Prairie View A&M University

Digital Commons @PVAMU

8-2023

Design And Implementation Of A Renewable Energy Research Platform In The Power Generation

Anthony Duran Hill
Prairie View A&M University

Follow this and additional works at: https://digitalcommons.pvamu.edu/pvamu-dissertations

DESIGN AND IMPLEMENTATION OF A RENEWABLE ENERGY RESEARCH

PLATFORM IN THE POWER GENERATION

A Dissertation

by

ANTHONY DURAN HILL

Submitted to the Office of Graduate Studies
of Prairie View A&M University
in partial fulfillment of the requirements for the degree of

DOCTOR OF PHILOSOPHY

August 2023

Major Subject: Electrical & Computer Engineering

DESIGN AND IMPLEMENTATION OF A RENEWABLE ENERGY RESEARCH

PLATFORM IN THE POWER GENERATION

A Dissertation

by

ANTHONY DURAN HILL

Submitted to the Office of Graduate Studies
Prairie View A&M University
in partial fulfillment of the requirements for the degree of

DOCTOR OF PHILOSOPHY

Approved as to style and content by

Dr. Penrose Cofie	Dr. John Fuller
Chair of Committee	Co-Chair of Committee
Dr. Kevin Kirby	Dr. Justin Foreman
Member	Member
Dr. Annamalai Annamalai	Dr. Pam Obiomon
Head of Department	Dean of College
Dr. Emmanuel Dada	Dr. Tyrone Tanner
Member	Dean of Graduate School

August 2023

Major Subject: Electrical & Computer Engineering

COPYRIGHT PAGE

Design and Implementation of a Renewable Energy Research Platform in

the Power Generation

Anthony Duran Hill

ABSTRACT

Design and Implementation of a Renewable Energy Research Platform in

the Power Generation

Anthony Hill, M.S., Prairie View A&M University.

(August 2023)

M.S., Prairie View A&M University

Chair of Dissertation Committee: Dr. Penrose Cofie

Over the past century or two, the interest in energy efficiency, Renewable Energy Generation in the power grid, energy cost, environmental protection, cyber-security, and the development of electric vehicles (EV) technology have been increasing. A research study on air pollution regulations in the USA, Asia, and Europe, as well as other major countries, showed that fossil-fueled vehicles were chosen as the significant source of emissions that created air pollution, leading to the global warming crisis. The oil resources on the earth are decreasing, and the new discoveries of these resources are at a more sluggish stride than the increase in demand by the world population. Therefore, the need for an alternative source of energy is becoming extremely critical. This research discussed the design and implementation of a Renewable Energy (RE) generation platform, solar power generation system. The design analysis and computations employed the Newton-Raphson load flow method, curve fitting, and other heuristics approaches. The design procedure is outlined in the body of the dissertation. The research study defined a RE platform consisting of a network of interconnected devices

collaborating to produce clean energy employing real-time measurements. The important components of the designed platform are detailed in the dissertation. These are various parallel and series combinations of solar cells, dc to dc converters including Maximum Power Point Tracking (MPPT), that are required to fine tune the dc output of the solar cells to charge the batteries and to activate the dc to ac inverters, e-Gauge data loggers, communication networks, parallel and series batteries configurations, buses, breakers, and 200 Amp panels. The partial designed blueprint of the overall system is included in the dissertation. The designed system minimized losses due to shading of the PV and overloads, maintained voltage levels, increased reliability, decreased power outage occurrences, and improved power management. The daily data collected on the system through the designed communication network allows system operators to rapidly identify the best power management and security strategy against cyber-attacks rapidly. The study also includes a working prototype to analyze crises condition, battery discharging and charging current, and implements a solution for solar efficiency.

Index Terms: Photovoltaic, solar power generation and converters.

DEDICATION

As I sit down and reflect on the four years since I started this journey, I would like to dedicate this work to my Lord and Savior, Jesus Christ. Also, I am grateful for the prayers, support, encouragement, and guidance my family provided me throughout this journey. Your unwavering belief in my abilities and potential has been the driving force behind my success.

Thank you, my wife, Shelia; our children, Keely (Arieus), Aisha (Bilah), Avis, Cody, Anthony, and Bryon; my sisters, brothers, and grandchildren. You have been my rock, my confidant, and my mentor. You were there to celebrate my victories and to pick me up when I stumbled. Your wisdom, experience, and kindness have been invaluable to me, and I am forever grateful for your contributions to my life.

I also want to dedicate this achievement to my parents, Robert, Ora Wallace, Clarence, and Edna Hill. Without your belief in me, I would not be where I am today. To my brother and sisters, Dalphana (Nate), Cathy, Julie (Mark), Tim (Candance), Juanita (Ronnie) and Rosita (Wayne), your unwavering support has given me the courage to passionately dream big and pursue my goals. Thank you for being my role models, mentors, and friends. You laid the foundation, and your dedication, hard work, and perseverance inspire me to be the best version of myself every day. I am honored to dedicate this achievement to my entire family.

ACKNOWLEDGMENTS

TABLE OF CONTENTS

Page

NOMENCLATURE

Abbreviation	Description
US	United States
RE	Renewable Energy
EPA	Environmental Protection Agency
CO_2	Carbon Oxide
CCS	Carbon Capture Storage
BSER	Best Emission Reduction
GHG	Green House Gas
PV	Photovoltaic
IC	Internal Combustion
EV	Electrical Vehicle
DC	Direct Current
AC	Alternating Current
IGBT	Insulated Gate Bipolar Transistor
kW	Kilo-Watt
H_2O	Water
MSL	Minimum Sea Level
AI	Artificial Intelligent
CAD	Computer Aided Design
A&M	Agriculture and Mechanical

LIST OF FIGURES

FIGURE

Page

LIST OF TABLES

1. INTRODUCTION

A.   History of Fossil Fuel

Over the past decades, climate variations have been observed not only across the US, but throughout the world. It has been discovered that a large amount of renewable energy resources is needed to offset these changes and this renewable energy resource will assist in minimizing the negative effects on the ozonosphere. The Environmental Protection Agency (EPA), monitors and protects the ecosystem and enforces regulations. The EPA suggested renewed procedures for charcoal and natural gas-fired power factories. These standards seek to avoid more than 500,000 metric tons of CO_2 greenhouse gasses, 300,000 asthma attacks and loss of 1,300 early human lives by 2030 [1]. The proposed standards for 2030, would attempt to avoid the following:

- an estimate of 1,300 premature casualties
- more than 800 emergency visits and hospital care.
- 66,000 employees lost their workdays. and asthma cases.

EPA is attempting to reduce detrimental pollution that affects the US residents, due to fossil fuel consumption [2]. The current proposed rule delivers on President Biden's and Congress's commitment to curtail the pollution resulting from the Fossil fuel energy sector.

This dissertation follows IEEE.

New energy source performance standards could attain up to less than 500,000 metric tons of CO2 emission decrease. Section 111 of the Clean Air Protections Act also outlines some upgraded regulations and emission procedures to reflect the best emission reduction (BSER) system that will advance the emissions performance of power generation sources, bearing in mind expenses, energy requirements, and other factors.

1.   Environmental Degradation

Fossil fuel-based pollutions are declining but as technology changes, fuel costs have gripped consumer wallets, and luxury has come at an exceedingly high price. Global warming is caused by the release of high fossil fuel by-products such as Carbon dioxide (CO2) and Carbon monoxide (CO) into the air through the use of many outdated machinery [3]. Health costs has increased across the country. The country's healthcare dollars are spent on treating the environment and cutting-edge research methods to reduce global air pollution. This study introduces various power systems derived from clean and renewable energy sources. The first system is the Photovoltaic or Solar power generation, which is making major advancements in creating clean and renewable energy. Solar panels can be set up to convert the sunlight into electrical power.

The second system is Wind power generation. This type of energy has been around for many years. Across Texas, especially in the northeast, Wind turbine towers have been installed to generate clean, renewable power. This type of renewable source converts the wind's kinetic energy into electrical power.

The third system is the Hydroelectric power. This system produces power by gravitational force using water by constructing concrete dams. And finally, the fourth renewable energy power system to discuss is Biomass power generation. The energy source for biomass is derived from organic matter. The process uses waste materials, crops, and various types of wood to produce heat, which generates electric power for daily use.

2. Encouraging Renewable Resources

As of 2023, the leading countries for Renewable Energy (RE) consumption were:

- China,

- United States and

- Brazil

with Russia and Italy trailing behind (see Fig. 1) [3].
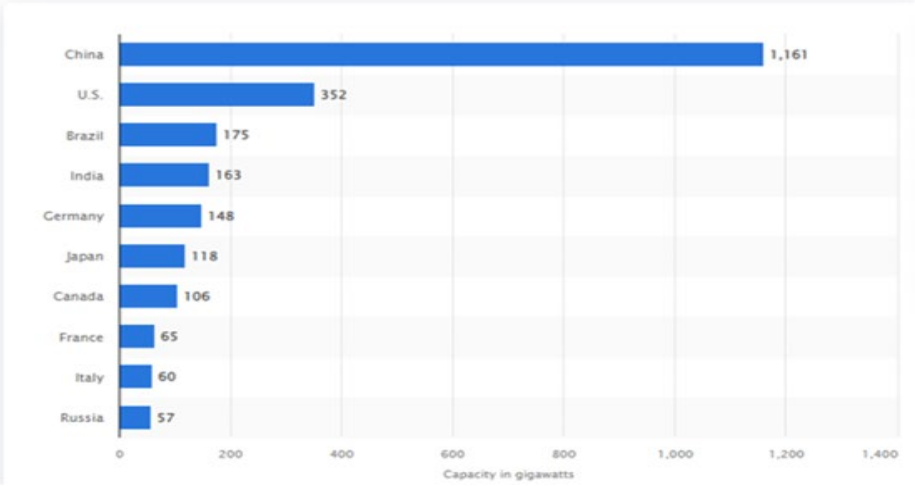
Fig. 1 Leading countries in Renewable Energy Wattages as of 2023 [4].

3. Photovoltaic (PV) Power Generation

Solar energy is the most available power that can provide a significant amount of energy for residential, industrial, and commercial use. Even though China is number one in solar power capacity generation, it is 30th in the world for reduction in climate change efforts. China still relies heavily on non-renewable sources of energy such as coal and natural gas for its electrical power production [5]. The US also depends heavily on oil, coal, and natural gas for power production [6]. The US is currently ranked number 40 for climate change efforts in the world as seen in Fig. 2.
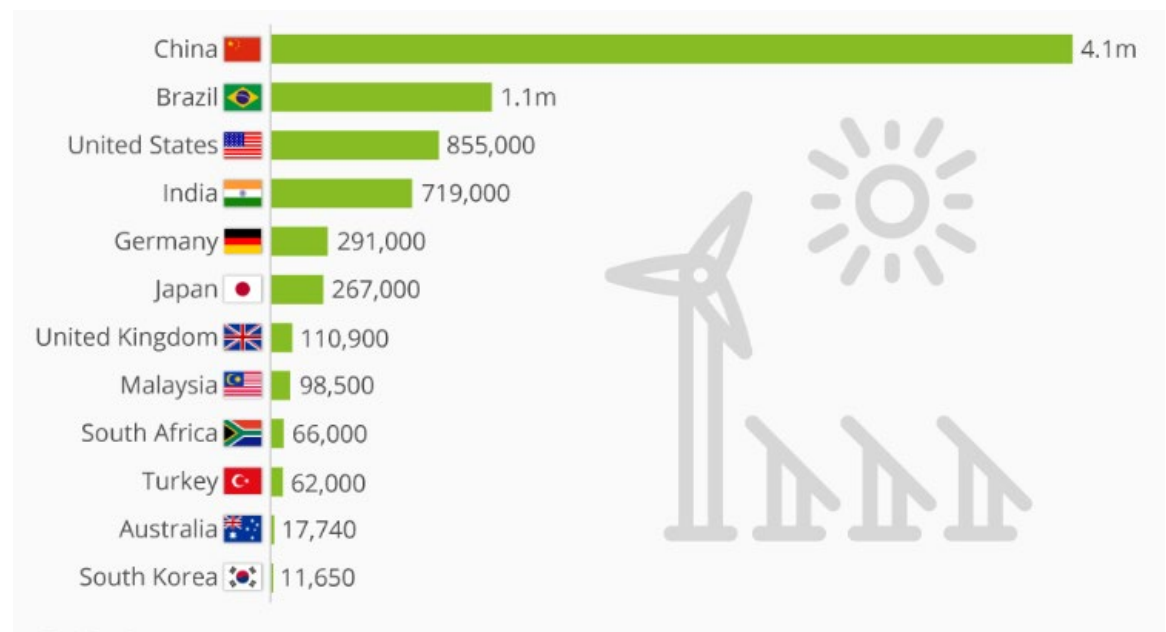
Fig. 2 Renewable Energy by Country [7].

In an effort to be among the leading countries that are implementing reduction strategies in global warming, the US government set an ambitious goal

of deploying 30 gigawatts of renewable energy by the year 2030 [8]. Photovoltaic (PV) power generation operation and maintenance cost are low, and it has a long lifespan. The reliability of the panels is very good. The energy produced is not seasonal like wind energy. PV energy can be used directly or stored in energy storage components such as super-capacitors, lead acid, and lithium batteries. Solar cell power generation uses series and parallel connections of the solar panels. The series connection increases the total voltage to drive a DC-AC power inverter. The two sources, solar and wind, can work together to complement each other to produce electricity. The wind can produce its energy in the winter months, and solar systems can produce power in the summer months.

4.   *Overview of Solar*

As explained by the EPA, greenhouse fumes are causing the Earth to heat and the heat travels into the atmosphere [9]. The emissions from Internal Combustion (IC) engine vehicles cause impurities to be released into the atmosphere, resulting in climate change. Solar systems on EVs are studied by transportation manufacturers worldwide. In this report, it was recommended that a fast off-grid solar array configuration be deployed to relieve the future charging issues for EVs. Recently, quite a few doctoral study projects were centered on the construction of appropriate educational platforms to enhance the training of students in various academic fields [10]. Many higher education institutions are challenged in designing or creating a power grid platform due to the rapid development of

technology in renewable energy sources. This has resulted in only a few universities actively involved in renewable energy research.

Renewable energy sources, such as solar with a remote laboratory, have become widely accepted for conducting hands-on lab-type experiments in the academic arena. The platform is suitable for renewable energy-based research on the smart grid. In this study, a web-based access portal formed part of the Solar Array Power system that included renewable energy sources application. Such solutions will significantly increase student interest in PV power generation (see Fig. 3).

Fig. 3 Renewable power-wind [11].

The platform will provide a facility for testing and tools to engage various applications with vigorous research in solar energy. The overview and architecture shown in Fig. 4, explains the main components of the platform as follows:
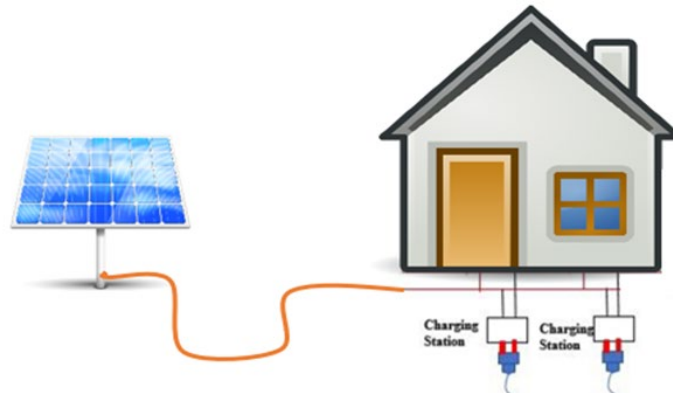
Fig. 4 The Impact on the grid [12].

a. An interface to the web with database

b. Two-factor log in systems

c. Solar Power Grid Tools

d. PV resources

e. Data application servers

f. Consumer Solar panels

g. Wind turbines

h. Converters and Inverters

An instrumentation and data acquisition system are housed in a portable metal

building that will allow students to work on new or previous research

demonstrated in Fig. 5.
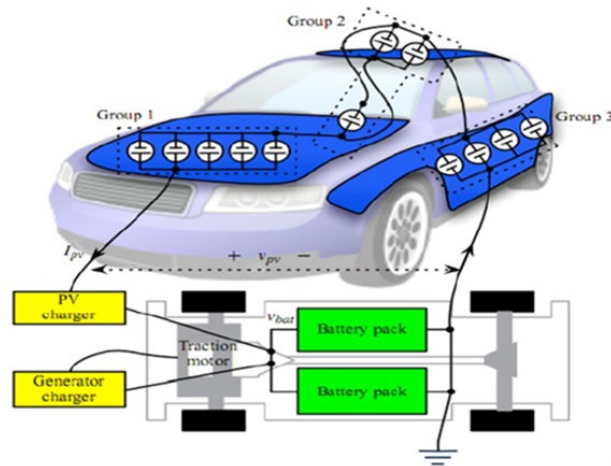
Fig. 5 Proposed Solution to Assist Power Grid [13].

A 45 Kw Solar panel system is placed on the roof and in the open field area of the

University landfill as seen in Fig. 6.
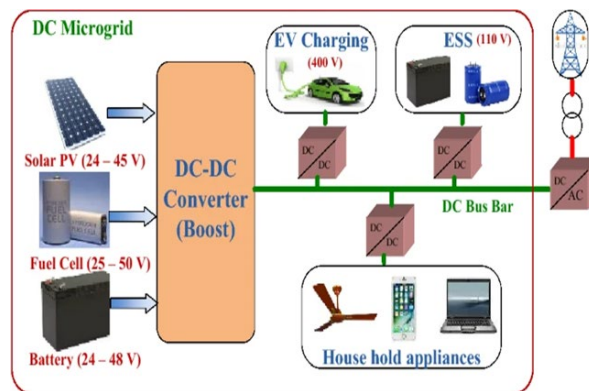
Fig. 6 Proposed Off the Grid Solar Network Infrastructure [14].

A Web portal application will open other research developments in cyber security protection for the grid. The key items and components of the platform are shown in Table 1.

TABLE 1

SOLAR PLATFORM PROPOSED EQUIPMENT

No.	Experiment Subject
1	Voltage and current of solar cells
2	Series and parallel connection of solar cells
3	Data acquisition for renewable energy systems
4	Maximum power point tracking (MPPT) for photovoltaic systems
5	Buck converter
6	Closed-loop control of buck converters
7	Boost converter
8	Closed-loop control of boost converters
9	Battery charging and discharging
10	A Microgrid using Renewable Energy

5. Renewable Energy Research

The proposed research was to study solar power and the EV impacts on the power grid. Also, the study will focus on generating enough power to support the University and surrounding communities' future needs. The US must move forward with other resources that can replace oil and gas. The US remains reliant upon an unsustainable power source such as fossil fuel [15]. As fuel technology advances for transportation and petroleum supplies reduce, it is crucial to discover power sources that are sustainable and safe for the environment and society [16]. Fig. 7 breaks down the estimated time necessary to create various power and renewable sources. The graph shows that between 1975 and 1980, oil production

took a significantly increased in its daily production. Currently, gas has become the fuel for energy needs [17].
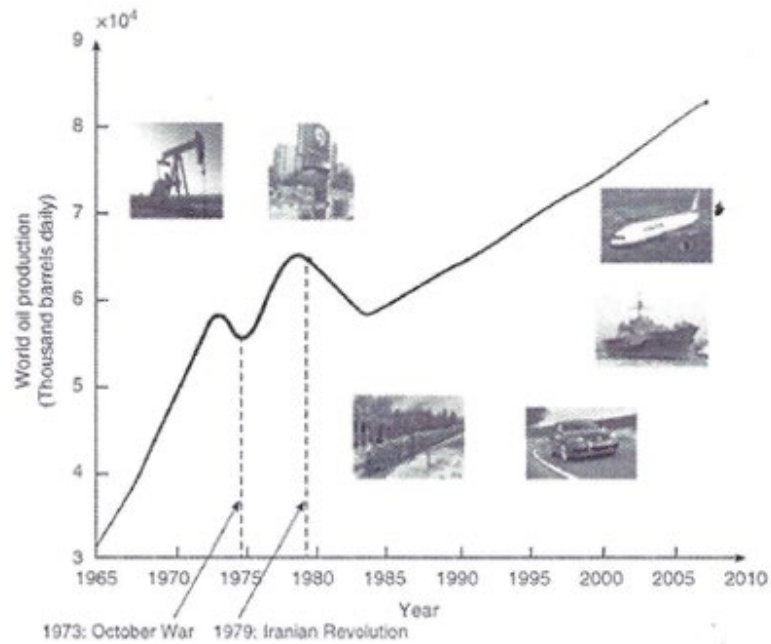
Fig. 7 The World's Oil Production (consumption) [18].

6.   **The Hydroelectric Power**

The Hydroelectric power was conceived in the US in the late 1800s. Hydroelectric power development and deployment were not encouraged by the US government and gas generation technology was actively pursued during the 1900s [19]. Currently, to forestall the contribution of global warming due to fossil fuel use in utility power generation, the US government allocated funds for research in hydropower generation. Where possible, hydroelectric dams can replace the use of fossil-fuel or coal power plants [20].

The coal industry is becoming obsolete and could be one of the causes of the country's global warning [21]. The Texas Water Development Board in 1968 had many small hydroelectric power plants. The board terminated their facilities even though local communities wanted to maintain operations for various important reasons, such as jobs and control of their revenue intake [22]. Plants located in the southern region of the state were also affected by shutdown. The initial settlers used water energy to operate the grinding machines for their grain and a water pump for the farms.

There are various power plants in the Colorado River region and in Travis County (see Fig. 8).
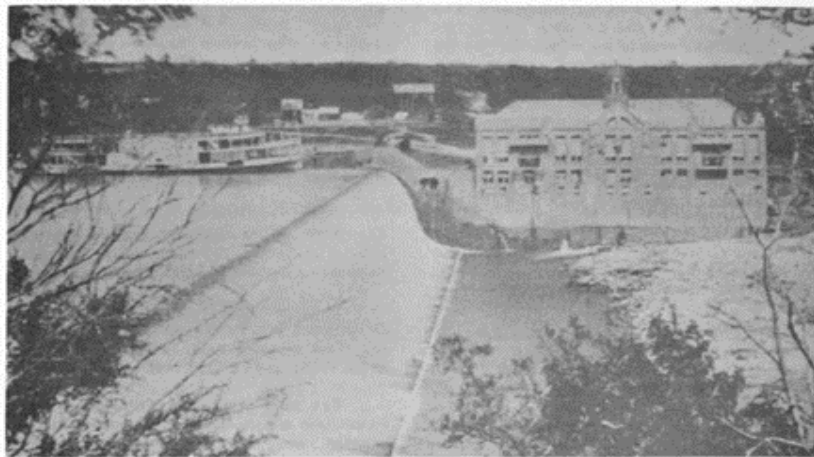
Fig. 8 The Hydroelectric Powerplant and Austin Dam [23]

The city of Austin owns the power plant. The Lower Colorado River Authority (LCRA) is one of the major hydroelectric power plants on the Colorado River.

The Hydroelectric powerplant listed in Table 2, in Austin, Texas, was destroyed by flooding in the late 1900s, and LCRA listed it as discontinued. Other plants not shown in the Table were also discontinued in 1965 [24].

TABLE 2

SUMMARY OF MAJOR HYDROELECTRIC POWERPLANTS

No.	Hydroelectric	Owner	Reservoir Lake	Stream	Built	Completed	Generating Capacity-KW
1.	Austin, Tx	City	McDonald	Colorado	1890	1893	5,227(hp)
2.	Austin, Tx	LCRA *	Austin	Colorado	1937	1939	13,500(hp)
3.	H-4-DAM	GBRA	H-4	Guadalupe	1929	1931	2,400
4.	Dunlap (TP_1)	GBRA	Dunlap	Discontinue	1927	1928	3600
5.	Eagel Pass	CPLC	Canal	Rio Grande	1931	1938	9,600
6.	Marshall Ford	Discontinue	Lake Travis	Discontinue	1937	1942	67,500
7.	Dennison	US Army-Corp of Eng.	Lake Texoma	Red	1939	1943	70,000
8.	Buchanan	LCRA	Inks	Colorado	1931	1938	33,750

It was discovered that Lake Buchanan was built first in 1938 and was used for storage so that the system could endure the water surge to generate power downstream of the plants.

Lake Travis provided backup storage as needed. Establishing this storage allowed the renovation process for the upstream dam and the powerplant. The LCRA plant was a key power source of the South Texas interconnected water system. The data in Table 2 was furnished by the LCRA. The blade propeller type is a 200-rpm unit with a capacity of 10,500 hp at a 64.8-foot head. The combined turbines are designed and equipped with mechanical metal blades. To receive the

highest power, the system must provide an excellent power output for any mechanical gate position. The powerhouse is water-sealed and the elevation is 476.0 feet above sea-level, which is elevated more than any known flood stage in Texas [25].

The LCRA is essential to the unified network, containing restricted energy and has a relationship with enormous metropolitan utility facilities in South Texas. They also provide power for local consumption and peaking loads of interconnected water systems. The prearranged total energy at the power plant was supplied by LCRA for at least 23 years.

7. **The Wind Turbine**

The energy from wind is also increasing to help implement clean green technologies, providing safe, renewable electricity generation. There are Scaled Wind Power Generation Systems in Texas near Lubbock (see Fig. 9) [26].

Fig. 9 Brazos Wind Turbine Towers [27]

The key elements of a wind turbine include various systems such as yaw, pitch blades, a hub, the base, and tower. Today, the installation of more wind power generators impacts the wind farms across the state. Research for replacements for

fossil fuels is urgently being pursued in most states in the US and other countries around the world, however, this research in RE is still faces many political and technological challenges.

8. **The Biomass**

Biomass fuel is obtained from agriculture feedstocks and plant residues, domestic and biodegradable industrial waste. Biomass has its advantages as well as disadvantages. There are some cost methods that are very expensive. The process and quality of biomass production faces challenges. These challenges include improvement in feedstock, conversion performances, and product distribution to consumers. It is the appropriate and cost-effective option for treating wet waste since very little energy is required [28]. A stand-alone smart grid system usually contains solar, wind, biomass, and battery energy system. The system is designed with Artificial Intelligence (AI). The AI diminishes the power supply loss probability and supply for at least 30 minutes, which can be observed in Fig. 10.
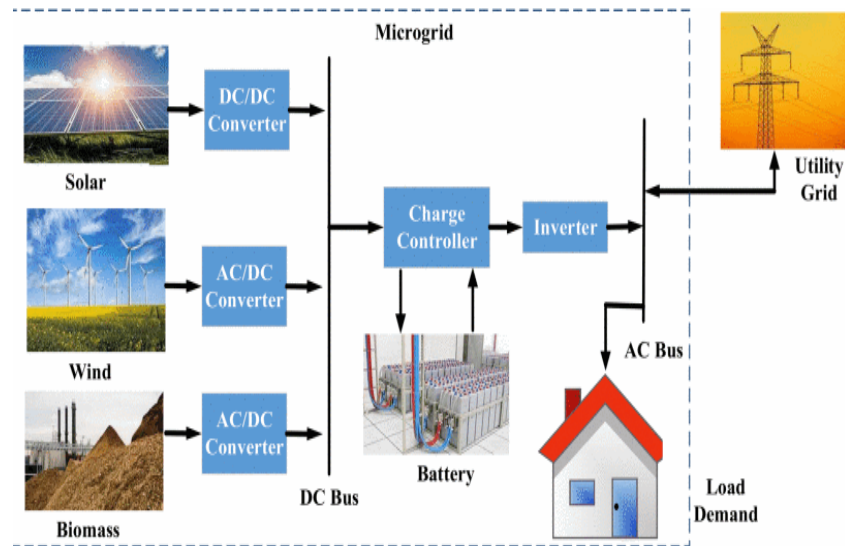
Fig. 10 Grid-connected Microgrid System [29].

9.   Motivation and Objective

The Industrial Revolution used Coal. Research has shown that humanity has used fossil fuel and wood energy for approximately 10,000 years. Fossil fuels are not renewable. Fig. 12 shows that US oil and gas usage skyrocketed and there is a need to conserve energy to reduce pollution [30]. Oil production reached its highest in 1970 in the US, and due to fracking technology, oil production in the US has rapidly increased. The US produces 20 billion barrels of oil. This needs to be reduced tremendously if the government wants to accomplish its ozone layer pollutions concerns by going green to produce clean energy (see Fig. 11).
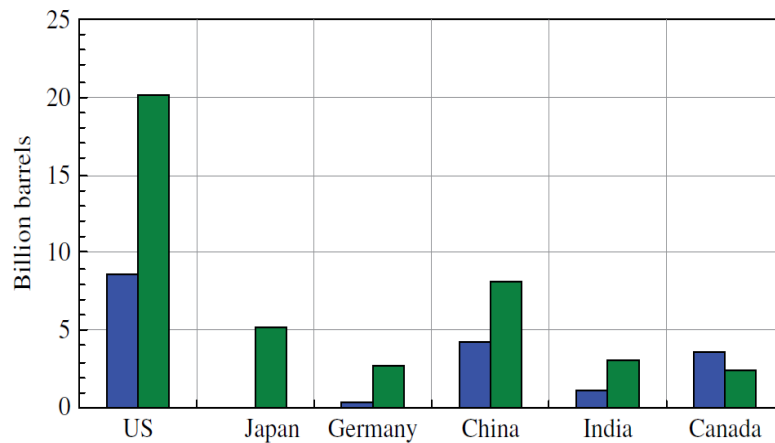
Fig. 11 The World's Crude Oil Consumption [31].

Other countries are ahead of the US. The barrels of oil production in the US should decline as more EV systems take to the highways of this country. Solar energy could facilitate, if the implementation and research is conducted thoroughly and consistently. The US still has not solved the country's air pollution problems. As mentioned before, the crucial objective of this study is to design, and build a platform through the development of algorithms to control the components of a PV platform that will produce and generate clean power. The proposed project is completed and will continue to phase two and three, in the future to assist with local communities struggling with high utility bills. It is anticipated that from this study and theoretical results, the PV Solar system can be integrated with the utility grid that will improve the campus power reliability and reduce utility cost. Prairie View A&M University has the opportunity to design and create a clean energy system that could surpass some of the other leading entities in the area of creating

renewable engineers. Table 3 also displays how other schools are producing power using PV cells that generate DC voltages from the sun.

TABLE 3

TOP FIVE SCHOOLS WITH RENEWABLE SOURCES IN PLACE

The top five schools for percent of electricity that is generated by energy projects that are owned and operated by the school			
Rank	School	State	% Self supply
1	Butte College	CA	79%
2	University of Minnesota, Morris	MN	58%
3	Carleton College	MN	22%
4	University of Missouri	MO	20%
5	Luther College	IA	20%

Butte College in Oroville, California, is number one in the nation for renewable energy installed systems. The college has about 75% of their school's electricity generated by solar projects. The campus is the first in the country to generate more electricity than it uses. Prairie View A&M University wants to be on the map of the Renewable Energy source consumers and aims to be a leading University in that direction. It is worth noting from the Table that little attention is given by the government to renewable energy curriculum in US Higher education institutions [32].

2. LITERATURE REVIEW

B. **Introduction**

The energy cell is a device that transforms light from the sun to electric power energy using the PV effect. A large volume of solar cells is engineered from silicon. Since silicon, which is basic sand, abounds everywhere, it lowers the cost of solar cell manufacturing. There are different types of solar cells: amorphous nanocrystalline, or single crystal silicon form. The PV cells do not require fossil petroleum to generate energy, nor do the modules have moving parts. The solar cells are put together in panels. These panels are then configured into thousands of arrays, as shown in Fig. 12. Solar cells can also be installed on rooftops of homes to supply power from the roof.

Fig. 12 International Space Station [33].

The PV cells also provide energy in many remote global areas where powerlines are not implemented. The RE is inadequate for space probes when using them for solar system's project in outer space due to the diffusion of radiant

energy and by the sun being far away [34]. Fig. 13 displays a demo system that can be implemented into cities across the country.

Fig. 13 Solar Cells Array [35].

Solar cells are used in customer related everyday items such as, calculators, robots, and mobile radios. The solar panels used in devices utilize LED and serve as secondary source by charging batteries to supply power when the sun is not available. It has been documented that current solar cells operate at about 20 percent efficiency [36]. Engineers are researching how to improve the efficiency of the panels to recover the 80% loss of energy. It has been discovered that silicon is the second abundant component in the Earth. The PV cells allow the light to pass through the device optical coating layer. This process uses reflection to reduce the losses. The panels trap the light falling on it and is then converted to energy using a spinning or vacuum process [37].

1.   The History of Photovoltaic (PV) Systems

Solar power was introduced in the 1800s. A scientist from France named Edmund Becquerel performed experiments with wet cell batteries in 1839, which led to his discovery of solar power [38] (see Fig. 14).
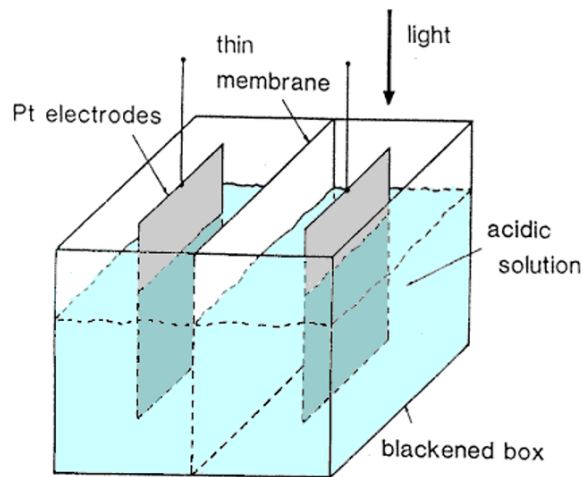
Fig. 14 A diagram of apparatus by Becquerel (1839) [39].

The PV uses outdoor installation panels such as roof or ground mount systems. When a Positive-Negative (P-N) junction begins to form inside the silicon material, electrons are excited due to the self-built electric field. The holes of the electrons move in opposite directions, especially those in the junction layer area [40]. When this happens, it creates positive and negative poles. Therefore, if a load is connected to the electrodes, the current flows through the cell. The solar cells create positive and negative charges, when exposed to light from the Sun. The two charges are then collected by a circuit, which converts the source into usable

electricity. The photovoltaic effect mentioned in Chapter 1 results when a photon's energy is absorbed, producing some free-electron spillover from the panel's surface (see Fig. 15). Fig. 15 also, displays the structure of cells.
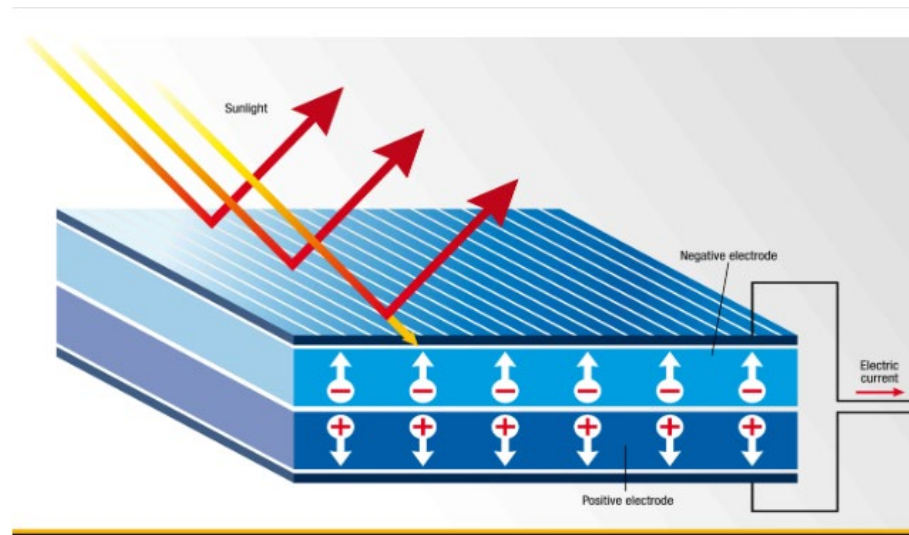
Fig. 15 Structural Crystalline Silicon Solar Cell Copper cuprous oxide PV cell [41].

The design was based on the junction of copper-cuprous oxide. A coil of Pb wire is used to give a grid contact to the irradiated surface of the PV-cell. This method was afterward refined by spinning the metal on the outer surface and removing a part of it to form a grid. The power can then be used to power items such as artificial satellites in space, homes, factories, and city electricity [42]. Although other materials comprise the panel, Silicon-based solar cells are favored and account for 95% of the PV production [43]. The batteries are used as an energy storage device for the energy produced from the solar panels.

The following are three generations of panels.

• Monocrystalline or polycrystalline silicon solar cells

• Thin Film Solar cells

• Organic Thin Film technology solar cells

The Monocrystalline is made from monocrystalline silicon that is commonly used in the residential market. The panels have a life span of more than 25 years [44] (see Fig. 16).

Fig. 16 Three Types of Solar Cells [45].

The thin film panels are extremely flexible, which makes the application highly manageable. Table 4 displays the advantages and disadvantages of each cell type.

TABLE 4

PANEL COMPARISON

Cell type	Efficiency rate	Lifespan	Advantages	Disadvantages
Monocrystalline	20 %	25 years	Highly efficient, durable	Expensive
Polycrystalline	16 %	25 years	Lower cost	Less efficient
Thin-film (Amorphous)	10 %	15-20 years	Less expensive, easily produced	Lower efficiency/ shorter lifespan

The second generation comprises the amorphous silicon thin film solar cell mixed with perovskite solar cell technology. The efficiency rate is lower than other types of solar panels. The global industry of solar cell manufacturers has increased 17 times in 10 years. The production of these panels is mainly distributed in US, Europe, and Japan. Twenty-two years ago, the installation scale of solar power was 1,744 MW, exceeding the ten-billion-dollar mark. Today, the scale has risen by almost 120. Ten thousand plus companies have generated more than 33 billion private investments through the US economy (see Fig. 17).
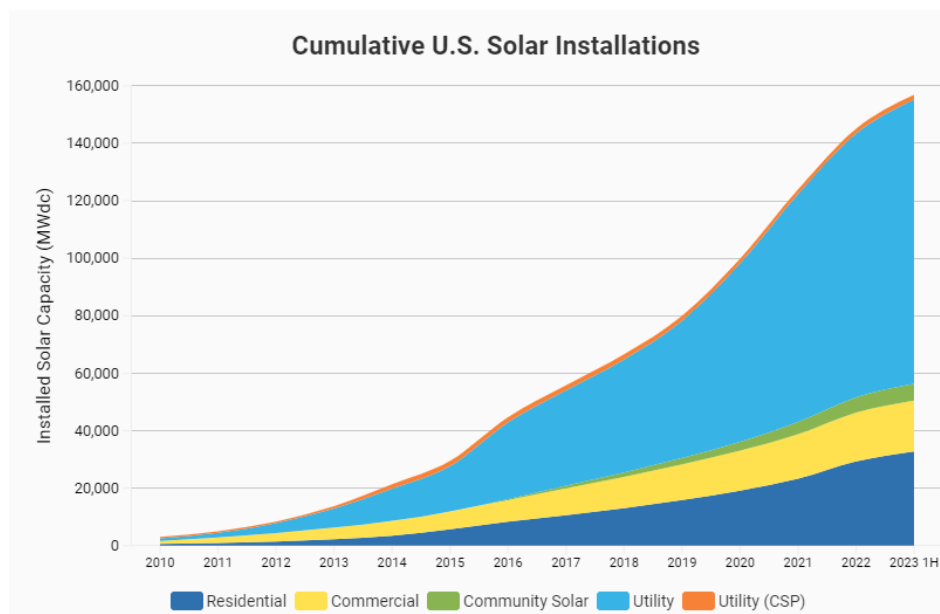
Fig. 17 Solar Installations in the US [46].

During the last century, the solar industry has an average growth rate of 24%. As the federal government continues to provide funding for the increased demand for clean, green energy, the 155 Gigawatt PV system was installed to provide enough power to 27 million homes [47].

2.   *Solar Cell Power Energy Operations*

Homeowners and industry demand that PV systems be implemented cheaply. The challenging component of solar cell power generation with an enormous cost is the storage sub- system. Today, utility companies recognize that if they fully participate in the solar power producing industry, they can positively affect their overall yearly revenue. California is pushing renewable energy projects by 2030 (see Fig. 18).
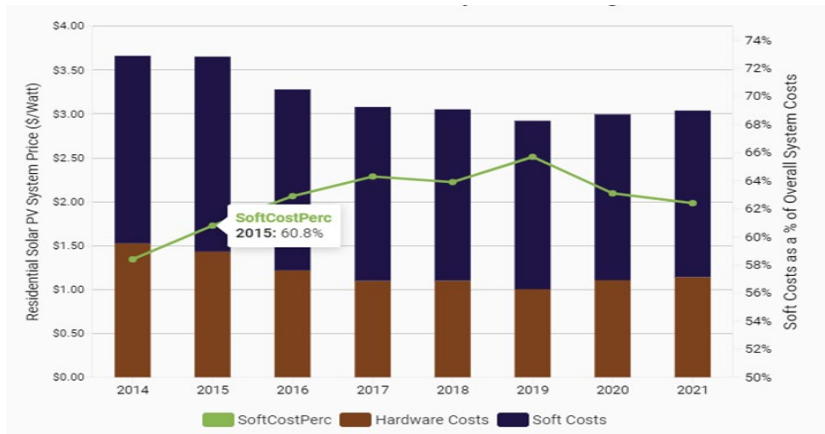
Fig. 18 Residential Solar Power Installation Cost [48].

The solar systems installation has diversified and impacted the market, creating large pipelines in the near future (see Fig. 19 and Fig. 20).
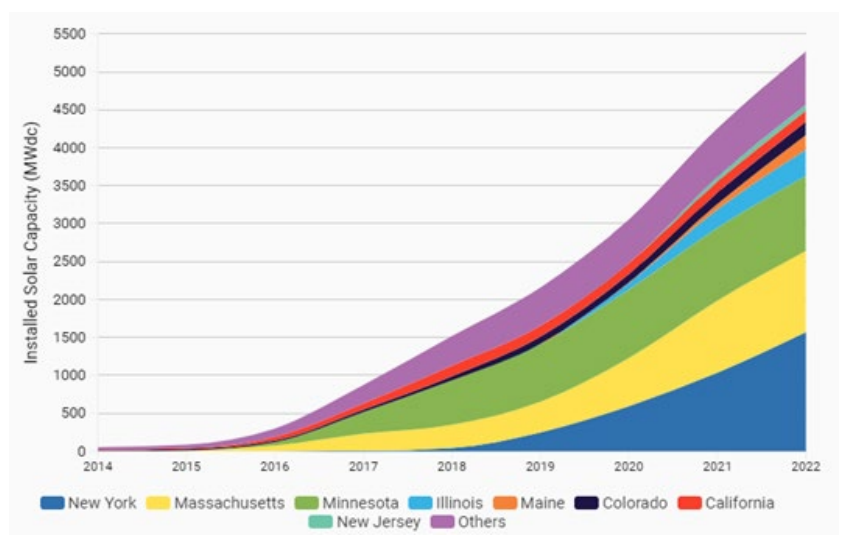
Fig. 19 Cumulative US Community Solar Capacity Installations [49].

Commodity	Consumption
Electricity	116513.4 kWh
Natural Gas	119964025.8 mmBtu
Water	No Data

Fig. 20 Prairie View A&M University FY 2012 Energy Consumption [50].

The growth in renewable sources will influence other state renewable community programs to accelerate the deployment of PV systems, allowing residentials and industries to realize considerable savings in their power yearly cost. As can be observed from the previous graphs, the renewable energy space for the US overall is not bright. Here at Prairie View A&M University, the demand for renewable energy sources is rising to reduce yearly electricity bills. The University's power consumption has increased tremendously over the past 10 years (see Fig. 21).

Commodity	Consumption
Electricity	46,178,722 kWh
Natural Gas	138,916 mmBtu
Water	272,290 kgal

Fig. 21 PVAMU FY 2022 Energy Consumption [51].

The University should submit the proposals for future solar farm as part of utility infrastructure for the entire Prairie View A&M system created a five-year master plan which included several new building developments, such as, New Engineering Research building, Business and Ag building, (ENCARB) four new student's housing complexes, and new police station. The university's master plan aims to aid in reducing and improving overall campus power consumption and optimization over next five years. The university and Texas A&M University system completed a capital plan investment encompassing the following to aid in optimization and life cycle of HVAC and Central Plant equipment throughout the campus, but it did not include any type of renewable energy concepts. The campus has a contract with San Bernard Electric Company (SBEC) for its utility services [49]. PVAMU has been a member since 1981 benefiting from $0.0026 per kWh utility rate. The University currently uses around 76 MWh annually with a base charge of $5,000 per month.

3. Solar Cell Specifications and Technical Data

The datasheets of the solar panels are furnished by JINKO Solar. The model number for the solar panels that is to be used on the platform is JKM 300P-72(530 W) [51]. The solar panel technical data are displayed in Table 5 [52]. The performance ratio is given by Equation 2.1.

TABLE 5

TECHNICAL PROPERTIES (SOLAR PANEL JKM 300P-72 300W)

Electrical Characteristics

Module	HT72-18X Transparent				
Maximum Power at STC(Pmax)	530W	535W	540W	545W	550W
Open-Circuit Voltage(Voc)	49.20V	49.35V	49.50V	49.65V	49.80V
Short-Circuit Current(Isc)	13.76A	13.83A	13.90A	13.95A	14.00A
Optimum Operating Voltage (Vmp)	41.35V	41.50V	41.65V	41.80V	41.95V
Optimum Operating Current(Imp)	12.83A	12.90A	12.97A	13.05A	13.12A
Module Efficiency	20.5%	20.7%	20.9%	21.1%	21.2%
Power Tolerance	0 ~ +5W				
Maximum System Voltage	1500V DC(UL/IEC)				
Maximum Series Fuse Rating	25A				
Operating Temperature	-40℃ t o + 85℃				

*STC:Irradiance 1000W/m², module temperature25, AM=1.5
Optional black frame or white frame module according to customer requirements

This is derived by subtracting the highest performing rate of 100% from 15.6 % of the deficits. The platform's complete outcome is 84.4%. The simulation studies done on this project displayed the detailed profit, the unit energy generation needed for the platform. The final calculation for the load ratio result is 1.17 [53]. The load's ratio can be derived by Equation 2.1 [54].

Load ratio= (DC POWER INSTALLED)/ (AC POWER) = 233.7KW/200Kw = 1.1

There are some disadvantages of Solar Cell panels that need to be considered when designing off-grid systems:

- Orientation-Tilt shortfall

- Shading

- Soil test for the PV foundation pads

- Mismatch loss due to environments, and apparatuses.

- Wiring Loss: due to resistance

- Clipping and Inverters.

4.   **Solar Cell Technology Detailed Overview**

Solar panels have many different voltage specifications as listed in Fig. 22.
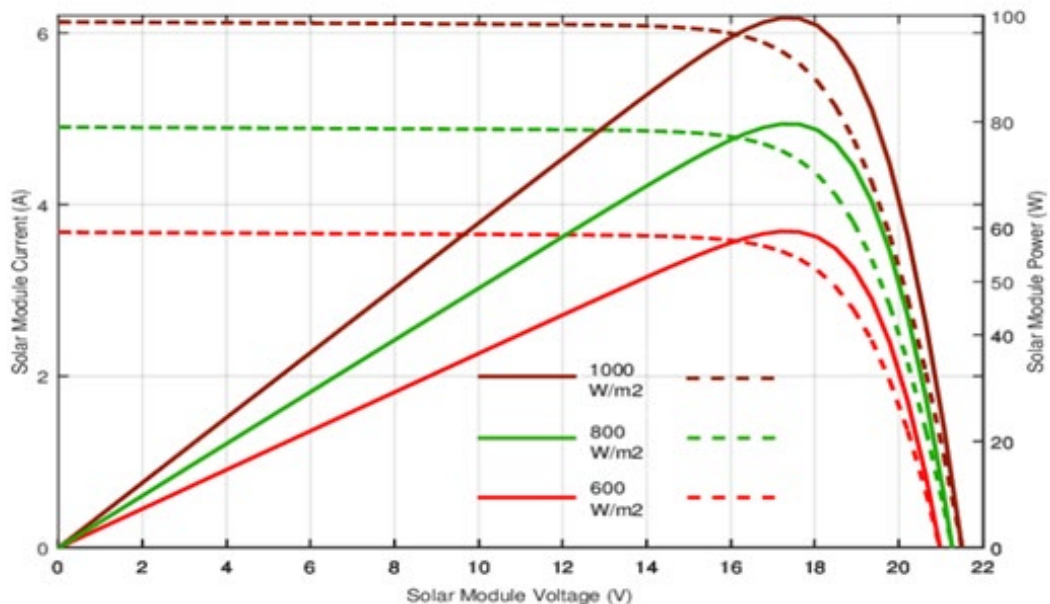
Fig. 22 Solar Irradiance P-V and I-V Curves [55].

Voltage at Open Circuit (VOC), and Nominal Voltage (V_n). During installation, the field test will include measuring all parameters for the PV Panel. The V_{oc} is measured with a volt-multimeter before the panel is connected to the load, as shown in Fig. 23.
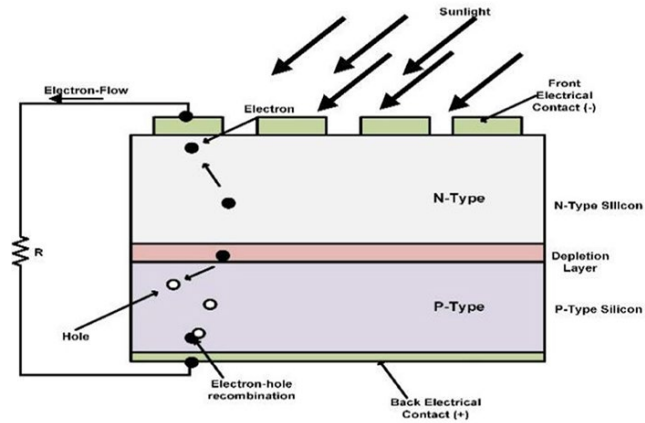
Fig. 23 Solar Cell Electric Circuit [56].

Table 6 displays the breakdown of the solar panels dimensions that will be used

in this study,

TABLE 6

SOLAR PANELS DIMENSIONS WEIGHT WATTS & EFFICIENCY

Dimensions (mm)	Number of Cells	Weight /Watts	Panel Efficiency
2285 x 1133 x 35mm-Tri	144	27.2 kg / 470	21.2%
75.2 x 44.6 x 6 – Alt E	182	158.1 lbs / 450	High Efficiency
79.96x39.69x1.57 -Aris	144	51.3 lbs / 500w	24.2%
1762x1134x30mm-Vertex	144	21.2 kg /435	21.2%
2278x1134x35mm-Jinko	144	27kg / 500w	22.8%

5.   Advantages and Disadvantages of Electric Power

The complex microgrid has several benefits. The power grid is a massive

and complex network. Electricity can be arranged and deployed throughout the

US [57]. The extensive transmission networks:

- Allows microgrid users to deal with known and unknown losses while providing the demands for more power;

- Provides flexibility. The smart-grid permits delivering power to locations far away;

- Allows economic competition.

A power blackout in Texas in 2021 indicated why Renewable Energy sources platforms are essential. In February of 2021, the largest blackout for the state of Texas occurred due to low temperatures and an erroneous prediction of energy demand that resulted in winter freeze throughout the state. The blackout spread across every major city, including the deep south areas. The Electric Reliability Council of Texas (ERCOT) allowed the events of forced outage of its generators for fifteen consecutive days [58]. The load consumption request of 20,000 MW was pushed through the system beyond its maximum limits. The request caused forced outages that went across 90% of the state. During this time, the first for Texas, EROCT of Texas, attempted to address the problem by implementing a process called rolling blackouts [59]. The process was to ensure that power is supplied to critical loads (see Fig. 24).
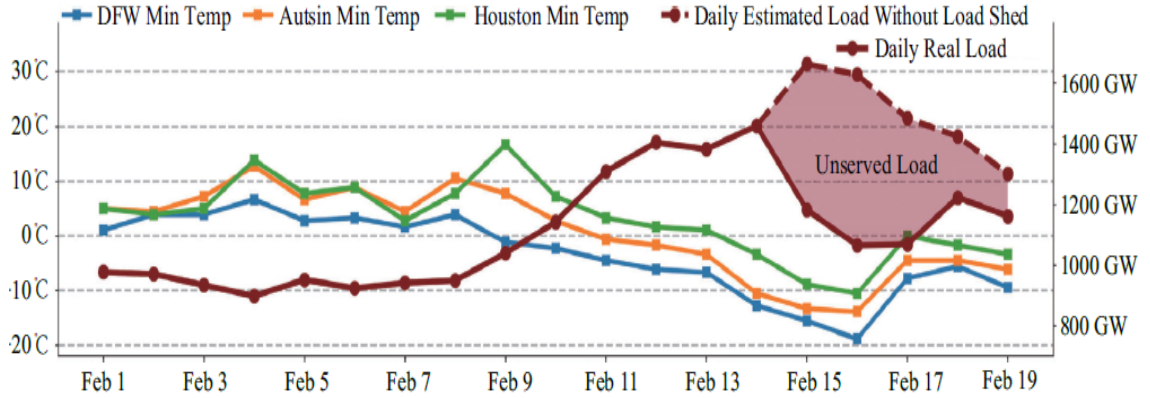
Fig. 24 The Overload Request for Texas Outage [60].

The Federal Energy Regulatory Commission (FERC) investigated the rolling blackouts from the nighttime light data from the sixth to the 15th of February 2021. NASA's satellite imagery system provided the data for Fig. 25.
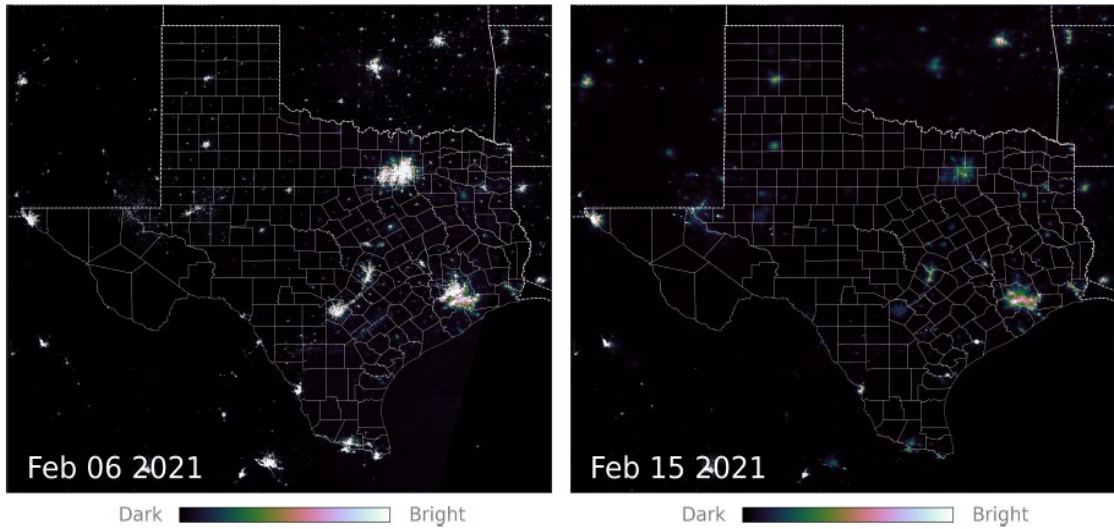
Fig. 25 Satellite Imagery power blackout (left). Satellite Imagery Power Restored (right) [61].

The outage ended on February 19th, and the power system returned to normal operations, but by then, it was approximately 195 billion dollars' worth of property damage occurred and several people passed away. The satellite observation revealed that the daily minimum temperatures in the major cities caused the system to overload. The nighttime light (NTL) data was beneficial in showing dark areas with no power. This disaster would not have occurred if the state of Texas had adequate renewable energy supply [62]. ERCOT has suggested some major changes to prevent future disasters:

- Execute an assessment worst winter condition;

- Engage RE engineers in the control room to monitor and make necessary modifications to the Texas grid;

- Update the rules and procedures for previous severe weather.

This study presents in Chapter 3 three types of configurations of Solar Arrays: 1) Ballasted Fixed tilt 100 Monofacial, 2) Fixed Tilt Monofacial 250, 3) Dual Axis Tracker Bifacial, and 4) Flush mount rooftop Monofacial (see Fig. 26).
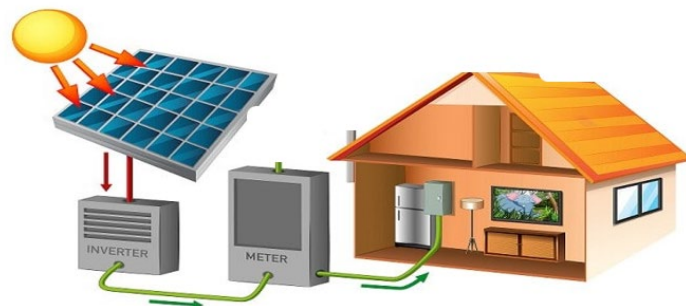
Fig. 26 Roof Top Monofacial Solar Cells - Off Grid [63].

6.   PV assisted EV charging

The prediction made by President Biden to build a US strong network of 500,000 EV chargers using PV generating stations along America's highways and in communities will bring relief to the power grid. A solar powered generating station should be pursued in current and future research studies (see Fig. 27).

Fig. 27 Solar Charging Unit [64].

The kit is a solar chaining kit designed to provide 50W of power. It is used in an off-grid application. The chaining feature allows the unit to connect multiple solar panels for increasing power generation. The Sun produces a tremendous amount of clean energy and this unit is a convenient and sustainable solution for powering and charging off the grid. This unit can charge the batteries and supply energy to

the local and commercial charging stations. Every community, company, and commerce would do what is needed to save and produce power from a renewable source. Although all these needs are fulfilled, choosing to go green with clean resources will hopefully eliminate the concerns of the polluting the Earth atmosphere [65]. The US needs to continue the research on RE to provide a complete solution to the world's environmental pollution problems. Fig. 28 is a complete setup of the recommended solution to President Biden's plan to instruct charging units across the US.

Fig. 28 PV Solar Charging Stations [66].

Various types of devices can use this station to charge employing clean and renewable energy. This type of units is setup to be environmentally conscious.

7.   **Battery Energy Storage in PV Solar Power Station**

Solar and wind power configurations, and the battery cost, are challenges. Table 7 displays a comparison between Lead-Acid battery, NiMH battery, and Li-ion battery.

TABLE 7

BATTERY COMPARISON

		Lead-Acid		NiMH		Li-Ion	
Nominal Cell Voltage	V	20		1.2		3.3-3.8	
Energy Density	Wh/l	60		100		150	
Specific Energy	Wh/kg	25		50		90	
Power Density	W/l	1200		2000 - 2500		3500 - 9000	
Specific Power	W/kg	500		1000 - 1300		2000 - 4000	

Most renewable energy generation systems use lithium-ion batteries to cut back acid vapor released into the atmosphere. Even though the Li-ion batteries are costly, the Table indicates Li-ion has a better energy density and therefore most RE generation system uses this type of battery [67]. The disadvantage of the Li-ion battery is that it is combustible and has a history of catching on fire [68]. The battery has power cells that can cause short-circuiting if it is damaged by water or manufactory error [69].

3. METHODOLOGY

C.   Design Simulation Implementation of the PV Generator Prototype

The RE solar platform is designed to introduce graduates as well as undergraduate students to RE applications and research. Students can conduct experiments outside and inside the lab as well as in remote locations on campus. The systems allow the students and graduate researchers to design a single and three-phase power system with various testing points for data collection. Also, the RE solar platform is implemented to counteract the negative impact of climate change.

1.   Mathematical Modeling and I-V Characteristics of PV Cell

Fig. 29 indicates the ideal PV cell model. This report details how to simulate a PV cell's behavior.
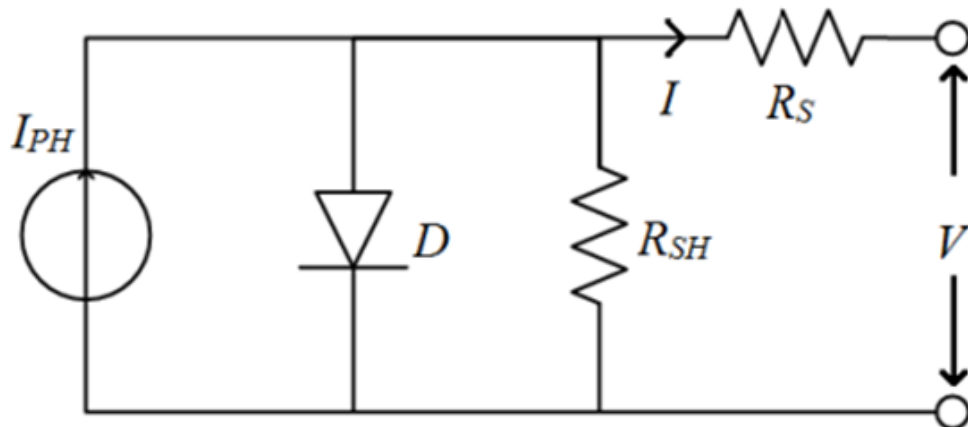
Fig. 29 PV Cell breakdown [70].

Equation 3.0 provides I-V basic characteristics for testing samples of the prototype PV cells [71].

$$I = I_{PH} - I_S \left[exp \ \frac{q(V+IR_{S)}}{NkT} \ - \ 1 \right] - \frac{(V+IR_{S)}}{R_{SH}} \ \text{..} \ (3.0)$$

- I_{PH} $= Sunlight \ generated \ current;$
- $I_s = Diode \ satutation \ current \ ;$
- $V_t = Thermal \ votlage \ of \ the \ PV \ cell;$
- $N = Ideal \ Diode \ factor;$
- $k = Boltxman \ constant;$
- T=operating temperature and;
- $q = Electron \ Charge;$
- $I - cell \ current \ (A);$
- R$_{SH}$ -cell shunt resistance;
- V = output voltage;
- R$_{s\ =}$ cell series resistance.

Fig. 30 shows how the testing of the cells is accomplished. This includes the variable load and two meters for measurements of the voltage and current.
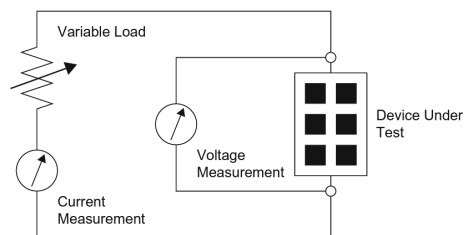
Fig. 30 PV Panel testing [72].

Some of the basic required parameters are located on the back of the solar panel. These parameters are:

- Maximum Power - (P_{Max});

- Voltage - V_{mp};

- Short Circuit Current - I_{sc};

- Open Circuit Current - V_{oc};

- Sun-Light Intensity - (S_o);

- Temperature - (T_{ref}).

Normally the values of R_{SH} and R_S are given and the values represents internal losses due to the current flow. Finding the two values require solving a non-linear equation using Newton- Raphson, curve-fitting, and other trial and error methods used in mathematical modeling [73].

Gauss-Seidel method was applied to the prototype. The research was performed with power flows analysis using Fast-Decoupled method. The study the efficiency of the prototype focusing on three main components:

1. The PV cell performance;

2. Battery Storage;

3. The algorithm that controls the Maximum Power Point Tracking (MPPT).

Another method to obtain R_{SH} and R_S, is to measure the open circuit

voltage V_{OC} of the module, and the short circuit current, I_{SC} [74] . The MPPT operates at the maximum power point, which is the knee of the current -voltage curves indicated in Fig. 31 [75].
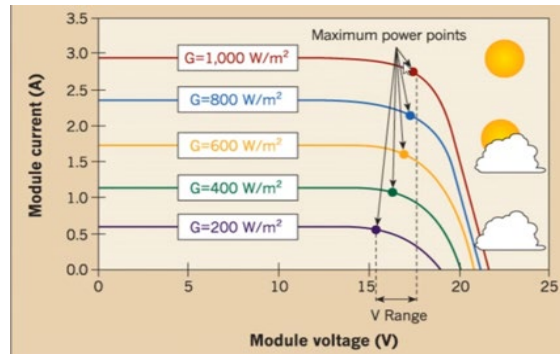
Fig. 31 Power Curve and Irradiance Characteristics [76].

The MPP is key for optimizing the performance of the cell modules in a practical application. The prototype used the data in Table 8 for the solar cells.

TABLE 8

PV MODULE PARAMETERS

Solar Module	Value
Voltages at Pmax (V_{mp})	17.6V
Maximum Power (P_{max})	100W
Current at Pmax (I_{mp})	5.69A
Voltage Open Circuit (V_{oc})	22.6V
Short Circuit Current (I_{sc})	5.90A
Number of cells (N_c)	36
Irradiance @ STC (T=25° C)	1000 W/m^2
Material Type	Monocrystalline silicon

A special design meter was used to obtain the values in Table 8. Power-Sim (PSIM)

simulation software was used to obtain the PV cell characteristics.

2. **The Off-Grid PV Prototype Design and Implementation**

The off-grid solar prototype is a PV system that operates without local utility power. The system is entirely stand-alone. When the sun is shining, the solar cells can provide power to the load simultaneously as it charges the batteries. Here are the essentials components for the off-grid prototype:

- The PV Modules;

- Charge Controller;

- Off-Grid Inverter;

- Battery Bank.

3. **Advantages and Disadvantages of an Off-Grid PV Power Generation:**

The main advantage of the Off-Grid PV Power generation system is that it can function anywhere within the US. The system can be used for many applications, such as:

- Agriculture - to power water pumps and irrigation sprinklers;

- Recreation use – to power boats, RVs, mobile devices, etc.;

- Industrial – to power hospitals, factories, ocean platforms and satellites;

- Residentials – to power homes with no access to regular utility services.

A disadvantage of the off-grid systems is that the battery cost is 70% of the total project cost. Another disadvantage is the short lifespan of the batteries. The batteries need to be replaced at least every four to five years during the lifetime of the PV system.

4.   Off-grid PV Power Generation Energy Flow

A typical off-grid PV power generation is composed of the following components:

1. The Production unit;

2. The Storage unit;

3. The Usage unit.

The production unit starts where the solar irradiance reaches the PV module's surface to generate DC. The current flows through the connecting wires into the storage unit. This unit uses a charge controller to manage and control the power. In Fig. 32, the Charge controller protects the batteries by preventing them from being overcharged or undercharged.
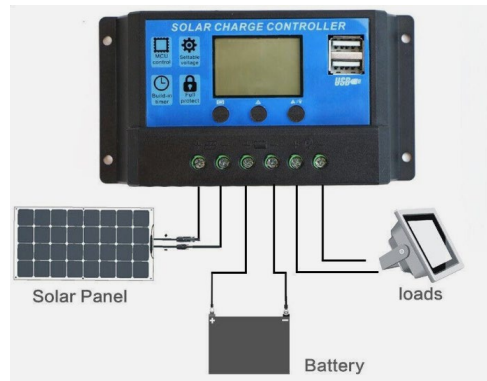
Fig. 32 Charge Controller Battery Connection with Load.

The usage unit is made up of the inverter that converts DC to AC. The generated current is clean enough to operate appliance and components. The off-grid system can also send the DC directly from the charge controller to the outlets or ports where DC loads exist (see Fig. 33).
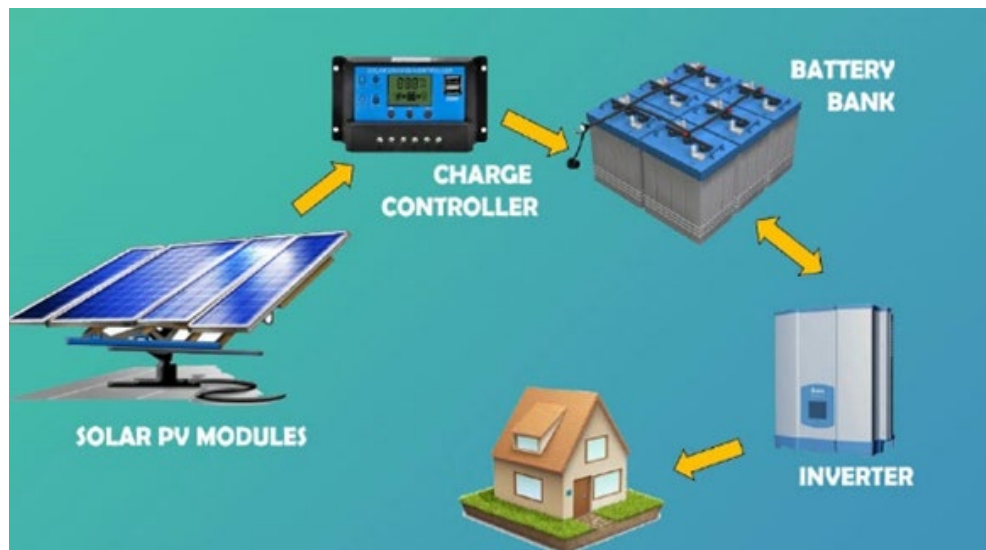
Fig. 33 Energy Flow [77].

5.   **The Off-Grid PV Power and Energy Production**

A PV system supplies energy in kilowatts hours (kWh) to the various loads [78]. One kilowatt hour equals 1000 watts of power used in one hour. The maximum current (I_{mp}) is the current below the short circuit current (I_{sc}), and (V_{mp}) is the maximum power point voltage just below the maximum power output point (P_{max}) of the I-V characteristics of the cell.

6.   **Sun Peak Hours and Energy Curve Productions (Summer)**

The energy production curve in Fig. 34 for the off-grid PV system was used to design and implement the prototype.
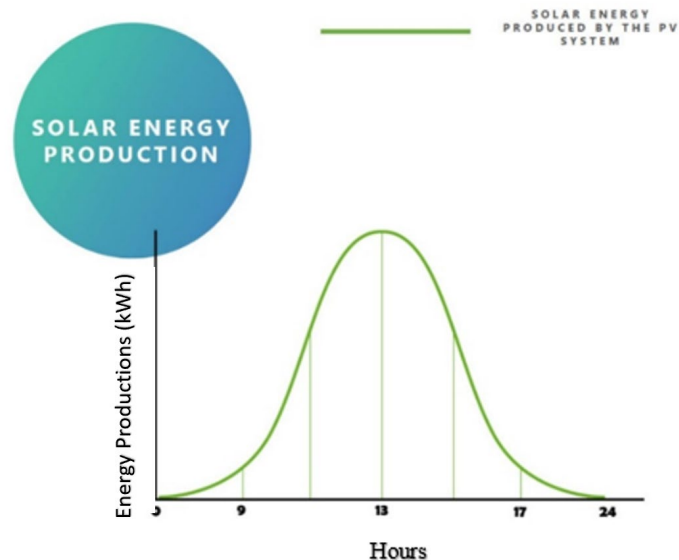
Fig. 34 Solar Energy Production [79].

The curve consisted of the solar energy production and the battery energy storage and usage. There was a 90 ° angle between the face of the solar panels and

the sun's position as it approached its lowest point in the sky [80]. Energy production decreased in direct proportion to the sun's position, clouds, and other atmospheric conditions. Fig. 35 shows the total energy produced by an off-grid PV system in a 24-hour time frame per day.
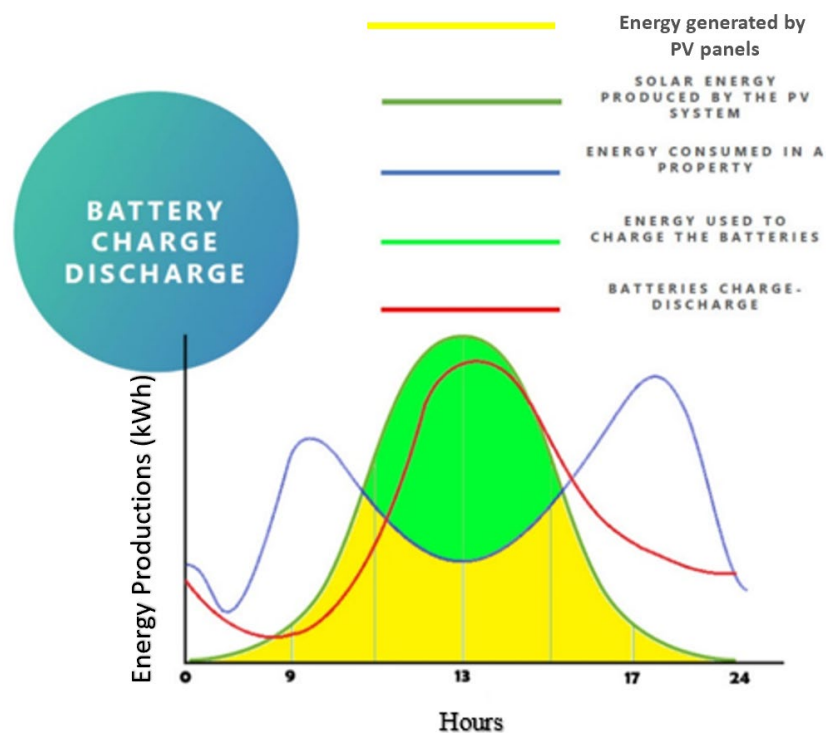
Fig. 35 Battery Charge and Discharge [81].

The blue curve represents the excess energy from the PV system stored in the batteries for nighttime usage. The blue curve starts above zero on the Y-axis of the energy production (kWh). The blue curve indicates the energy consumed by the load began to decline around 18.5 hours, and the PV system recharged the battery when sunlight returned. The yellow area under the curve is the energy

generated by the PV panels, and the green area is the excess energy used to charge the batteries. This process occurred around 10.5 hours to 15.5 hours. The red curve represents the period when the PV panels were not producing energy, and the load drew energy from the batteries.

7.   Peak Sun Hours (PSH) Computations

The Peak Sun Hours (PSH) is a crucial factor in determining the number of solar modules needed to build the prototype of the off-grid PV system [82]. If an area on the solar panel has an irradiance of 1000 W/m² and the sun hits that area consistently with the same value of irradiance for one hour then the PSH is the same. Ten hours of sunlight per day, maybe five to six hours on average of PSH, due to solar irradiance being inconsistent within the panel's area.

The location of the PV system in an area devoid of shading, must also be carefully considered. A website is used to assist with the computation of the parameters, and the components capacity ratings of the prototype. The PSH Web site results are shown in Fig. 36 [83].
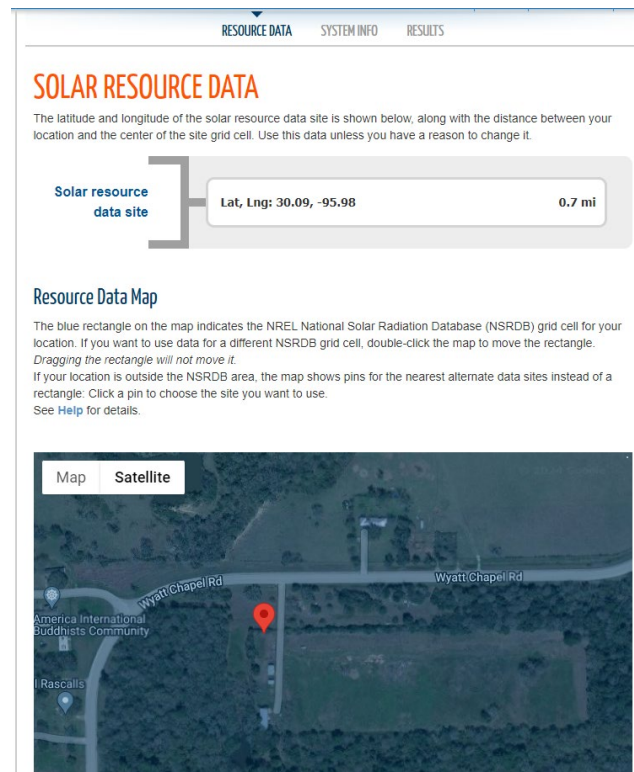
Fig. 36 PV Watts Calculator [84]

The zip code of the location is entered and the site presents its latitude and longitude. The site is displayed in two modes: 1) Map mode and 2) Satellite mode. The view in Fig. 36 is the satellite mode. When the system info tab is selected, the site provides various parameters to design and construct the prototype. A rooftop size estimator, bifacial, and efficiency rating are also listed in Fig. 37.

Fig. 37 PV Watts Calculator System Information (Info) [85].

When the Results tab is selected in the menu, the following parameters are displayed:

- DC System size (kW);

- Tilt Angle of the Solar Panel;

- Model Type of the Solar Panel;

- Azimuth Degree (Placement of the Solar Panels).

The total average PSH of Prairie View A&M University location is 5.30 kWh/m2 per day[86]. The total energy from the sun for Prairie View A&M University location is 5,872 kWh/m2 per year. The PV systems' solar radiation can vary each month, as shown in Fig. 38.

Fig. 38 PV Watts Calculator Site Parameters [87].

8.   PV Prototype Components Sizing

The steps for sizing and computation of the PV prototype components are as follows:

1. Determine the Load;

2. Size the Solar Array;

3. Determine the Battery Size;

4. Determine the Charge Controller Capacity Rating;

5. Determine the Inverter Size.

The first step is to determine the energy demand of each load. A small desktop fan, socket light bulb, and an oscilloscope are used to load the prototype.

The power consumption is listed in Table 9. The total wattage and watt-hour from the Table are 280W and 280 Wh.

TABLE 9

LOAD TOTALS FOR THE PV OFF-GRID SYSTEM

Load	Hours/Day	Wattage(W)	Load (Wh)
Light bulb	1 hrs	80	80
Fan	1 hrs	100	100
Oscilloscope	1 hrs	100	100

The tool from the website for larger projects was created by Unbound solar. This site is free, and computations are available for all electrical appliances and components [88].

The solar panels power generations by string:

String one, power: = (80 W/day)/(5.30 KWh/m)^2 x 96% = 15.97Watts

string two, power: = (100 W/day)/(5.30 KWh/m)^2 x   96% = 19.96Watts.

string three, power: =   ⟦(100 W/day)/(5.30 KWh/m) ^{2} x 96% = 19.96Watts.

Equation 3.2 is used to calculate the number of solar panels.

$$\text{Number of solar panels} = \frac{The\ power\ of\ the\ string}{Wattage\ of\ the\ Panel} \quad\text{.......................................} (3.2)$$

For String one, the number of panels = $\frac{15.97\ Watts}{100\ Watts}$ = 0.1597 (round up to one solar

panel). For Strings two and three, the number of panels = $\frac{19.96\ Watts}{100\ Watts}$ = 0.1996

(round up to 1 solar panel). The proposed prototype needs one solar panel or one

panel per charge controller and inverter to generate 0.01996kWh of energy for

strings two and three and 0.01597kWh for string one. Three charge controllers and

three inverters are used for the prototype. The next step is to select the battery

bank. Here, there are three essential steps to consider:

　　　1. Days of autonomy;

　　　2. Total Load;

　　　3. Maximum Depth of Charge (DoD).

The formula to size the battery bank is the following:

Battery Capacity (Ah) =

Total Watt-hours per day used by appliances　x　Days of autonomy ....(3.3)
　　　(0.85 x 0.6 x nominal battery voltage)

　　　The larger PV systems should have higher voltages and low Ampacity [89].

The calculations assume a 12V battery pack for use in the PV prototype.　The

prototype's current Amps Hour (Ah) capacity remains unchanged. It all depends

on the voltage of the prototype. For example, a 24-volt solar module will need a

24-volt battery bank as well. The batteries can be connected in series or parallel

configurations. To understand this concept in detail, [90] two batteries connected

in parallel, each with a rating of 6V at 45Ah, result in a voltage of 6V and an energy of 90Ah. The battery selected for the prototype was an Ever-start with a rating of 12V and 230CCA. For practical purposes, due to not being able to convert Cold Cranking Amps (CCA) to AH, it can be divided by 7.25 or use the data from Table 10.

TABLE 10

CONVERSION TABLE FOR THE BATTERIES

CCA Range	Approximate Ah Range
200-400 CCA	20-40 Ah
400-600 CCA	40-60 Ah
600-800 CCA	60-80 Ah
800-1000 CCA	80-100 Ah
Above 1000 CCA	Above 100 Ah

The Cold Cranking Current for the selected battery was equal to 230 CCA. From Table 10, the amp hour rating by interpolation is 23.0 Ah.

The energy of the prototype battery at any number of hours was determined using the Battery size calculator using Omni calculator web tool. The selected battery bank should be adequate to operate and deliver power to the load without sunshine. The environment will help a designer determine the size of the battery bank, knowing that the battery bank might be larger due to the days of autonomy.

The Depth of Discharge (DoD) for Lead-Acid batteries is about 40% to 60%, and the Lithium-ion is around 90% based on the manufacturer data [91]. Using

formula 3.3, and assuming days of autonomy is equal to 2.5, the load is 80 watts, and DoD for the systems is 40%, the Battery bank sizing in amp hours

$$= \frac{\text{(Total Watt–hours per day used by appliances)}}{\text{(0.85 x 0.6 x nominal battery voltage)}} \text{ x Days of autonomy}$$

$$= \frac{80}{.51x12} \text{ x 2 } = 156 \text{ Wh for string one.}$$

Similarity for strings two and three, each $= \frac{100W}{.51x12}$ x 2 = 196 Wh.

 The voltages for each battery in the bank are too equal to 80W/6.7A = 11.9 Volts, and for strings two and three, = 100W/8.3A = 12.04 V. The current for all strings was obtained from the online battery size calculator referenced above. A 12V battery bank was then selected. The remaining energy from the panels assisted in determining the number of prototype batteries. The solar charge controllers were rated based on the size of the solar array current and voltage. The rating of most MPPT charge controllers is 12,24 and 48 volts [92]. Twelve volts were used for this prototype. The amperage rating is typically in the range of 1 to 80 amps. The prototype had a 12-volt battery bank for a 140-watt system. The solar panel output power was 100W.

The controller's output current was 8.3 Amps. To account for bad weather conditions that might cause the PV module array to produce more power than its standard rating, the value needed to be increased by 25%. This adjustment brought the current value to 10.40 A. The selected charge controller for the prototype is shown in Fig. 39.

Fig. 39 Solar Charge Controller for the Prototype [93].

The rating was 12V/24V at 20A. It had multifunction features using the USB port. For larger PV systems, the current is increased by 20% to cover all environmental issues or concerns. The inverter supplied power directly to the load, and for future growth, it should have a power rating of ten times that of the PV systems. For example, if the size of the solar system is 200 watts, then the inverter should be 2000 watts or higher. Besides, if more panels are installed in the future, the extra capacity of the inverter will handle the PV power increase. Also, a bigger inverter can handle the following loads:

- Short-term overload;

- Loads that are 5 times higher than the rated continuous load.

Future load tests were performed to configure a three-phase circuit for a single phase and the lower wattage inverters were able to handle the flow of current due to the unbalanced loads produced by the tested equipment. The one that is recommended in this research is the KISAE SW1210 for the prototype. It can produce a very clean sinewave for PV array systems to generate clean power. The MPPT charge controllers can be used in 400-watt systems, but it is recommended

to use the hybrid that can perform both functions due to high voltage produced by panels if set up in parallel-series configurations. It was also discovered during data collection that the MPPT was designed to power on with the battery voltages only (see Fig. 40).

Fig. 40 Various type of Inverters [94].

Further research is needed to review and create a controller that will operate when it recognizes 12 volts applied. The prototype systems produced enough AC voltage that an oscilloscope was used to measure the output data points after the utility meter. The Power was reduced to 0.5 Watts after 30 minutes, and the inverters sounded an alarm signal. The battery began to fail due to the power generated by the solar panels being lower. The battery was about to reach its nominal charging voltage threshold of 11.6V. Dropping below this value affected the SOC of the battery. The final consumption during this period was 0.09 Watts.

9. Simulation of Power Flow for the Photovoltaic Prototype

The power systems network is very complex. Because of this complexity, it is additionally challenging to obtain valuable information on its hundreds of buses and transmission links [95]. In addition, solving the steady-state solutions of the power system network requires substantial mathematical computations. The load flow (LF) study of the electrical power system is called Power Flow analysis. The power companies and engineers use it for designing, controlling, planning, and future improvement of the electrical power network. The process can derive the voltage magnitude, phase angles, and reactive(Q) and active power (P) flows and losses of the power system network under various loads and generation conditions [96]. The Power-World Simulator software is used to determine and present examples of software implementation of the approaches.

In recent years, numerous mathematical analysis approaches have been used to solve power load analysis problems [97]. The continuous increase in power demand leads to a vast increase in the dimension of the grid network [98]. This abrupt increase makes it more challenging for numerical mathematical approaches to converge to the correct answer without the iteration process. The following sections review the Newton-Raphson method.

10. Simulation of Power Flow for the PV Solar Prototype

The prototype for a central station PV system with a working solar cell at the point of interconnection that is available in the market consists of a customer

node labeled as a bus, a 15KW Hybrid inverter, and a distribution line, as shown in Fig. 41 [99].
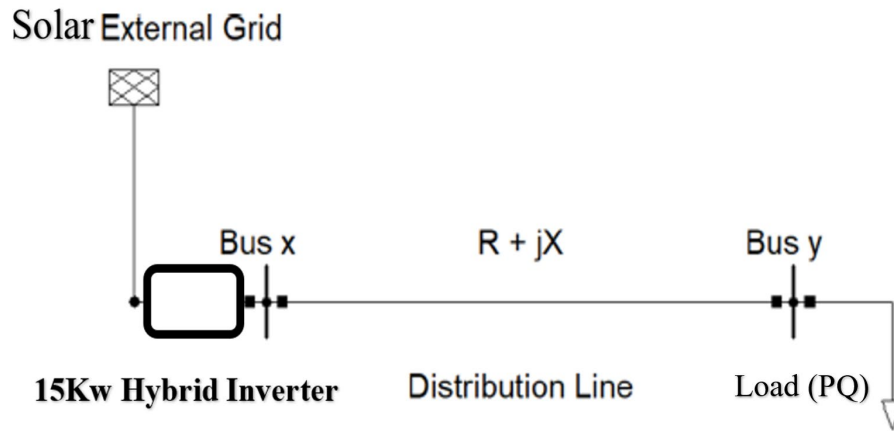
Fig. 41 Ideal Solar Cell [100].

The voltage control bus, known as the (PV) bus, is shown as bus x. A low voltage exists the hybrid inverter and the load. The load apparent power is presented as $(S_L) = P_L + jQ_L$.. (3.5)

P_L represents the active power and Q_L is the reactive power of the load for the system. The Line current is derived by:

$$I = \left(\frac{S_{xy}}{V_y}\right)^* = \frac{P_{xy} - Q_{xy}}{V_y^*}$$ .... (3.6)

V_y is the nodal voltage, and S_{xy} is the complex power that flows through the line from bus x to bus y. The complex power at bus (i) that corresponds to the injection on the kth iteration is derived by:

$$S_i = P_i + jQ_i \text{ where } (\ i = 1....N) \ \text{...} \ (3.7)$$

S_i is the injection of the apparent power at the *n*th node. The current at that injection of *k*th iteration is derived by:

$$I_i^k = \left(\frac{P_i^k + jQ_i^k}{V_i^k}\right)^* = \frac{P_i^k - jQ_i^k}{(V_i^k)_*} \text{...} \ (3.8)$$

The voltage at bus y is derived as $V_y = V_x - I\ (R_{xy} + jX_{xy})$ .... (3.9)

The voltage at bus i at the kth iteration is given by $V_i^k = V_x^k - I^k(R_i + jX_i)$ .... (3.10)

Now, V_x *is* the voltage at bus x, and V_i^k is the voltage at bus-*(i)* at the kth iteration

and impedance of the line $Z = R_i + jX_i$, so $V_i^k = V_x - Z(\ I_i^k)$ .... (3.11)

In a transmission system, the total power loss is $S_{ij} = \ VI^*$ .... (3.12)

The active power loss is given by $\left(\frac{Pi}{Vi}\right)^2 R_{ij}$ .... (3.13)

The reactive power loss is given by $\left(\frac{Qi}{Vi}\right)^2 X_{ij}$ .... (3.14)

11.   PV Load Flow Analysis using Newton Raphson - Power World

The Newton-Raphson method was used to analyze a three-bus system shown in Fig. 42. The three-bus system consisted of three transmission lines, and three sets of eight Solar panels connected in series.
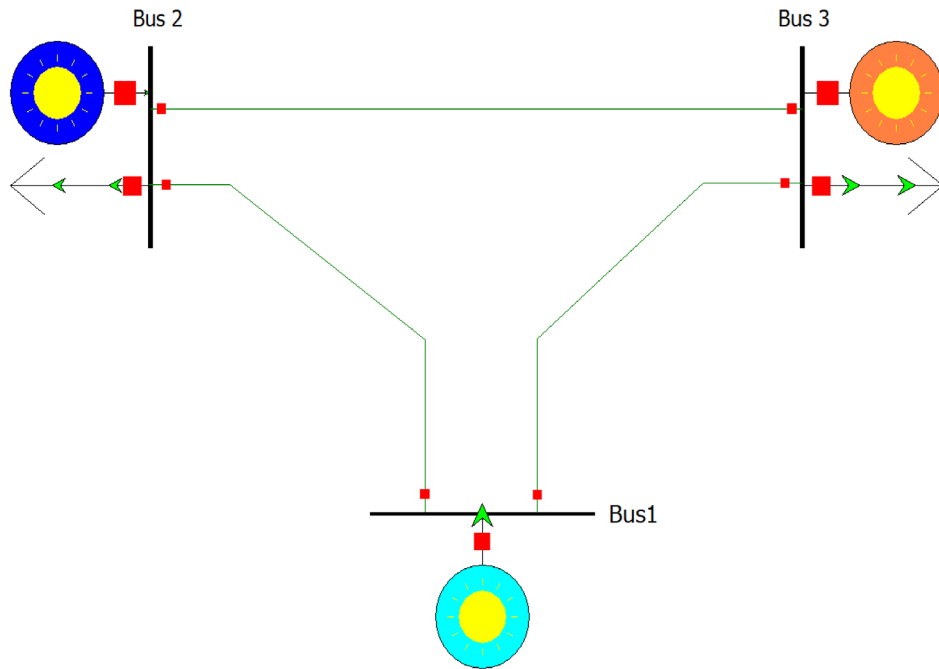
Fig. 42 Diagram of the PV Solar 3-bus system [101].

The relevant equations for the power network in polar coordinates at bus – (i) are as follows:

$$P_i = P_{GI} - P_{DI} = \sum_{k=1}^{N} |V_i||V_k| \left(G_{ik} \cos\delta_{ik} + B_{ik} \sin\delta_{ik} \right) \quad \text{........................ (3.15)}$$

$$Q_i = Q_{GI} - Q_{DI} = \sum_{k=1}^{N} |V_i||V_k| \left(G_{ik} \sin\delta_{ik} + B_{ik} \cos\delta_{ik} \right) \text{............................(3.16)}$$

In Fig. 42 above, bus one is the slack bus, and the given line impedance is 0.1 per unit (p.u.). These equations are used to calculate bus 2 voltage, magnitude, and angle [102]. Therefore, assume an initial flat start of $V_{21} \angle 0^o$ p.u. and simplify equation 3.10 by inserting the following values:

$$|V_1| = 1, \delta_1 = 0, B_{ik} = 10, B_{ii} = -10, \text{ and } G_{ik} = G_{ii} = 0.$$

The real power injections at bus 2 and an estimated value for $|V_2|$ and δ_2 are obtained as:

$$P_{2calc} = |V_2| \, 10\sin\delta_2 \quad \text{...} \quad (3.17)$$

$$Q_{2calc} = |V_2| \, (-10)\cos\delta_2 + 10|V_2|^2$$

Now we can define the function:

$$F(x) = \begin{bmatrix} f_1 & (x) \\ f_2 & (x) \end{bmatrix} = \begin{vmatrix} P_{2calc}(x) & -2 \\ Q_{2calc}(x) & -Q_2 \end{vmatrix}$$

Where $(P_{cal} - P)$ is the mismatch between the real and reactive power, this above equation will calculate the estimated values of $|V_2|$ and δ_2. To calculate the roots of f(x), we will define the i_{th} iteration as:

$$X^{(i+1)} = x^{(i)} - J^{-1}\,(f(x)) \mid x^{(i)} f(x^{(i)}) \quad \text{..} \quad (3.18)$$

The Jacobian for this 3-bus system is as follows:

$$J(f(x))|_{x^{(i)}} = \begin{bmatrix} \frac{f_1(x)}{d\delta_2} & \frac{f_1(x)}{d_{|V_2|}} \\ \frac{f_2(x)}{d\delta_2} & \frac{f_2(x)}{d_{|V_2|}} \end{bmatrix}_{x^{(i)}}$$

For the first iteration, the study initially guessed $x\,(0) = \begin{pmatrix} 0 \\ 1 \end{pmatrix}$. The calculated $f(x(0)) = \begin{pmatrix} 3 \\ 1 \end{pmatrix}$.

The inverse of the Jacobian matrix is:

$$J^{-1}(f(x))|_{x^{(i)}} = \begin{bmatrix} \frac{f_1(x)}{d\delta_2} & \frac{f_1(x)}{d_{|V_2|}} \\ \frac{f_2(x)}{d\delta_2} & \frac{f_2(x)}{d_{|V_2|}} \end{bmatrix}_{x^{(i)}}^{-1}$$

The PowerWorld simulator is used for the simulation and analysis.

Various cases for different PV systems give simulated output data. Table 11 is for

bus voltage, generation & load data for case one.

TABLE 11

FOR CASE ONE: BUS VOLTAGES & LOAD DATA

Bus No.	Bus Code	Voltage (P.U.)	Generation		Load	
			MW	MVAR	MW	MVAR
1	(Slack)	1.04	0	0	0	0
2	(PQ)	1.025	0	0	5	0
3	(PQ)	1.025	0	0	25	0

The reactive power on the three buses is assumed to equal zero. This resulting

data was analyzed under contingencies such as shading and full sunlight

conditions [103].

Table 12 is the corresponding line data.

TABLE 12

LINE /BRANCH DATA THREE-BUS SYSTEM

Line From	Line To	R	X
1	2	0.004700	0.0474
1	3	0.004700	0.0474
2	3	0.006200	0.0632

Table 12 tabulates the N-R method results for case 1. The results indicate the two

power values, reactive power and real power, for the slack bus, the line losses, and

the voltage magnitudes. The base results for Case 1 using Newton Raphson (N-R)

are displayed in Fig. 43.
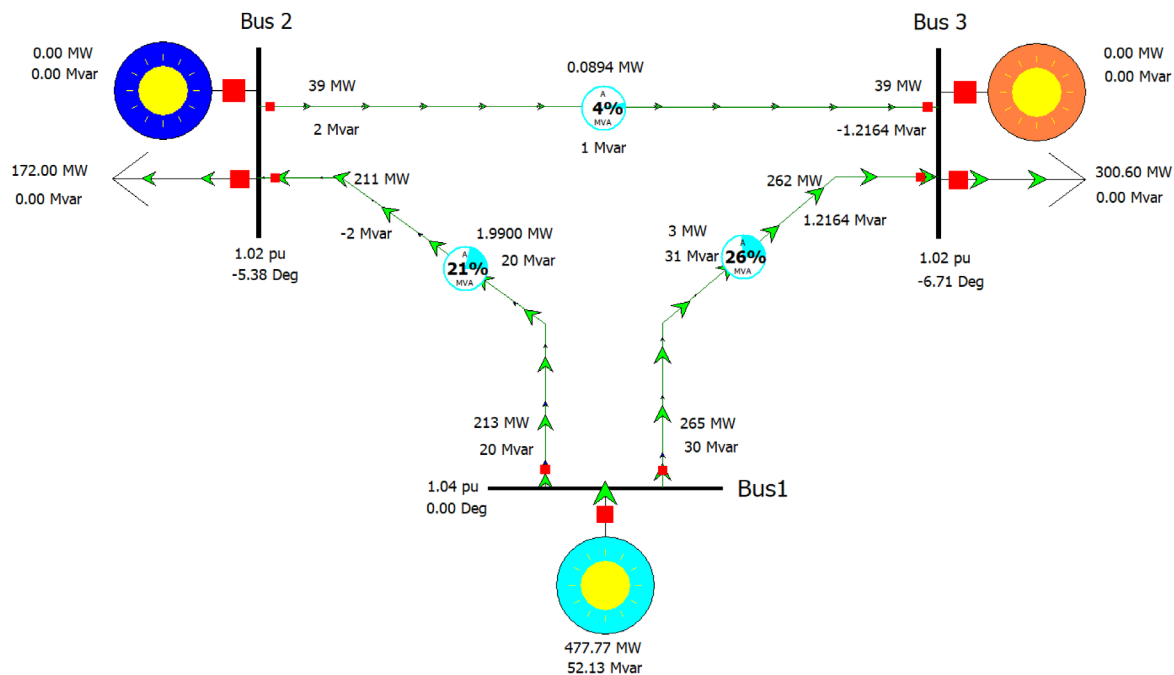
Fig. 43 Slack bus injection for Case one [104].

The real power for the slack bus was 30.02 MW, and the reactive power was 0.23 MVAR. The line losses are shown in Table 13.

TABLE 13

LINE LOSS AND SLACK BUS RESULTS FOR CASE ONE

Bus Nodes	Real Power (S) Losses	Reactive Power (Q) Losses	Real Reactive	
			(MW)	(MVAR)
1 to 3	3 MW	31 MVAR	265	30
1 to 2	1.99 MW	20 MVAR	213	20
2 to 3	0.0894 MW	1 MVAR	39	2

The largest load of 26% was transmitted in the line between bus one and bus two. This occurred because the generations on buses two and three were experiencing full shading, and the slack bus supplied power to the entire system. The power factor was assumed and set to be 0.9 and was leading. The voltages for buses two and three were within 1.02 to 1.04 (p.u.) for case one. Case two again attempted to perform a load study on when the generation on bus three was experiencing shading during peak time. The PV source at bus 1 generated 150MW, as shown in previous Fig. 43 and the data in Table 11. Bus one was the slack bus of case two, shown in Table 14. The results for case two are shown in Table 14. In Case two, the PV source at buses one, two, and three provided power for all three loads.

TABLE 14

LINE / BRANCH DATA OF THREE – BUS SYSTEM

Bus No.	Bus Code	Voltage (P.U.)	Generation		Load	
			MW	MVAR	MW	MVAR
1	(Slack)	1.040	0	0	0	0
2	(PV)	1.025	70	0	172	0
3	(PV)	1.025	38.50	0	300.60	0

The generation's partial shading was at bus two and bus three. The line losses for case three are shown in Table 15.

TABLE 15

LINE LOSS AND SLACK BUS RESULTS FOR CASE 2

Bus Nodes	Real Power (S) Losses	Reactive Power (Q) Losses	Real Reactive (MW)	(MVAR)
1 to 2	1.0014 MW	10 MVAR	151	10
1 to 3	2 MW	21MVAR	216	20
2 to 3	0.1367 MW	1 MVAR	48	2

The line loads comparison in case one showed a decrease of six percent transmission loss from bus one to two, and the supply to bus two was 150MW. The remaining 48MW flowed to supplement the supply to the load of 300.60MW at bus three.

The real power was 70 MW for bus two and 38.50 MW for bus three. The reactive powers on the buses were set to zero. Fig. 44 shows case two in which the real power and reactive power at the slack bus decreased to five percent and seven percent, respectively.
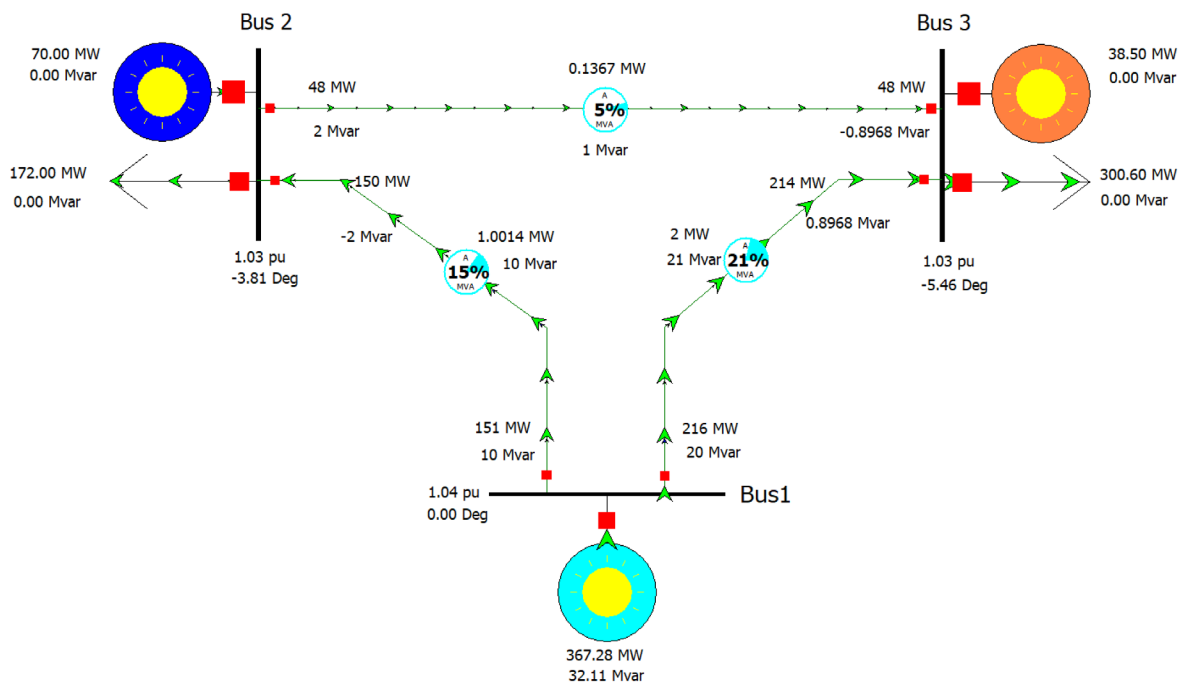
Fig. 44: Slack Bus injection at Bus one and two Case two [105].

In case three, the solar PVs at buses one, two, and three supplied power to all three loads. Fig. 45 shows all the buses supplying the loads for cas3 three.
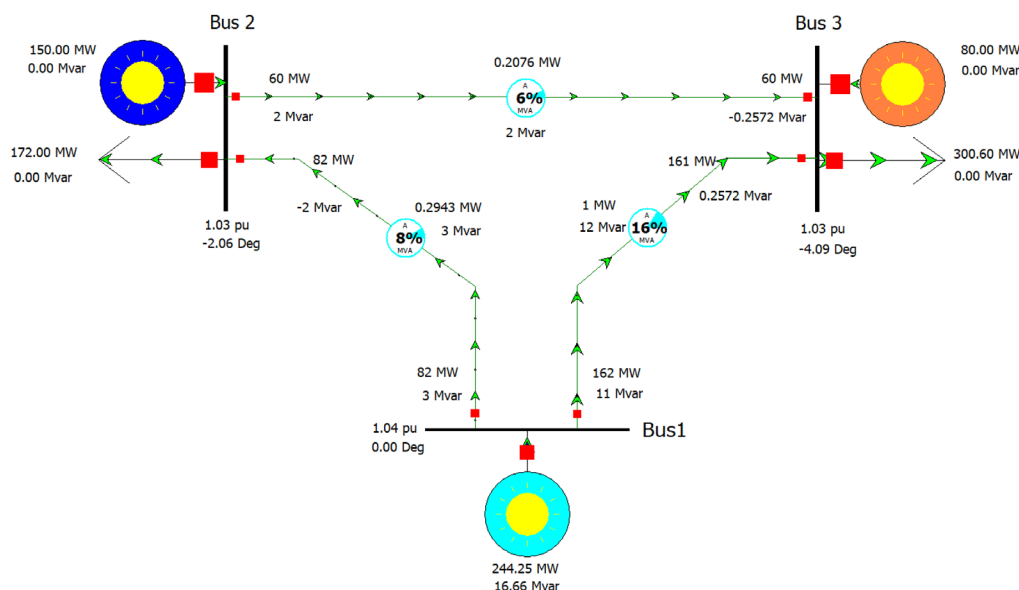
Fig. 45 Case three Bus simulation for the Slack Bus injection at Bus one, two and three Case two [106].

The data for case three is shown in Table 14. The Power Load Flow solutions was obtained from all the case verified the capacity of the PV generation. The generation was varied to determine its optimality and cost efficiency that improved the congestion flow and to discover if there were any effects on the transmission lines. The line data is shown in Table 16.

TABLE 16

LINE / BRANCH DATA OF NINE-BUS SYSTEM CASE THREE

Bus No.	Bus Code	Voltage (P.U.)	Generation		Load	
			MW	MVAR	MW	MVAR
1	(Slack)	1.04	0	0	0	0
2	(PV)	1.027	150	0	172	0
3	(PV)	1.027	80	0	300.6	0

It was observed that the power losses in the line and the load flows can be obtained through simulations. See Table 17.

TABLE 17

LINE /LOSS AND SLACK BUS RESULTS FOR CASE THREE

Bus Nodes	Real Power (S)	Reactive Power (Q)	Real Reactive	
			(MW)	(MVAR)
1 to 2	0.2943 MW	3 MVAR	82	3
1 to 3	1 MW	12 MVAR	162	11
2 to 3	.2036 MW	2 MVAR	60	2

The scenarios of the cases were used to determine the risk factors for each section of the PV arrays. The three-bus system detected the load bus with the minimum voltage and the maximum reactive power demand. It was evident from each case that the real and reactive power improved for each case, and power was produced and generated on the grid. The load flows' final results revealed the compensation of both the real and reactive powers through the network.

12.   AC and DC Power Converters

In power electronics, there are four types of converters: AC to AC, DC to DC, AC to DC, and DC to AC. This study focused on DC to DC and DC to AC converters. The PV system used MPPT or solar charge controller. This study focused on DC-

to-DC voltages because the PV panels produced a higher DC voltage, and the converter converted it to a lower voltage to charge the storage batteries [107].

13.   The DC to DC Buck Converter

The Buck converter analysis as shown in Fig. 46, steps down the DC input voltages.
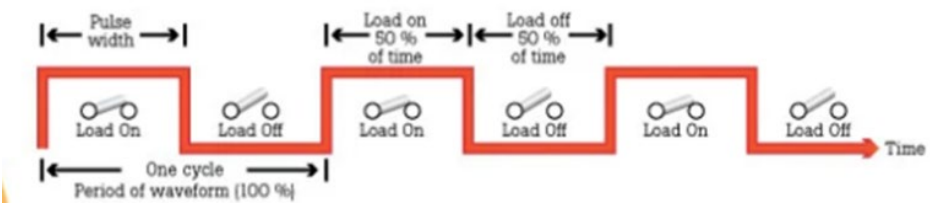
Fig. 46. Duty Cycle Ratio with respect to time [108].

The buck converter is very popular in PV application. When a high frequency of 10kHz or higher is used in the circuit, the switch turns on and off periodically. The duty ratio (D) equation of the switch is:

$$D = \frac{time\ on}{period} = \frac{T_{on}}{T} = T_{on}\ x\ switching\ frequency, f_s \dots\dots\dots\dots\dots (3.18)$$

The MPPT charge controller will generate a large amount of power at the highest point. The power equation can be derived by equation 3.19:

Power(P) = Voltage(V) * Current(I)... (3.19)

The converter operated on time, as the switch was closed. When a high frequency of 10kHz or higher was used in the circuit, the switch turned on and off periodically. Equation 3.19 of the switch is

$$Duty\ ratio\ D = \frac{time\ on}{period}\dots\dots\dots\dots\dots\dots\dots\dots\dots\dots\dots\dots\dots\dots\dots (3.20)$$

$$= \ \frac{T_{on}}{T} = T_{on} \ x \ switching \ frequency, f_s$$

Fig. 46 shows the pulse width measured when the switch was on. The converter was designed to decrease the DC bus voltage to the battery charge voltage. The converter operated when the switch was closed. This is shown in Fig. 47.
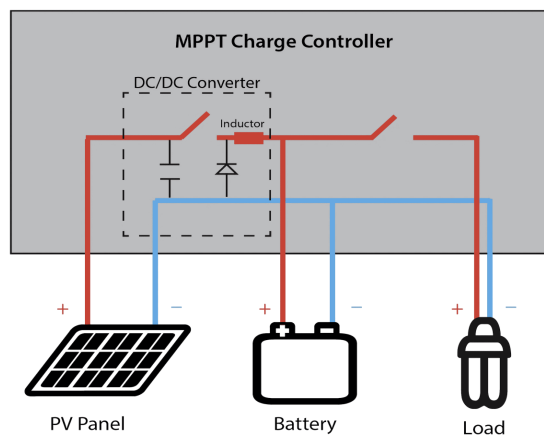
Fig. 47 MPPT Charge Controller Diagram [109].

The PV dc source charged the inductor as well as the capacitor, then current flowed throughout the circuit [110]. The diode allowed the current to charge the capacitor and prevented the flow of current back into the inductor. The purpose of this capacitor in the circuit is to maintain a relatively stable output voltage across the load resistor [111]. The buck converter has some advantages. It reduced the voltages at the input, but it stepped up the current. Unlike other circuits such as voltage divider circuits that reduce the voltages and dissipate power as heat,

the buck converter does the opposite. The inductor current is derived by equation 3.20:pplication [112].

$$i_L\,(t+T) = i_L(t) \dots\dots\dots\dots\dots\dots\dots\dots\dots\dots\dots\dots\dots\dots\dots\dots\dots\dots\dots\dots (3.21)$$

And when the average inductor voltage is zero:

$$V_L = \frac{1}{T}\int_o^{t+T} V_L(\lambda)\,d\lambda = 0 \dots\dots\dots\dots\dots\dots\dots\dots\dots\dots\dots\dots\dots\dots\dots (3.22)$$

The capacitor current average is zero,

$$I_c = \frac{1}{T}\int_o^{t+T} I_C(\lambda)\,d\lambda = 0 \dots\dots\dots\dots\dots\dots\dots\dots\dots\dots\dots\dots\dots\dots\dots (3.23)$$

The power associated with source is the same as the load, plus the losses.

$$P_s = P_o \text{ which ideal} \qquad P_s = P_o + \text{losses non-ideal [113]}.$$

At the closed state of the switch, $V_L = V_{out} - V_{in}$. In this way proves that this type of circuit reduces the voltage of the circuit (see Fig. 58).

$$V_S = V_{in}$$

$$V_l = V_S - V_0 = L\frac{di_L}{dt}\dots\dots\dots\dots\dots\dots\dots\dots\dots\dots\dots\dots\dots\dots\dots\dots\dots\dots (3.24)$$

To solve for $\qquad\qquad\qquad \dfrac{di_L}{dt} = \dfrac{V_s - V_o}{L}$

The positive current is derived by taking the derivative:

$$\frac{di_L}{dt} = \frac{\Delta i_L}{\Delta t} = \frac{\Delta i_L}{DT} = \frac{V_s - V_o}{L}$$

And to solve for Δi_L

$$\Delta i_L(closed) = (\frac{V_s - V_o}{L}\,)\,DT \dots\dots\dots\dots\dots\dots\dots\dots\dots\dots\dots\dots\dots\dots\dots (3.25)$$

The current across the capacitor will change (see Fig. 48).
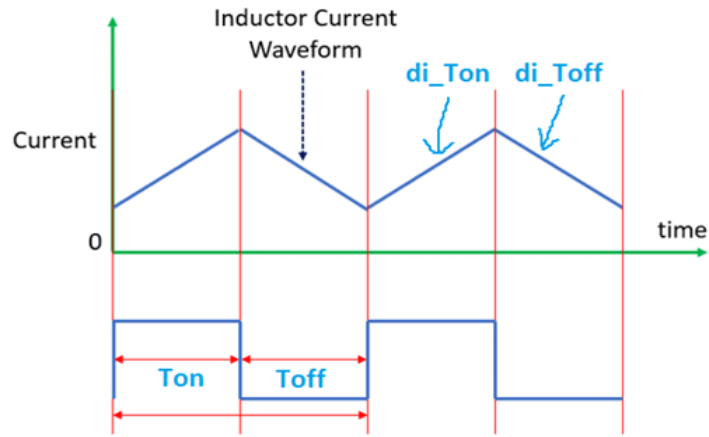
Fig. 48 Buck Converter Circuit and Switch Duty Ratio [114].

The voltage across the inductor is:

$$V_l = -V_0 = L\frac{di_L}{dt}$$ .... (3.26)

To solve for $L\frac{di_L}{dt} = \frac{-V_o}{L}$

When the inductor value was negative, this caused the current to decrease, and that change is represented by equation 3.27:

$$\frac{\Delta i_L}{\Delta t} = \frac{\Delta i_L}{(1-D)T} = -\frac{V_o}{L}$$ .... (3.27)

$$\Delta i_{L_{open}} = -\frac{V_o}{L}(1-D)T$$

And to solve for V_o, using the previous equations:

$$(\frac{V_s-V_o}{L})(DT) - \frac{V_o}{L}(1-D)T = 0$$ .... (.3.28)

$$V_o = V_s D$$

The average current equation is:

$$I_L = I_R = \frac{V_o}{R} \qquad \text{... (3.29)}$$

And the inductor minimum is:

$$L_{min} \quad \frac{(1-D)R}{2f} \qquad \text{... (3.30)}$$

Where f is the frequency and L_{min} is required minimum conditions. Now the power from the source must be equal to output voltage across the load resistor:

$$P_s = P_o$$

$$V_s I_s = V_o I_o$$

$$\frac{V_o}{V_s} = \frac{I_s}{I_o}$$

The formula for this converter is like a dc transformer equivalent circuit.

To determine the correct capacitance, the capacitor current is indicated in Fig. 52. The equations are as follows:

$$i_c = i_L - i_R \text{.. (3.31)}$$

The charge of the capacitance:

$$Q = CV_o$$

$$\Delta Q = C\Delta V_o$$

$$\Delta V_o = \Delta \frac{Q}{C}$$

the required capacitance: $C = \dfrac{1-D}{8L(\Delta^{V_o}/_{V_o}) f^2}$ .... (3.32)

The output voltages depend on two effects, the voltages going in the circuit, and the duty cycle. The duty cycle is equal

to: $\frac{t_{on}}{T}$. Where t_{on} is when the switch is divide by the period, T.

If the circuit is on for 1 ms and off for 3 ms , then the Period T is time for one complete cycle would be 4 ms and the

Duty Cycle (D) $= \frac{t_{on}}{T}$ D $= \frac{1\,ms}{4\,ms} = .25 = 25$

Now that D is known, the output voltage can be calculated. The formula for the output voltages is:

$V_{out} = V_{in} \times (D)$. Therefore:

The output voltage can be controlled by adjusting the duty cycle. The Buck converter was implemented into the prototype designed to control the DC from the PV panels, and the input voltage was assumed to be equal to 10 volts. A current of 4 amps flowing through the buck converter and a 555 timer was added to the circuit with a duty cycle of 50% [115]. The output voltages were calculated, the current was assumed, and the buck converter had an efficiency of 80%. On the first initial step, the Power was derived to be, $P_{in = 10 \times 5} = 50\,W$

Then the $V_{out} = V_{in} \times (D)$.

$$V_{out} = 10 \times 50\%$$

$$V_{out} = 5v$$

Now that the efficiency of the circuit is given at 80%, output power can be derived [116]. So, the output is

The output power, P_{out} is equal to 0.8 x 50 W;

$$V_{out} = 24\ x\ .25 \text{ and } V_{out} = 6v$$

Now that the efficiency of the circuit is given at 80%, output power can be derived [116]. So, the output is

P_{out} is equal to $0.8 \, x \, 50 \, W$;

$$P_{out} = 40 \, W$$

Then $P_{out} = V \, x \, I.$

$$I_{out} = \frac{P_{out}}{V}$$

$$I_{out} = \frac{40 \, W}{5 \, v}$$

$$I_{out} = 8 \, amps$$

The Buck converter circuit's voltage decreased, but the current increased. The voltage decreased by a factor of two, and the current increased by a factor of two. The circuit was not rated at 100 % efficiency due to voltage loss across the resistance of the circuit, and the voltage drops across the diodes [117].

14. Testing Conditions for PV Panels

The sunlight shined on a certain area of the solar panels. In Fig. 54, some of the crucial points are as follows:

1. The Azimuth;

2. The altitude;

3. The panel is installed towards the south;

4. How long is that area covered by Solar irradiance.

The solar panels manufactory ratings for the prototype is 200 W/m2 at 17.6Volts. The PV module power was equal to the *Total consumption average daily* divide by the *irradiance*yieldfactor*. This information was considered for the prototype as the data was collected from the panels, and research will continue for future studies. Testing was done using the panels at the site to verify the parameters provided by the manufacturer that are located on the back of the panels.

The first step was to collect the PV array datasheet specifications for the Standard Testing Conditions and the Worst Testing Conditions. The conditions for this study for the solar irradiance were:

- The Standard Testing Condition (STC) of 1000 $W/_{m^2}$ @ 25°.

- The Worst Testing Condition (WTC) of 50 $W/_{m^2}$ @ 25°.

The PV cells had multiple voltage ratings which were determined under the standard test conditions (STC) or the worst-case condition (WTC) [118]. One of the ratings was the maximum power voltage (V_{mp}) which was the operating voltage of the solar panel. It dropped significantly at high temperatures (see Fig. 49) and will vary slightly depending on the amount of light from the sun.

ELECTRICAL DATA (STC)

Peak Power Watts-P_{MAX} (Wp)*	470
Power Tolerance-P_{MAX} (W)	
Maximum Power Voltage-V_{MPP} (V)	36.1
Maximum Power Current-I_{MPP} (A)	13.02
Open Circuit Voltage-V_{OC} (V)	43.0
Short Circuit Current-I_{SC} (A)	13.73
Module Efficiency η m (%)	20.0

STC: Irradiance 1000W/m², Cell Temperature 25°C, Air Mass AM1.5.
*Measuring tolerance: ±3%.

Fig. 49 PV Cell Datasheet [119].

For the tracking to operate smoothly, the cells (V_{mp}) must always be several volts greater than the battery charge voltage in every condition, including elevated temperatures. The second rating was the open-circuit voltage (V_{oc}), which is always higher than the V_{mp}. The V_{oc} also decreased at a higher temperature but significantly increased at a lower temperature.

The data sheet for the PV array had the following settings:

Standard Testing Condition   **Worst Testing Condition**

$1000 \; W/m^2$ @ 25° ; $50 \; W/m^2$ @ 25°;

$P_{mps} = 1800 \; W$; $P_{mpw} = 0.005$;

$V_{mps} = 106.5 \; V$; $V_{wps} = 106.5 \; V$;

$I_{mps} = 16.9 \; A$. $I_{wps} = 16.9 \; A$.

15. Standard Testing Conditions (STC) of the PV Module

For standard testing conditions, the following steps are implemented:

a. Data from the Solar Panel module is added to the PSIM software;

b. Build the circuit using PSIM;

c. Run STC simulations;

d. Compare results

16. Worst Testing Condition (Shading & No sunlight) of PV Module

The procedures below are essential:

a. Adjust the S value for the Solar panel array, and choose any three.

b. Build the circuit.

c. Run the WTC simulations.

Fig. 50 shows the current and voltage in the simulation situation. Fig. 50 is a breakdown description of its PV energy conversion characteristics.
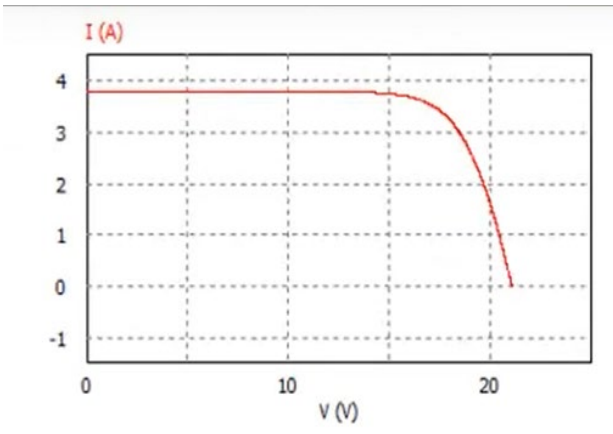
Fig. 50 PSIM IV Characteristic Curve [120].

The P_{max} is critical in deriving the device's performance results and the panels' efficiency. The prototype project demonstrates the PV panel parameters using the practical prototype in PSIM software. The entire process of modeling the solar module prototype and setting up the PV array is even suited for anyone who has a basic level of comprehension of the application. Once the final calculations were done, the values were tested with simulations (see Fig. 51).

Electrical Characteristics

SOLAR CELLS	POLY-CRYSTALLINE 156 × 156 MM 72 PCS. (6×12) – 4 BUS BARS				
Maximum Power (Pmax)	300 Wp	305 Wp	310 Wp	315 Wp	320 Wp
Voltage at Pmax (Vmp)	37.23 V	37.24 V	37.32 V	37.46 V	37.62 V
Current at Pmax (Imp)	8.06 A	8.19 A	8.31 A	8.41 A	8.51 A
Open-Circuit Voltage (Voc)	44.71 V	44.72 V	44.76 V	44.82 V	44.84 V
Short-Circuit Current (Isc)	8.947 A	9.094 A	9.234 A	9.371 A	9.515 A
Maximum System Voltage (V DC)	1000 V (iec), 600 V (UL)				
Cell Efficiency	17.46 %	17.75 %	18.05 %	18.34 %	18.63 %
Module Efficiency	15.46 %	15.72 %	15.98 %	16.23 %	16.49 %
Number of By-pass Diodes	6				
Maximum Series Fuse	15 A				
Temperature Coefficient of Pmax	- 0.45 % / °C				
Temperature Coefficient of Voc	- 0.34 % / °C				
Temperature Coefficient of Isc	- 0.05 % / °C				
Nominal Operating Cell Temperature	47 ± 2 °C				

Fig. 51 Solar Panel PSIM configurations [121].

17.   PSIM I-V Curve of a PV CELL Characteristics

The cells are designed to be placed outdoors to generate electric power from the sun. When there is a load, the current flows within the cells. The output voltage cannot go beyond the value of the forward bias voltage of the diode. The actual value of this diode is between 0.5 to 0.7 volts. The panels consisted of several modules fastened to a common metal frame.   Fig. 52 shows the panels set up in series.
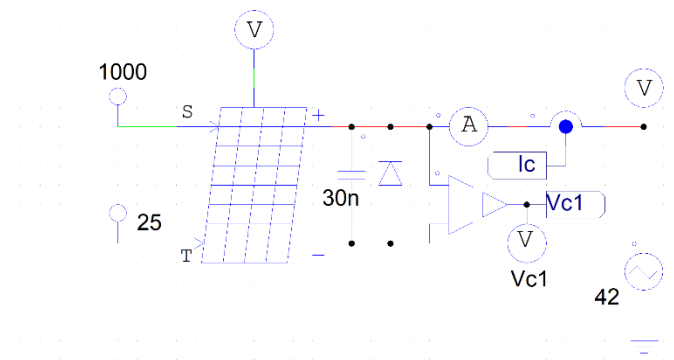
Fig. 52 Solar cell PSIM schematic [122].

PSIM was used to create the schematic. All values from the datasheet were entered. For this physical module, the temperature is rated at 25 ° C and the standard testing condition is 1000 $W/_{m^2}$ [123].

18.   PSIM Thin File Models

Fig. 53 shows the solar cell array module for the i-v characteristics. The module is simple to use because a user inserts any manufacturer's data from the datasheet.
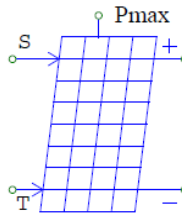
Fig. 53 PSIM Thin File Model [124].

This study focused on the Physical prototype due to the environment of the designed area. There are terminal nodes, positive and negative. "S" is the light concentration input (in W/m2), and "T" is the ambient temperature input (in °C). P_{max} is the operating conditions, as shown in Fig. 54.
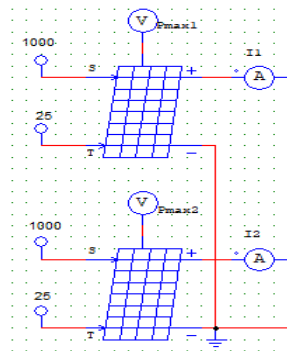
Fig. 54 Solar Array Configured in Series [125].

19.   The PSIM Simulation of Solar Panel Characteristics

This study used PSIM software to pull the characteristics components and generated an I-V curve waveform to compare the results with rated parameters. The curves study was very critical so that the prototype could generate the maximum power using the PV cell characteristics. A prototype model of the PV cell is shown in Fig. 55.
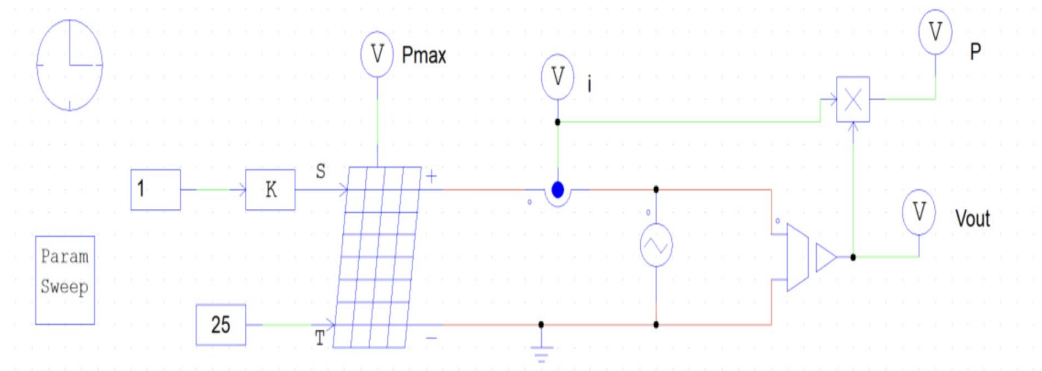
Fig. 55 I-V Solar Panel Characteristics using PSIM [126].

The schematic is used to study the proposed prototype and the model design so that the system can be optimized for the maximum power point to ensure that the design systems will run efficiently. All components and behaviors were monitored during operation in the land field. There are some key functions that must be considered:

- The total irradiance environment on the PV Cell;

- The temperature of PV cell;

- The spectral content of the irradiance;

- The input parameters and Cell Array setup: Series or Parallel.

The results present the values of both the series equivalent and parallel resistances. PV cell IV characteristics were done with a standard light source and temperature controller. The test was done in PSIM and used the sunlight as well. The results are shown in Fig. 56.
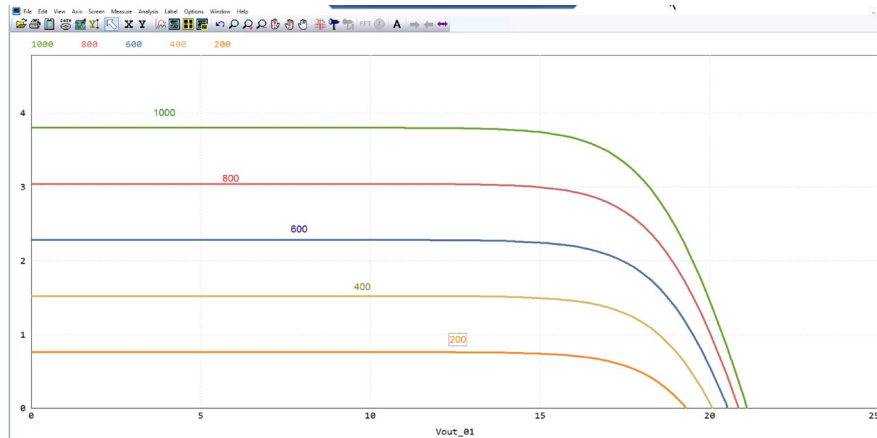
Fig. 56 IV Characteristics Results using PSIM [127].

The reading 200 is when the system is about to turn on and the concept is to run the systems so that it reaches its maximum point from the sunlight as it approaches its highest peak. The components of the circuit were set with proportional blocks to vary the irradiance and an initiative point using a constant value. A voltage sensor and a multiplier were used to calculate the power flow through the system. The results for the String A of the system were very controversial. The results can turn out to be a modified sine wave (see Fig. 57).
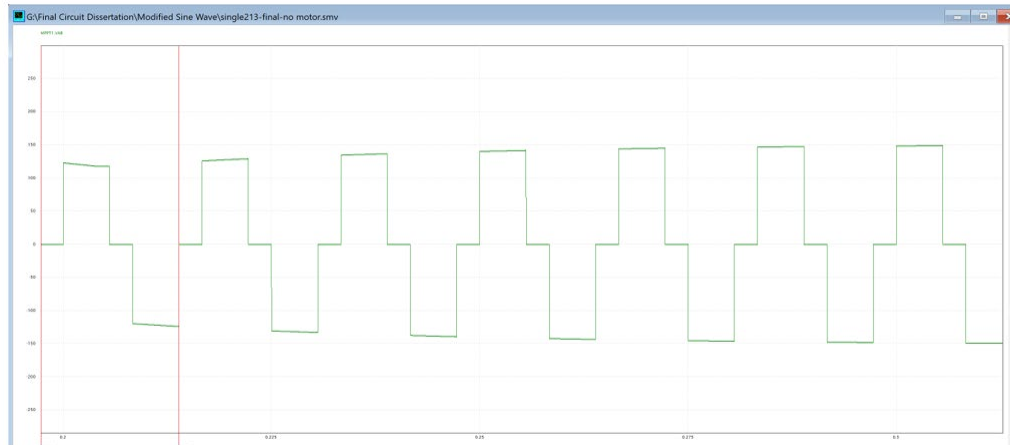
Fig. 57 Prototype Modified Sine Wave [128].

When purchasing the inverters, consider that the output of the inverter must be a pure sine wave to operate electronics properly. An inductor and capacitor (LC) filter were added to clean up the sine wave, which is discussed in the next sections. Most inverters are classified as pure sinewave. The demand for sinewave inverters is increasing rapidly [129]. The modified sine wave results in Fig. 58 were unsatisfactory and did not transition directly from positive to negative maxima. The output results displayed a zero level at a period of the graph with respect to time, which gives dead spots between the positive and negative cycles. There are many techniques to correct this output and to generate a pure sinewave in alternating current. However, in this project, SPWM was employed to regulate the switching of the MOSFET full bridge. This provided clean power AC output after incorporating an LC filter, which resulted in a full sinewave, as shown in Fig. 58.
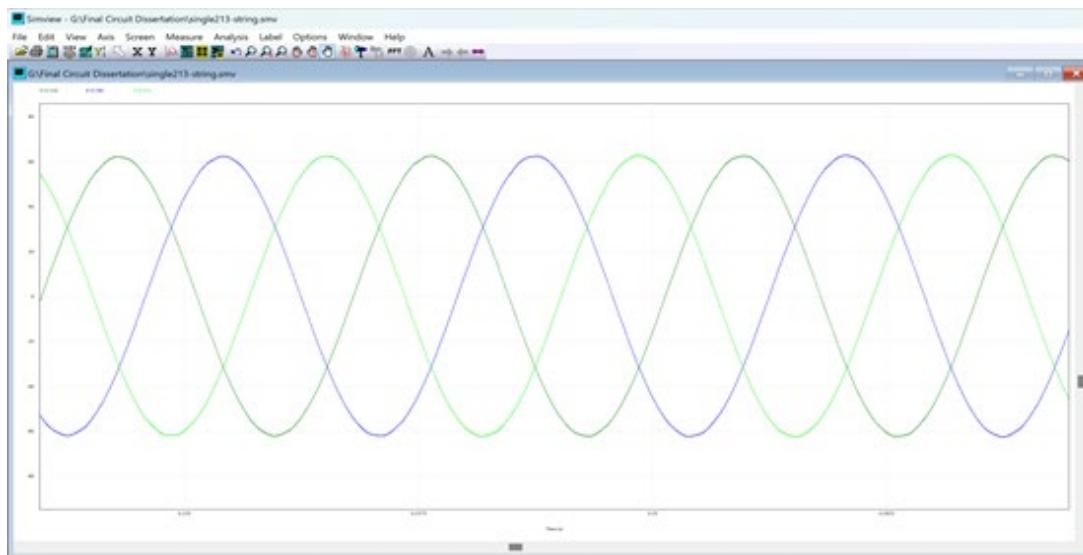
Fig. 58 Filtered output with an LC Load [130].

20. *The Effect of Partial Shading on PV Panel Operation*

When a single solar panel was shaded, it no longer provided full power at its output (see Fig. 59).
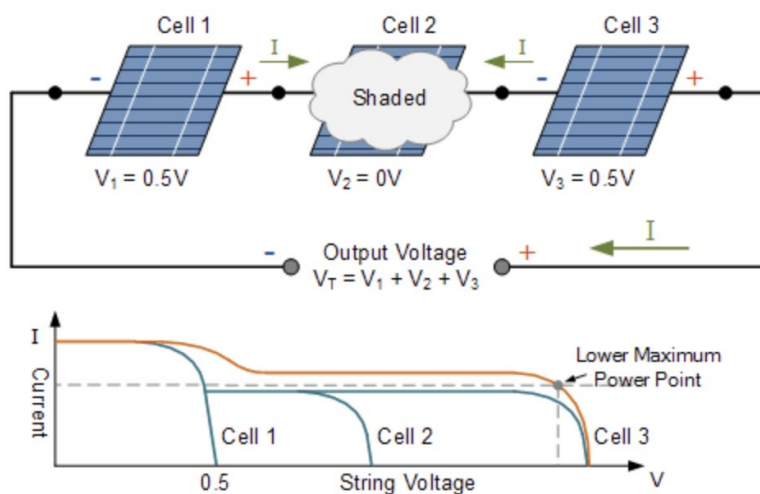
Fig. 59 Partial Shading [131].

The current produced was affected when the shading occurred. In other words, this shading caused a slight drop in PV module output. Partial shading occurs during poor sunlight or cloudy days. The result voltages of each panel are different. The negative effect of shading was solved satisfactorily by inserting a bypass diode in parallel with each solar module. This allowed the current to move within the cells, and the voltage at the cell terminals equaled the applied voltage, as shown in Fig. 60 [132].

Measure								×
	X1	X2	Δ	1/Δ	Average	Average |X|	RMS	
Time	68.33038m	84.54242m	16.21204m	61.68256				
VAB	6.61838	-5.93114	-12.54952		-16.24938	96.26370	107.99008	
VBC	-80.97769	-156.01841	-75.04073		14.23751	92.33304	103.27963	
VCA	74.35931	161.94957	87.59026		2.01187	96.54948	110.84357	

Fig. 60 Simulations results at 200 W/m² Irradiance [133].

As the sun rotates, a partial shading effect occurred. The installation had an uneven impact on its power production. This proposed study presents an experimental result from an off-grid renewable energy solar system covering all types of solar conditions. A shadow reduced the power production by the solar panels as shown in Fig. 61, and shows the relationship between shading and power reduction.
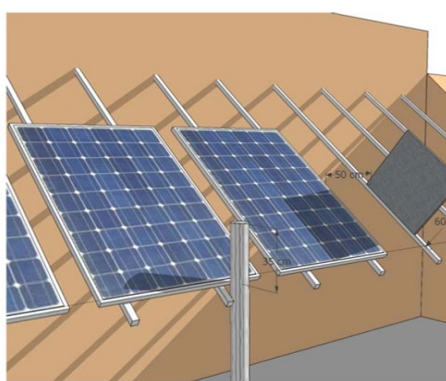
Fig. 61 Shading example [134].

As shade is produced by clouds or some obstacles, the current decreases through each string. The PSIM software used the datasheet parameters to research the solar panel output results for future studies (see Fig. 62).
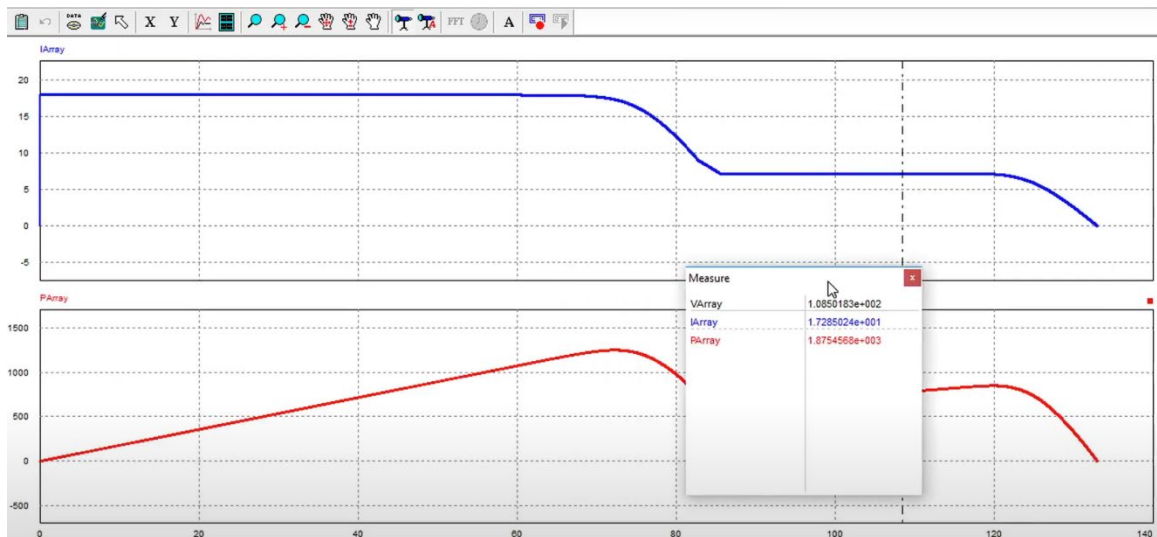
Fig. 62 Partial shading and Power Results [135].

21.   *Solar Irradiance and Panel Configurations*

The device's main operation was to control the voltages produced from the panels. The voltage controller also controlled the current flow in the solar cell array and was selected to withstand maximum flow. Sizing the inverter included the configuration of the power usage applied to the prototype. All the current sources flowed through the cell output terminals, and the cell output voltage was zero Amps, as shown in Fig. 63.
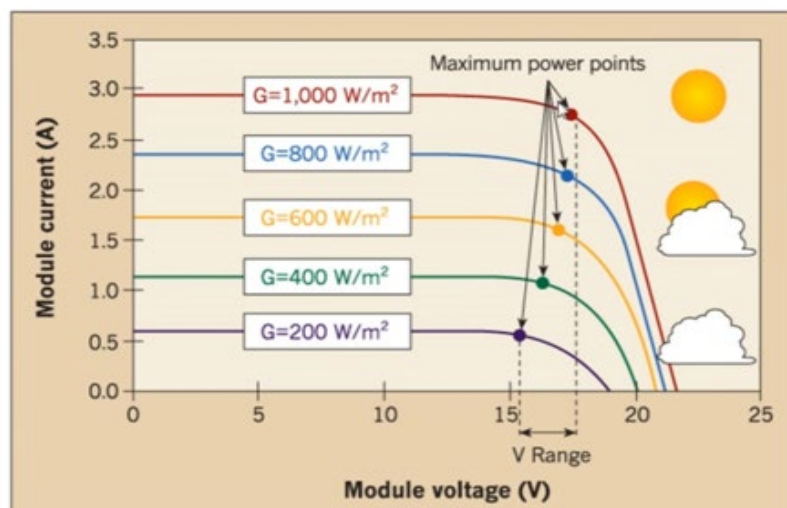
Fig. 63 Worst case conditions and I-V Curves Results [136].

22.   **Partial Shading Awareness**

The prototypes can be partially shaded by houses, light poles, or buildings at any time of the day, which impacts their power performance output. Consumers can obtain an efficiency of around 22% [137]. Efficiencies of 46% have been

demonstrated in laboratories for the most advanced concentrator applications, and efficiencies continue to rise for various categories of RE panels, as well [138].

23.   Panel Configurations

To meet the goals of designing high-power systems, the N-number modules was configured in series and parallel, which are called strings. The series configuration of the cells increased the system voltage, as shown in Fig. 63. For example: $V_T = V_{series} = 12 + 12 + 12 + 12 = 36\ Volts$

$$I_T = I_{series} = 8\ A$$
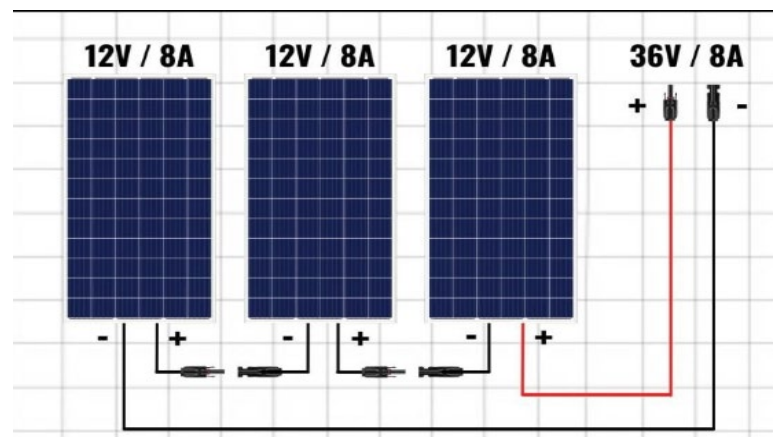
Fig. 64 Series Configurations [139].

The cells configured in parallel added the output currents, and the voltages remained the same. For example: $I_T = I_{parallel} = 8 + 8 + 8 + 8 = 24A$

Fig. 64 Parallel connected PV modules.
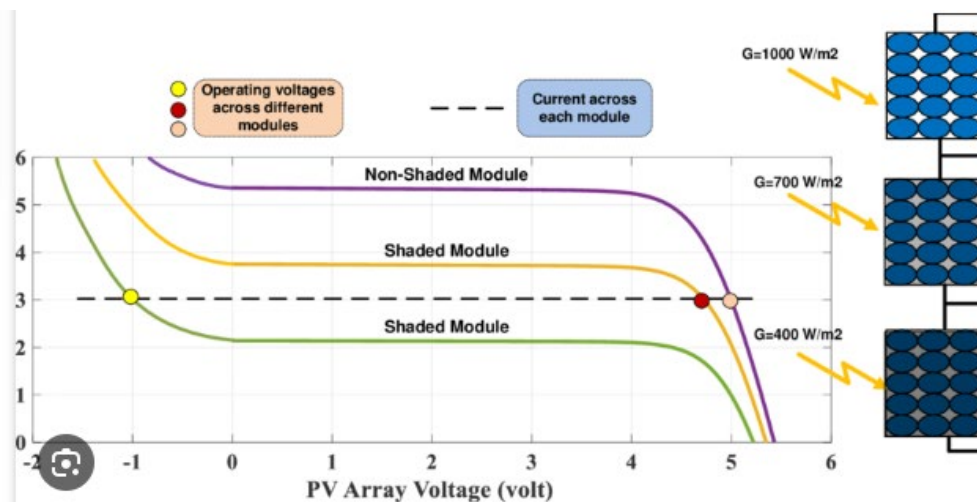
Fig. 65 Shading Examples [140].

$$V_T = V_{parallel} = 12V \quad \dots\dots\dots\dots\dots\dots\dots\dots\dots\dots\dots\dots \quad (3.35)$$
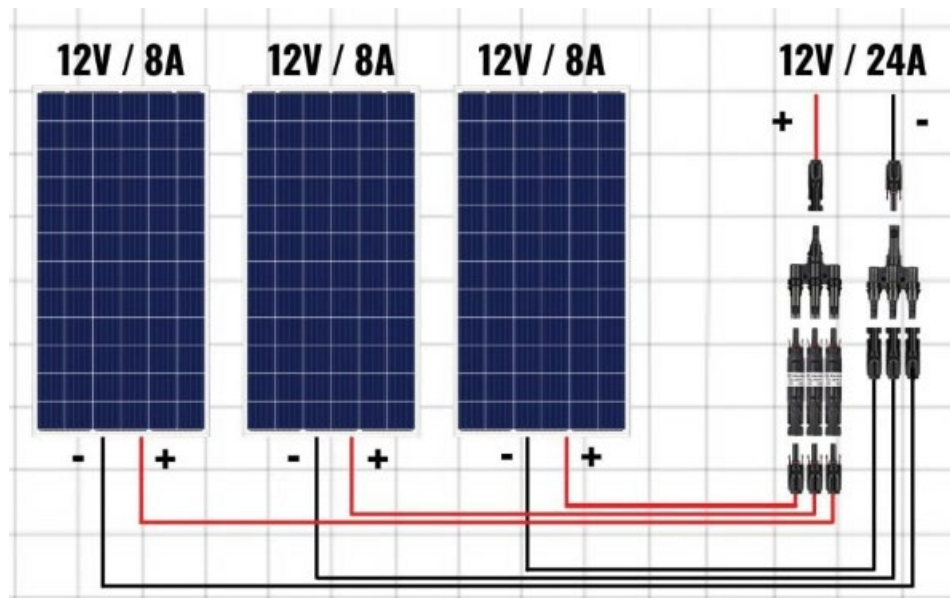
Fig. 66 Parallel Configurations [141].

For example, 14.4 volts is required for the lithium batteries to operate and charge. It will take at least 100 watts to produce a 18-26 volts for a solar module. To receive 14.4 volts and for the batteries to charge, solar panels were connected in parallel in order to reach at least 75% capacity as shown in Fig. 66.
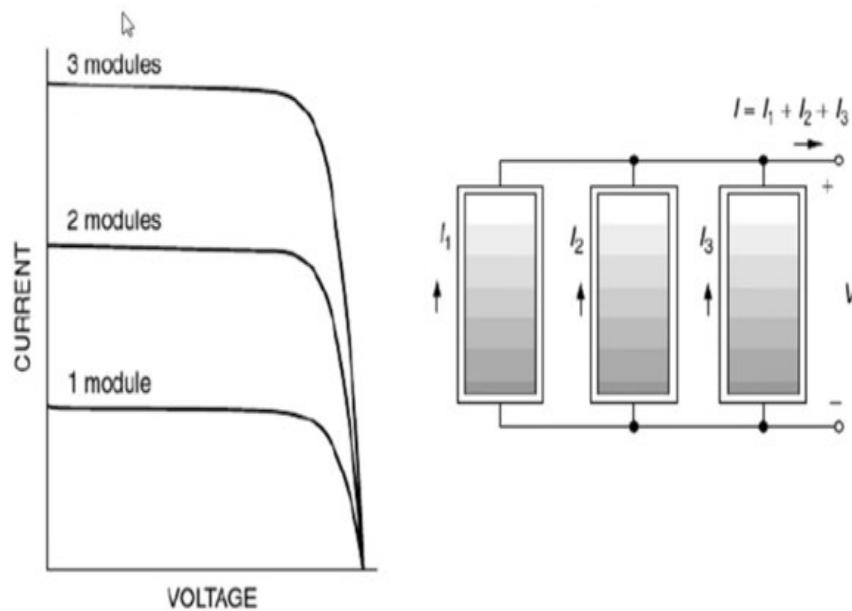
Fig. 67 I-V Characteristics for 3 Parallel and Series [142].

A string is when N-number of cells are configured in series. Fig. 67 shows a diagram of combination of parallel and series parallel (2S2P) connected PV modules.
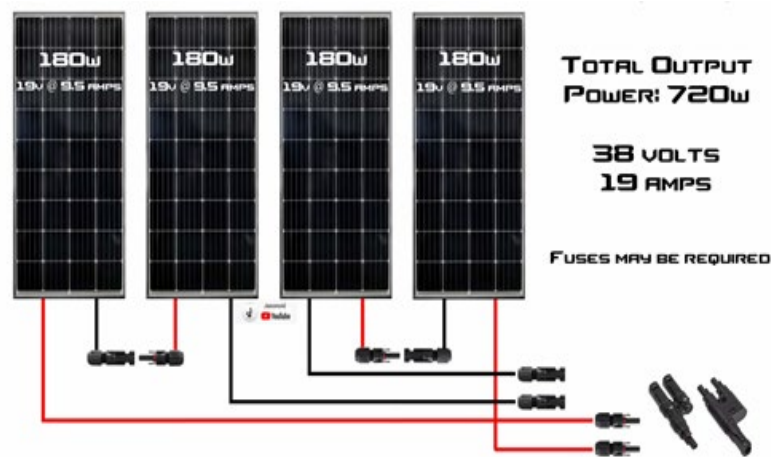
Fig. 68 Parallel and Series Combination (2S2P) [143].

A Special plug was needed to complete this configuration. This allowed the voltage to increase and to maintain a stable current as well. The configuration also assisted in the partial shading issue as well. The power remained without losing the entire system that was connected parallel.

24. Battery Types and Specifications

When freezing temperature is taken into consideration, the irreversible plating happens on the anode of the cells for the Li-ion. A lead acid battery costs $150 to $200 and the Li-ion cost is $40 to $100 per kWh. Now in a PV system, to attain the 12VDC to 120/230VAC system, both the solar panels and batteries storage must be connected in parallel. The two types of storage batteries that are widely used are lead acid and lithium batteries. The Li-ion also performs better but the cost analysis goes to Lead-Acid batteries. The lead-acid batteries have two electrodes and can be classified as follows [144]:

1. Flooded;

2. Sealed;

3. internal structure with removable plugs. Since photovoltaic applications demand deep.

The flooded lead-acid or ventilated lead-acid batteries have a small, ventilated access to their charges and discharges cycles, suitable for RE storage. There are also storage battery array's that are somewhat sealed to avoid evaporation and leakage of vapors. Another type is the valve regulated lead-acid (VRLA) battery. The VRLA comes in two types:

- Gel;

- AGM.

In the Gel type the electrolytes is in the form of gel and AGM type has a special glass mat separator as electrolytes. The batteries have low self-discharging rates with a high energy density, which means lesser sizes. The performing characteristics are higher than the lead-acid arrays. The characteristics allow the units to charge at a rapid speed.

25. Battery Architecture and RE Prototype:

A major disadvantage of lithium batteries is their price compared to lead-acid batteries. However, for solar power applications, lithium is the most powerful, efficient, and long-lasting solution [142]. Lithium batteries can be connected in series as needed.

The 300-watt prototype unit, as the sunlight activates the panels, was able to produce power. The batteries ensured a constant and dependable energy supply. The energy was stored in the batteries during the sunny periods and used during cloudy times and night hours [143]. It is recommended to use marine-type sealed lead acid batteries and to avoid acid fumes (see Fig. 68).
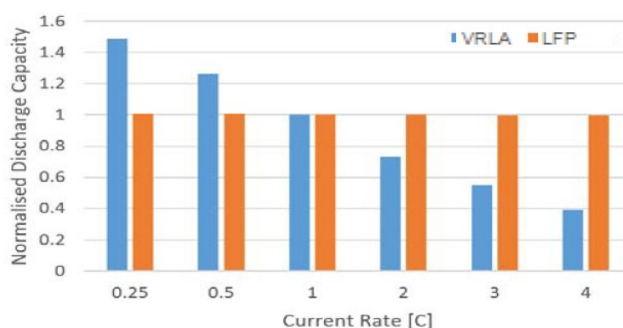
Fig. 69 Discharging Lead vs Li-ion Battery @ 25°C [144].

The batteries should be fully charged and should never be totally drained of their power. If this occurs, it will affect and deteriorate and shorten the life span of the unit. This is known as a flat process. The battery has three charging stages:

Stage 1: Bulk charging: a method of charging where the battery is supplied with the maximum current. The current is extremely high. This is the initial charging phase because the Battery capacity is quickly filled.

Stage 2: Absorbing charging: in this stage, the current is reduced to a lesser but very steady level. This stage prevents the battery from overheating and also stops the liquid inside the battery from boiling and giving off explosive gases.

If this process occurs, it will take the battery longer to charge, but safety is a concern for the end user.

Stage 3: Trickle charge: Also known as floating charging. As was observed during the testing of the prototype unit, the storage batteries reached charge.

The power's charging current was reduced to a mere trickle to maintain the battery at 100%. At times it could take a full day to charge the batteries. The Amp-hours (AH) were used to calculate how long the battery would provide power to the load and to supply power to devices such as, Lights, Laptops, phones, TVs. Suppose the rate is 125AH, the system should not use more than half of this, which would be 62AH. At this point, the battery recharged. During the testing of the prototype unit, it was noticed that the current was extremely high during charging time. The data showed that the battery's voltage decreased gradually at a discharge rate of 80%. When lithium-ion was compared to the lead acid battery, the constant flattened at a lower rate. For a non-permanent solar power installation, the Lead acid vs Lithium in the previous Table 17.0 displayed that the Lead-acid battery is the right choice for the prototype. It discovered that cloudy and sunny days has an effect the on the PV array's energy for the system, as shown in Table 18.

TABLE 18

SOLAR PROTOTYPE BATTERY RESULTS

Voltage (V)	Current (A)	Time of the Day	Sunny / Cloudy
12.6	3.2	9:25 AM	Sunny
12.1	3.5	9:45 AM	Partial Sunny
11.9	3.7	9:46 AM	Sunny
11.7	4.25	9:50 AM	Cloudy

If the prototype has future plans to implement a more efficient battery energy

arrangement system, see Table 19.

TABLE 19

LEAD-ACID VS LITHIUM STORAGE ARRAY

Battery	Weight	Discharge Rate	Maintenance	Efficiency	Cost /Venting
Lead Acid	Heavy	50%	Self-discharge	80%	Low / gases
Lithium	½ of Lead Acid	80%	Longer storage	95%	4x / sealed

The cost/venting was discovered for cycling the lithium battery and a lead-acid

battery.

26.   Series and Parallel Configurations for Batteries

The flooded lead acid and sealed AGM storage system can be configured for series or parallel. The systems in the series have a rating of 100 Ah, and the total voltage is 24 volts. Three batteries can be configured with the results of 36 volts, with the current remains the same (see Fig. 69).
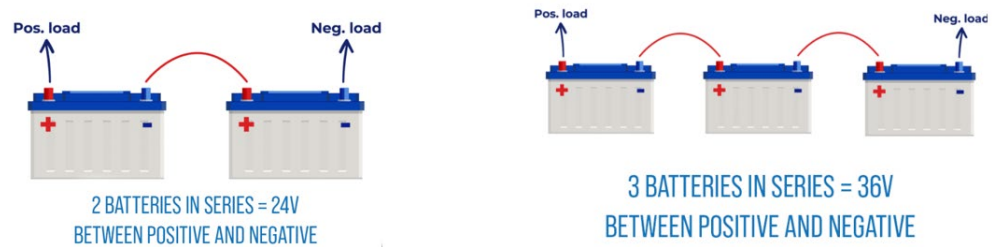
Fig. 70 Two and Three Batteries in Series [145].

The current increases but the voltages remained the same in a parallel battery configuration (see Fig. 70).
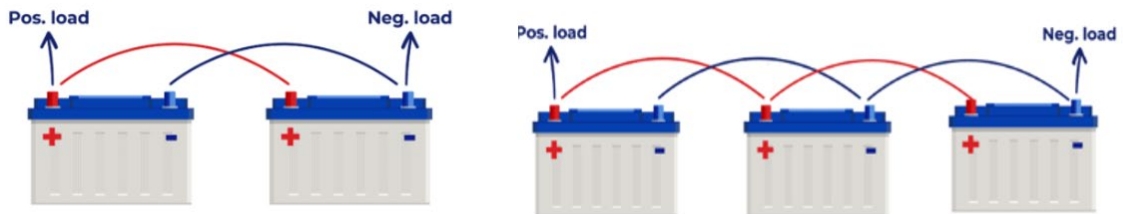
Fig. 71 Two and Three Batteries in Parallel [146].

27.   Advantages / Disadvantages of Series vs Parallel Configuration

The advantage of having batteries in parallel configuration was that the current increased. The amp-hour capacities were stabilized, and two parallel doubled the runtime, and so on. Another advantage was when one battery had an issue, the remaining batteries in the system could still perform. The disadvantage of parallel configuration was that the system voltage remained the same, and the current was higher. Higher current requires a larger AWG size and more resistance that will cause a larger voltage to drop [147]. The limit on how many batteries are in a series is contingent on the battery manufacturer's system voltage requirements, but there are constraints with the parallel configurations. The more batteries in parallel, the more capacity and longer runtime the system has available. The only disadvantage in the parallel battery configurations is that the charge time will increase for the system. For overall cost consideration for this prototype project, lead acid batteries were used.

28.   Building of an Off-Grid Solar Power Prototype

To design an Off-Grid Solar system, the operation of load that will be applied to the PV array must be considered. The daily operating hours of each appliance, through estimation and calculation, should be around 100 watts, as shown in Fig. 71.

Fig. 72 Section: Lead Acid battery (100-watt PV Testing Prototype) [148].

The estimated average daily irradiance is 0.54 using Table 14. The yield factor can be considered as well, with the calculation of the total power can start the installation of the PV modules for each string. The amount of solar radiation is studied after the site survey. The Sun covers the Earth's surface with angles that are consistent on Earth. The angles can start at 0° and go up to 90°. As the Sun's irradiance becomes upright, the surface of the Earth is considered to be the maximum power point. A small PV system prototype with three circuit breakers and three strings of modules, AC meters, AC appliances, and safety breakers was able to deliver up to 9A and was created and implemented (see Fig. 72).

Fig. 73 Prototype Components: CT's, DC Switches, MPPT, and Inverters.

The installation wire two to eight AWG size was considered, and multiple bus bars were implemented. The AWG size was considered to induce fire. The fuses acted as a precaution-protection device that detached the schematic from the rest by cutting off the power source from reaching the fuse internally when a specific current passed through the fuse to the network. These fuses are generally installed in line with the AC and DC combiner railing systems. As mentioned in previous sections, for small or bigger applications, consider using 12v and 24v battery designs, but the over-solid choice is 48V. A 1000-, 1100-, and 200-watt inverter are other options as well. It was calculated using the formula below:

$$12 \text{ VDC} \times 40 \text{ Amps} = 480 \text{ Watts} \dotfill (3.38)$$

It is vital to know the consequences of choosing a specific voltage for the renewable system, but there are some advantages and disadvantages that are covered later. There are three types of systems that can be considered: 1) 12 volts, 2) 24 volts, and 3) 48 volts systems. A single charge controller can handle a maximum of 80 Amps, equaling 960 watts of solar at 12 volts.

12v x 80A = 960 watts

The following components are shown in Fig. 73 and listed below.

Fig. 74 PV Off-Grid Prototype [149].

1. 100-W inverter x 2;

2. 1000-w inverter x 3;

3. 3 MPPT controllers rated at 50V input and 12.6 volts output;

4. 3 Solar panels rated at 100-W V_{oc} 22.6 Volts;

5. Various type of bus bars;

6. AC /DC Breakers;

7. 3 12V 260 AH Batteries;

8. Single Phase Meter;

9. Three Phase Meter;

10. Three AC Voltage Phase Shifters.

When the battery voltage is increased to 24 volts, the calculated power required for the prototype was 1920 watts. Using the current of 80 amps, the power is equal to:

$$24v \text{ x } 80A = 1920 \text{ watts}$$

Or even more with a 48-volt battery system

$$48v \text{ x } 80A = 3840 \text{ watts}$$

The conclusion is that the charge controller was less expensive with a higher voltage PV system.

The prototype used was a 2000 watts prototype.*12v x 24A = 288 watts*. The prototype system was able to display load current as well as the wattage and the consummation (kWh) (see Fig. 74).

Fig. 75 Solar Prototype Load Results [150].

The prototype systems were able to provide a single phase and a three-phase line for various types of applications. If a lead-acid storage array is implemented, the capacity needs to be doubled, because the lead-acid storage array has a 50% dischargeable rate. Testing was done outside near the proposed site to evaluate all types of situations that could occur on the prototype. The simulation data matched the practical data, due to the modified sine wave output results were noticed on the prototype measurements also. The solar array specifications, along with the rated parameters that were used are as follows:

- Solar panel Voltage: 22.6 V;

- Current: 5.21 A;

- R_L = 22.6 v /5.86 A = 3.866 Ω;

- Power Supply Load = 22.6 x 5.21= 117.75 W.

The PV Module Load voltage (R_{sh} = 313.40 Ω (From Simulink Module). The power supplied to load decreased significantly when cells were shaded. The voltage produced by only 35 cells was calculated to be: 35 over 36 x 24.3 v = 23.63

V. It was observed with the prototype that when the solar voltage increased, so did the current throughout the circuit. The Tables show that the three systems performed very well and were able to remain stable 95% of the time with a load of 36.5 watts and 60 watts. The system's three MPPT set off an alarm if the batteries dropped below its nominal operation voltage threshold (see Fig. 75).

Fig. 76 Prototype Modified Sinewave and Measurements [151].

The output for two inverters did not deliver clean power. Those units were replaced. The inverters set-off an alarm if the batteries dropped below its nominal operation voltage threshold. It was noticed that the MPPT shut down without the battery's input voltages of 12 volts (see Tables 20).

TABLE 20

DATA FOR PV SYSTEM PROTOTYPE (SUNNY)

RE Solar Voltage (V)	RE Solar current (A)	RE Solar No load (W)	Battery Voltages (V)	Output Sine Wave AC
20.2	5.3	107	12.9	noise
20.2	2.4	48	12.8	noise
19.8	3.4	67.3	12.9	noise

The output for two inverters did not deliver clean power. Those units were replaced. The Ever-start Lawn/Garden battery, with model number U1R was not designed to handle the energy supply for the prototype. See the Ever-start battery amp hour rating in Table 21.

TABLE 21

DATA FOR PV SYSTEM PROTOTYPE (PARTIALLY CLOUDY)

RE Solar Voltage V	RE Solar current A	RE Solar No load W	Battery Voltages V	Output Sine Wave AC
20.2	5.3	107	12.9	noise
20.2	5.5	48	12.8	noise
19.8	6.0	67.3	12.9	noise

This battery was designed with a 30-minute Reserve Capacity (RC). During the testing of the prototype, a few batteries were damaged when the voltage dropped from 12.5 volts to 10.5 volts. See Table 22.

TABLE 22

DATA PV SYSTEM PROTOTYPE (SUNNY)

RE Solar Voltages V	RE Solar current A	RE Solar load W	Battery Voltages V	Output Sine Wave AC
13.1	2.0	107	13.1	108.6 Modified
13.0	2.0	48	13.5	118.2 Pure
112.9	61.6	67.3	12.9	97.8 Pure /ripples

29.   Performance of Selected Components for Prototype

The batteries performed well. The testing results provided valuable insights on how the batteries performed during various cases with the sun light. The results assisted in assessing the overall efficiency of the PV platform and ensuring that the stored energy was available when needed. It was noticed that when the sunlight obscured by clouds, the current rose after the batteries carried the load of the system for about 15 to 20 minutes. The results are shown in Table 23.

TABLE 23

PROTOTYPE PERFORMANCE TEST DATA

RE PV Panels			Battery Voltages	Inverter Output
Volts	Amps	Watts	12.6	108.6 Modified
12.4	2.0	107	12.9	118.2 Pure
12.1	2.0	48	12.6	97.8 Pure / ripples
12.6	61.6	67.3	12.6	108.6 Modified

When fully charged, the prototype operated at 100%. Field test was done with 300-watt and 2000-watt prototypes to analyze full sunlight, partial shading, the effect on the battery, and the charging rate. See Table 24.

TABLE 24

DATA SOLAR SYSTEM PROTOTYPE (PARTIAL SHADY)

RE Solar Voltage V	RE Solar current A	RE Solar load W	Battery Voltages V	Output Inverter Sine Wave AC
12.4	2.0	107	12.6	108.6 Modified
12.1	2.0	48	12.9	118.2 Pure
12.6	61.6	67.3	12.6	97.8 Pure / ripples

The power generated reached 14.038 volts to operate the system loads (see Fig. 76).

Fig. 77 Solar Panels Prototype Site Assessment [152].

The panels were placed where sunlight could illuminate the unit. This study proposed installing a hybrid inverter in this prototype to test future on-grid applications.

30.   DC and AC Fuse Protection for Prototype

The fuse switches were installed to prevent an overload and to protect the system [153]. The switch will prevent damage to the inverter by cutting off the power source before it reaches the load. The switches were installed in line with the AC and DC combiner railing systems, as shown in Fig. 77.

Fig. 78 AC / DC Switches [154].

The prototype has an ambient temperature sensor and a module temperature sensor for each type of inverter. An instrument voltage and current transformer

assisted in collecting the data for each inverter and battery [155]. The data collected was analyzed for the solar panels, inverters, and batteries with the help of the e-Gauge.

31.   Testing Prototype Components Efficiency

The efficiency of a RE solar panel is defined as the amount of electrical power coming out of the solar panel compared to the power produced by the sunlight [156]. All the energy produced from this panel depends on the intensity and wavelengths of the light available and multiple performance attributes of the cell,

as shown in Fig. 78 and Fig.79.
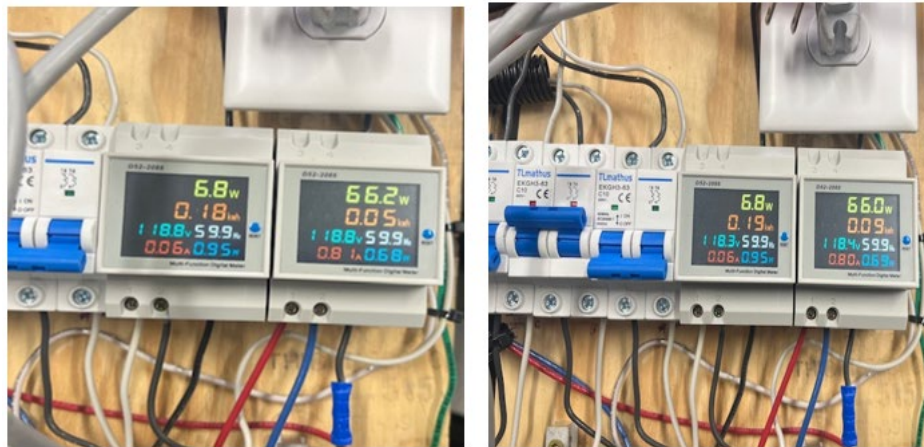
Fig. 79 Prototype Wattage Consumptions [157].
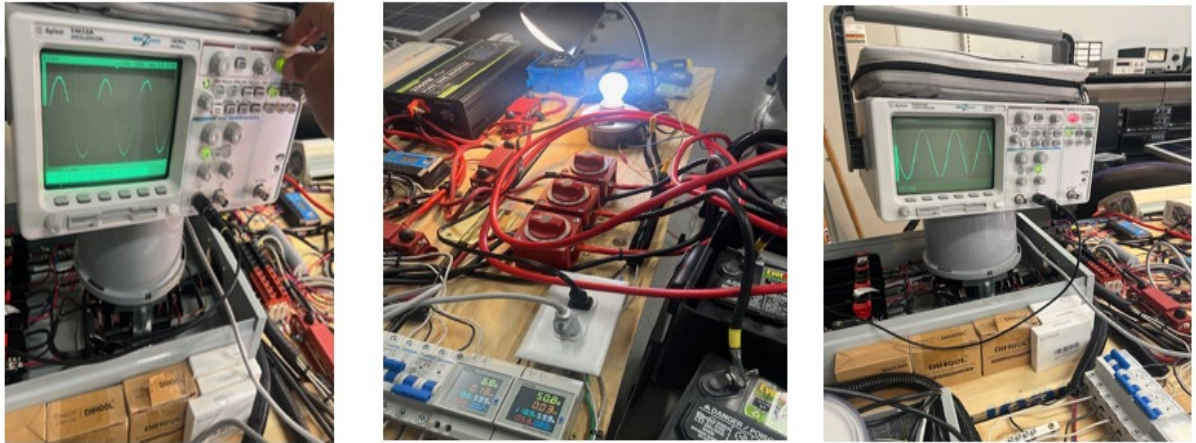
Fig. 80 Oscilloscope 60 and 100-watt Loads on the Prototype [158].

.

4. THE PLATFORM DESIGN

D.   Introduction

The design of the RE platform will follow the same steps as the prototype

described in Chapter 3.

The platform consisted of three types of panel installations:

1. Ballasted Fixed Tilt 10° Monofacial,

2. Dual Axis Tracker combination of Monofacial and Bifacial

3. Fixed Tilt 25° Monofacial

The load, MPPT, battery size, and number of solar panels were considered in the

platform's design (see Fig. 80).

AC Appliances

Device	Watts		Hours		Watt Hours	
AC-Heating	1000	W	6	h	6,000	Wh
Laptop	60	W	6	h	360	Wh
Lights-Cameras-EMS	860	W	24	h	20,640	Wh
Printer-Gate	1050	W	6	h	6,300	Wh
PC - Microwave	1270	W	6	h	7,620	Wh

Total Watt Hours

40,920	Wh

Future load expansion	30 % of the Total Watt Hours	53.196	kWh

Fig. 81 Projected energy demand for the Platform [160].

Based on the same procedure used in the design and implementation of the prototype, The platform needed an estimated total energy of 40,920 kWh that will also supply future load growth.

1.   Platform Solar Array Sizing

To calculate the wattage per string of the PV panels for the platform, using the PSH value and efficiency, the formula below from Chapter 3 section 3.1.11 was considered;

Power = (53.196 kWh/day)/ (5.65 kWh/m² = 9415.22 Watts.

Power = (9415.22 Wh/day)/ 14.08% = 66869.5 Watts

Watts hour = 66869.5 Watts x 30 days

Watts hour = 2006.kWh /month

Now to calculate Wattage of the Solar Panels

The number panels =   66869.5 Watts / 470W = 142.275 (150 Panels of 470 watts) (see Fig. 81).

ELECTRICAL DATA (STC)

Peak Power Watts-P_{MAX} (Wp)*	470
Power Tolerance-P_{MAX} (W)	
Maximum Power Voltage-V_{MPP} (V)	36.1
Maximum Power Current-I_{MPP} (A)	13.02
Open Circuit Voltage-V_{OC} (V)	43.0
Short Circuit Current-I_{SC} (A)	13.73
Module Efficiency η_m (%)	20.0

STC: Irradiance 1000W/m², Cell Temperature 25°C, Air Mass AM1.5.
*Measuring tolerance: ±3%.

Fig. 82 Trina Solar Specifications for the Platform [161].

The suggested panel is the Trina-Solar, has the maximum power of 470W, and the maximum current is 13.02A. This satisfied the calculations. A satellite land survey was performed for the suitability of the selected platform construction site. The energy that can be derived from the Sun for that site was 83,145,475 kWh/Year, and the annual solar radiation (PSH) was 5.65 kWh / m² per day, as shown in Fig. 82 and Fig. 83.

RESULTS
📇 Print Results

83,145,475 kWh/Year*

System output may range from 79,495,389 to 85,273,999 kWh per year near this location.
Click HERE for more information.

Month	Solar Radiation (kWh / m² / day)	AC Energy (kWh)
January	3.88	5,329,969
February	4.32	5,205,012
March	5.72	7,520,596
April	6.56	8,073,856
May	7.01	8,602,306
June	7.63	8,681,224
July	6.97	8,051,021
August	6.47	7,660,897
September	6.28	7,284,199
October	5.38	6,830,964
November	4.26	5,434,319
December	3.29	4,471,112
Annual	**5.65**	**83,145,475**

Fig. 83 PV Watts Calculator for 45kW Platform System information [162].

PV System Specifications

DC System Size	53196 kW
Module Type	Standard
Array Type	Fixed (open rack)
System Losses	14.08%
Array Tilt	20°
Array Azimuth	180°
DC to AC Size Ratio	1.2
Inverter Efficiency	96%
Ground Coverage Ratio	0.4
Albedo	From weather file
Bifacial	No (0)

Monthly Irradiance Loss	Jan	Feb	Mar	Apr	May	June
	0%	0%	0%	0%	0%	0%
	July	Aug	Sept	Oct	Nov	Dec
	0%	0%	0%	0%	0%	0%

Performance Metrics

DC Capacity Factor	17.8%

Fig. 84 PV Platform Specifications [163].

2. **Determining the Battery Bank Size**

There were three fundamentals steps to consider:

1. Days of Autonomy (DoA);

2. Total Load;

3. Battery maximum Depth of Discharge (DoD).

The formula to size the battery bank from Chapter 3 section 3.1.11 was the following:

Battery Capacity (Ah) =

Total Watt-hours per day used by load   x   Days of autonomy
(0.85 x 0.6 x nominal battery voltage)

The suggested platform had a load of 53,196 watts. The platform was designed to use a 55.6-volt solar module, rated at 470 watts. The batteries were connected in series, then parallel to obtain the required system voltage. It is recommended to connect the batteries for most systems in parallel to increase the system's capacity [164]. The platform battery sizing was determined by using the battery size online Omni calculator. For most systems, two to three days of DoA is sufficient. The manufacturer data showed that the Lithium-ion's DoD was around 90% [164]. The days of autonomy was calculated to be 5.65, which is typical for winter environment for the state of Texas. For the platform design, total energy was

40.920kWh, DoD is 90%, and the DoA was taken as one day. The Battery capacity

formula is repeated here for convenience.

Battery capacity (Ah) =

<u>Total Watt-hours per day used by appliances</u>   x   Days of autonomy
 (0.85 x 0.6 x nominal battery voltage)

$$= \frac{53.196 \; kWh}{(0.14085 \; x \; 0.96 \; x \; 40.96} \text{ x Days of autonomy}$$

$$= (9604.86) \text{ x } 5 \text{ (DoA)}$$

$$= 38.4194 \text{ kWh}$$

A total of 38.4194 kWh Battery capacity was required for the platform. A Storz

power battery bank, shown in Fig. 84, was selected.

Fig. 85 Storz Power Battery for the Platform [164].

The battery had an energy capacity of 5.12 kWh. Therefore, the battery

configuration was two sets of four in series to parallel combination as shown in Fig.

85.
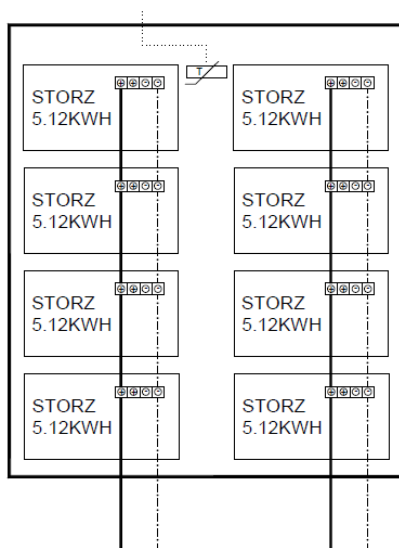
Fig. 86 Storz series to parallel configuration [165].

The selected battery for the platform was a Lithium-Iron Phosphate (LFP) 51.2 V Storz Power battery, which has a 100% depth of discharge (at 1C Rate at 77°F), 98% and a round trip efficiency – 100 (Ah). The battery current is designed to be continuous and the current charge is at 100 A. The nominal voltage of 51.2 volts for each battery pack was measured to confirm the DC required for the platform. The Storz power battery module has two batteries that were connected in series in one module which added up to 51.2 volts.

3.   The Sol-Ark DC - DC and DC - AC Converter for the Platform

Proper selection of the converter will safeguard the battery bank, which is also the key to the longevity and efficiency of the entire PV platform. The battery bank capacity was calculated to be 38 kWh from the previous section. The converter voltage must therefore be larger than the battery bank voltage for the

converter to be able to charge the batteries. The Sol-Ark15k-P converter was the suggested device for the platform. It is to be noted that the Sol-Ark converter had both an MPPT and inverter incorporated in the unit. A software program controlled the phase shift for each of the three inverters AC output voltages to give a three phase AC supply, as shown in Fig. 86.
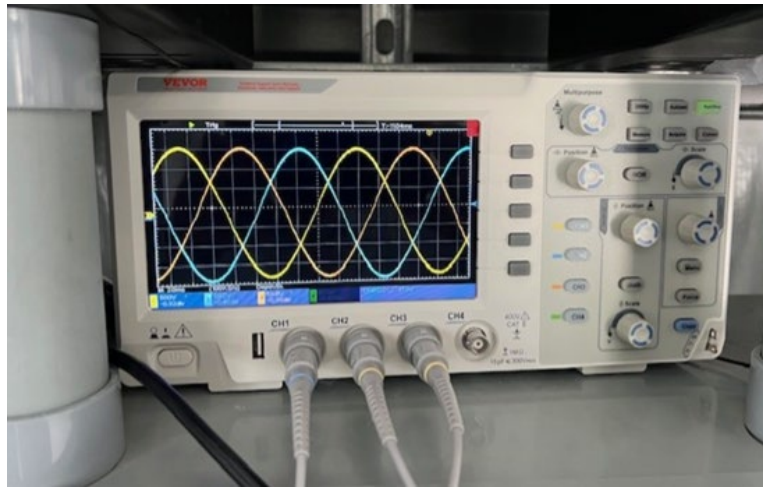
Fig. 87 AC Output Voltages from the Sol-Ark Inverter [166].

The converter is also capable for its high performance and reliability in converting the solar energy into electricity and supply the backup power. The Sol-Ark converter maximized the solar energy usage and reduced total reliance on the power grid as shown in Fig. 87.

Fig. 88 Solar Charge Controller for the Prototype [167].

The voltage level of the system was 120V / 208V and the maximum current was 200 A. Most PV platforms have their panels set at10 degrees or 25 degrees.

4.   Fixed 10° and 25° Tilted Monofacial - Dual Axis Bifacial Tracker

A research study done in 2017, found approximately 40% of utility scale RE platforms operating in the US have fixed or tilted PV panels [196] (see Fig. 88).

Fig. 89 Platform Solar Mount process [168].

The amount of electricity generated by the tilted PV system hinged on the alignment of the PV panels [117], as shown in Fig. 89.
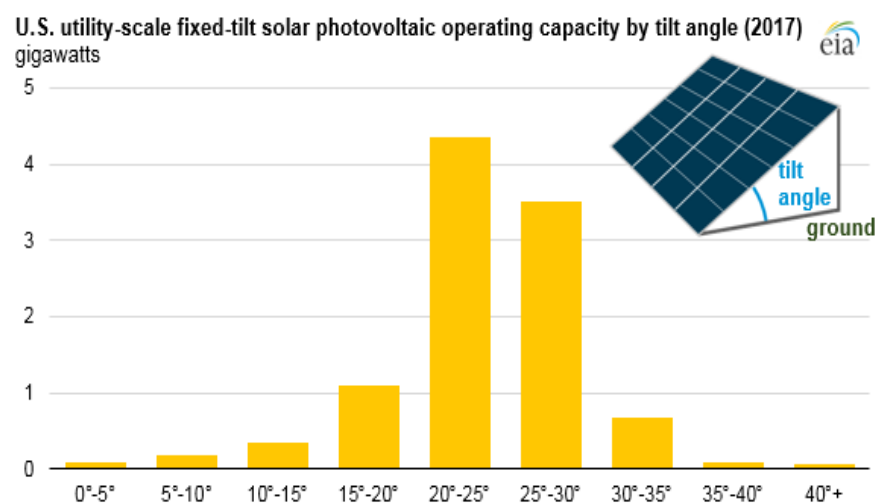
Fig. 90 US Scale for Fixed Title Angles of 20° to 40° [169].

The PV system's panels, when set at a 30 ° angle, maintained the manufacturer-rated panel efficiency (see Fig. 90).

Fig. 91 Fixed PV Degree Installation [170].

The azimuth stipulated the correct angle at which the panels should face the sun. Most panels face south (see Fig. 91).
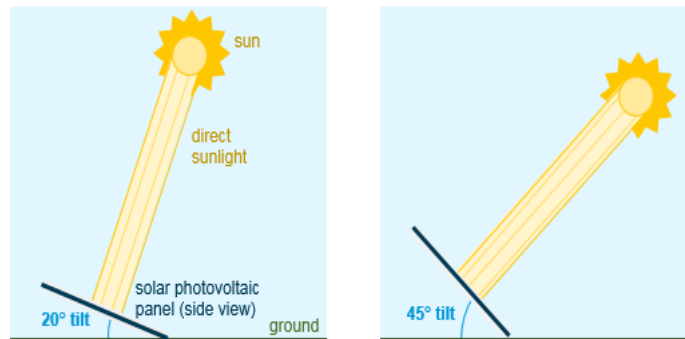
Fig. 92 Fixed Titled Solar PV System [171].

Zero degrees would locate the panel on the ground and 90° will align it perpendicular to the ground. At lower latitudes, it is noticed that the sun peaks at its highest point and the solar modules do not demand much of the fixed angle as shown in Fig. 91. But at higher altitudes, the sun is lower in the sky and PV panels are often installed at a greater tilt angle as viewed in Fig. 91 than 20°. The essential component that assisted in deciding the tilted angle was the coordinates. Over the recent decades, utility and RE power plants pressed towards installing tracking systems [172]. The advantages are that the system can rotate on a single axis, typically east to west to follow the sun, or on a dual axis. Even though these types of systems are expensive, the returns are very desirable (see Fig. 92).

Fig. 93 Dual Axis Solar Tracking System [173].

The Chassis used to mount and tilt the solar panel 10 ° was very strong, and light, and able to support any type of installation. This polyamides material is exceptionally hard plastic that is durable and has the strength for mounting in any angle. The mounting device as shown in Fig. 93, comes in 5° and 10° options with a 25-year warranty [174].

Fig. 93 Platform Ballasted mount [175].

The surface of the 10-degree mount has a secure mounting device fixed with two large patio bricks. The brackets, circled is located on the mount. The platform ballasted mount are secured by patio bricks [176]. The back side of the PV module is connected to another mounting bracket. This area is used as a secondary installation rack for other PV panels. The converters and batteries for the PV platform are installed in a temperature-controlled environment inside the platform building. The symbols in Fig. 94 are explained as follows:

- E_{net} = network energy from the storage and grid;

- E_i = dc input to the converter (efficiency n);

- E_c = energy delivered by the converter;

- E_p = energy generated by the PV panels;

- E_b = power stored in the batteries;

- E_l = energy demand by the load.
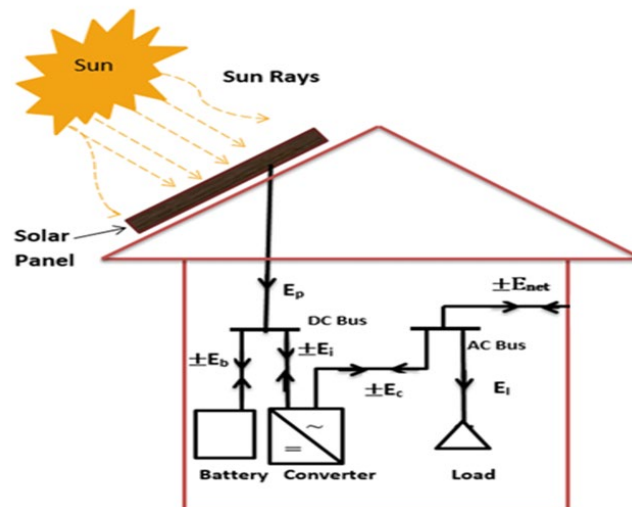
Fig. 94 Control Center Components [177].

The site satellite image layout is shown in Fig. 95.

Fig. 95 An Overview of the Proposed PV Site [178].

The facility platform construction is shown in Fig. 96.

Fig. 96 PV Platform under construction [179].

A custom designed gate is installed and is operating fully on solar energy, as shown in Fig. 96.

Fig. 97 The Entry Gate [180].

The Sol-Ark components consisted of the following items:

- Load connection;

- DC Breakers;

- AC Breakers;

- Battery connection;

- Internet Ports / Neutral bar;

- 6 lines output for the A and b leg.

The wiring scheme for the Sol-Ark converter was AC, BA and CA (see Fig. 98).

Fig. 98 Sol-Ark 3-Phase Wiring Configuration for the Platform [181].

The line–to-neutral voltage measured results is equal 120V AC, while the line-to-line voltage results is equal to 208V AC.

5. Electronic Gauge Smart Meters and Sensors

The PV platform has internet capability, with a composite smart meter and an E-gauge datalogger. There are two E-gauge meters. The WLAN port direct option allows users to connect to the campus network. A wireless modem was also installed with cellular cloud services. The students can access the logger using the built-in web application (see Fig. 99). The E-gauge records the current, wattages, VA, VAR, kWh, temperature, and wind speed, among other things [182].
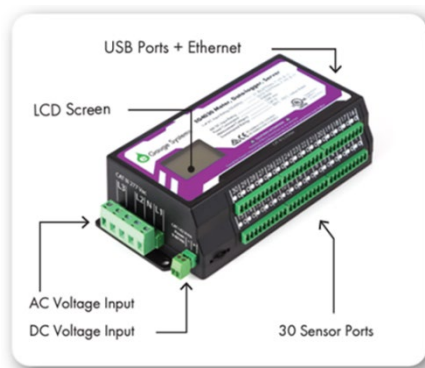
Fig. 99 E-Gauge Smart Meter [183].

6.   The PV Platform – Partial Blueprint and Implementation

Each PV cell string in Fig. 100 produced around 425 V at 12.5 A [192]. All

designed PV panel strings had the same voltages.
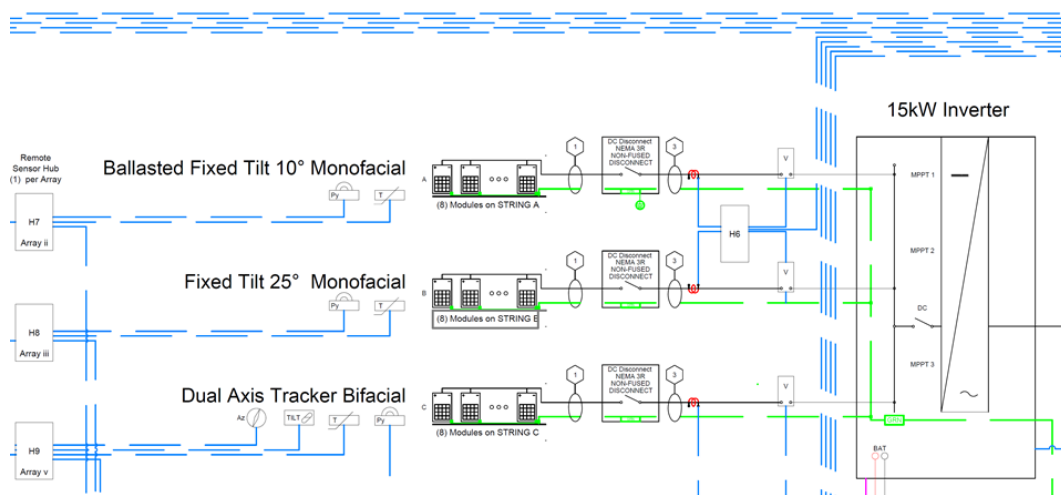
Fig. 100 PV One Line Diagram [184].

The Solar Panels, 15kW Inverter, sensors, DC disconnect, pyranometer, the

ballasted fixed Tilt 10, the Fixed Tilt 25 Monofacial and the Dual Axis Tracker

Bifacial are all shown in Fig. 101. Also included on the blueprint are voltage sensors and current transformers. Fig. 101 is a block diagram of the entire PV platform.
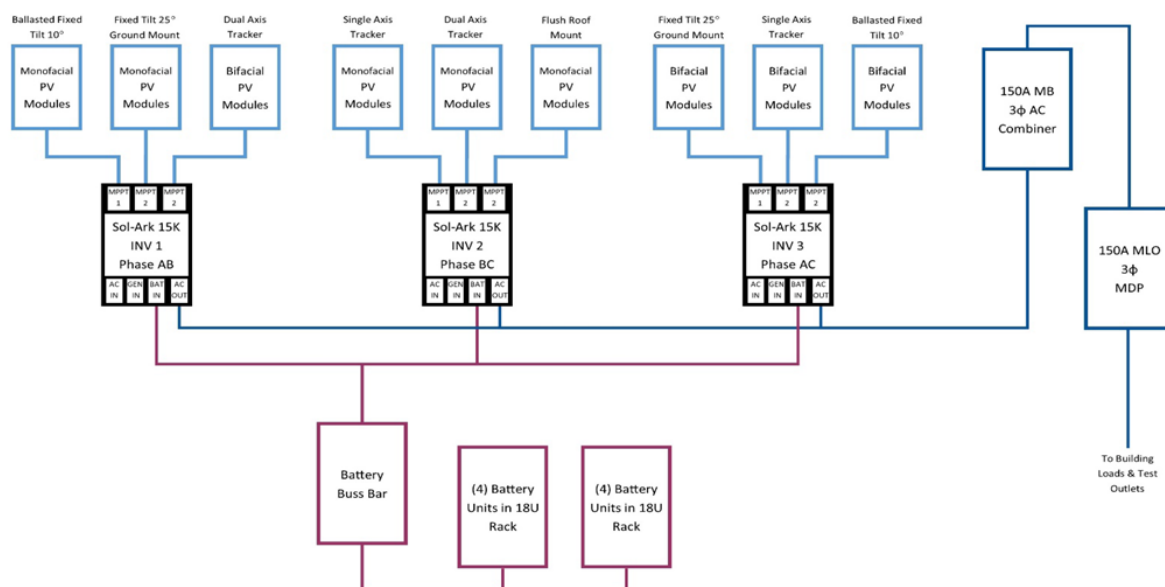
Fig. 101 Preliminary Concept Online Drawing of PV Solar Platform [185].

Fig. 102 is a constructed 10 ° PV array for the platform.

Fig. 102 Platform's Fixed 10 ° Monofacial and Bifacial Array [186].

This array has a mixture of bifacial and monofacial panels. Each bifacial panel captured light on both sides. The sunlight hit the panel and the environment and

it dispersed, thus suppling energy to both sides of the panel. The purpose of this 10° PV array tilt was to further capture more energy. Fig. 103 is a 25 ° tilt PV fixed array system for the platform.

Fig. 103 Platform's Fixed 25° Tilt Monofacial Array [187].

This tilt pointed the PV array toward the sun's average yearly path. The goal was to ensure the maximum yield of annual energy that can be adjusted slightly based on latitude to achieve optimization of power. The ability to dynamically track the sun's position makes the PV array a highly efficient renewable energy technology. This system ensures the panels are always angled in the correct position to produce maximum power output, as shown in Fig. 104.

Fig. 104 Platform's Dual Axis Array [188].

The ability to continuously rotate and adjust the PV array orientation ensures capturing the maximum amount of energy from the sun. The advanced dual and rotating technology ensures the panels are always at the best angle for maximum power output, as shown in Fig. 105.

Fig. 105 Platform's Rotating Axis Array [189].

The Polar Axis Rotation Unit (PARU) solar tracker of the platform shown in Fig. 106 allows the PV system to dynamically adjust the panels to the sun.

Fig. 106 Platform's PARU Solar Tracker [190].

The unit offers an optimal balance of simplicity, versatility, and energy production.

7. Platform Cellular Services

Cellular services are another key component of the network. It requires a dedicated power source and, of course, an active data plan. The system will connect to an e-Gauge meter using the TCP/IPv4 network capabilities. The meters are only compatible with one cellular modem called the In-Hand IR315, as shown in Fig. 107, to access the network.

Fig. 107 In-Hand cellular modems (left).   Wi-fi Switch (right) [191].

The device connects to the local router, and the built in Wi-Fi will handle the

WAN area.

5 CONCLUSIONS

E. **Conclusion and Future Work**

The future direction of Renewable Energy systems such as photovoltaic, wind turbine, hydro, and Biomass is well defined. Fossil fuel obsolescence imminent. This is evident in the massive deployment of solar and wind power systems in China, Europe, Brazil, India, and the US.

In the US, the previous President, Barack Obama, proposed the Department of Energy RE task initiative. The goal of this task was to form a collaboration of America's top scientists, engineers, and businesses to advance Renewable Energy systems and offset the effect of climate change by 2030 [192]. Meanwhile, the Department's Joint Center for Energy Storage Research at Argonne National Laboratory has been performing research to overcome barriers and improve lead-acid batteries for Renewable Energy storage.

This study researched, designed, and constructed an Off-grid PV platform that will assist in producing RE research engineers and building future infrastructure to reduce local utility power consumption. Most university programs do not implement efforts to train RE engineers, and this problem needs to be addressed if the US plans to lead the world in RE efforts. This study was intended to help address this challenge.

1.   **Future Work**

The opportunity is for university research to continue with renewable energy through proposals and grants. Prairie View A&M University has the opportunity to embark on:

• Developing microgrids; and;

• Increasing energy efficiency;

• Assist in energy burden in low-income communities;

• Continue to research clean energy technology (solar, storage) access;

• Implement and create a center for clean energy, and job training;

• Construct Solar-EV charging stations for Electric Buses;

Additional future work projects include:

• Install standalone microgrids in critical facilities or resilience centers to ensure continuation of services during natural disasters;

• Upgrade transmission and distribution lines, grid stability, and resilience with substation or other electrical infrastructure improvements.

The plan is to develop a larger renewable power generation system, and researchers will continue to observe the impact of the university utility consumption and the cost to the university.

REFERENCES

[1] Adil Salman, Arthur Williams, Hanya Amjad, M. Kamran Liaqat Bhatti, M. Saad *Simplified Modeling of a PV Panel by using PSIM and its Comparison with Laboratory Test Results.* The University of Nottingham, UK2,2015.

[2] Solar Energy Technologies Office, *The White House, Solar Energy Technologies Office How Does Solar Work*? Photovoltaic Technology Basics Solar Photovoltaic Cell Basics, The Office of Energy Efficiency and Renewable Energy (EERE),US 2023.

[3] K. Kaur, Perovskite solar cells-A futuristic approach, 2019 IEEE 2nd International Conference on Renewable Energy and Power Engineering (REPE), Toronto, ON, Canada, 2019.

[4] Fig. 1: *Leading Countries in Renewable energy wattages as of 2023 Enerdata World Energy & Climate Statistics* – Yearbook 2023.

[5] Fig. 2: *Renewable power-wind*: Shutterstock: 2020.

[6] Fig.3: *The impact of EV on the grid: Clean Energy Reviews: Solar.*

[7] Mahmoud Abdulwahed*, Towards Enhancing Laboratory Education by the development and Evaluation of the – A Triple Access Mode (Virtual, Hands-On and Remote Laboratory*, Loughborough University, 2010.

[8] Fig. 4: The architecture of a parallel HEV: Hybrid Electric Vehicles: Principles and Applications with Practical Perspectives, 2nd Edition Mi and Masrur October 2017.

[9] Tomislav Simeonov Kostyanev , *Building a European laboratory network to combat bacterial resistance by boosting the clinical development of anti-infective*, University of Antwerp, 2021.

[10] Fig. 5: *Proposed solution to assist power grid*, Bluettipower, 2021.

[11] Fig. 6: *Proposed off the grid solar network infrastructure*, Springer,2007.

[12] Fig. 7: *Renewable Resources link to power grid. Shuttle Images and Cooper Development Association Inc*, Shutterstock, 2023.

[13] Omali D, Buzibye A, Kwizera R, Byakika-Kibwika P, Namakula R, Matovu J, Mbabazi O, Mande E, Sekaggya-Wiltshire C, Nakanjako D, Gutteck U, McAdam K, Easterbrook P, Kambugu A, Fehr J, Castelnuovo B, Manabe YC, Lamorde M, Mueller D, Merry C. *SolarCity Corporation's "Photovoltaic Roof Tile,"* patented 2018.

[14] Fig. 8 F.A. Godfrey *The Hydroelectric Powerplant and Austin Dam.* Texas Water Development Board: 1968.

[15] F.A. Godfrey *The Hydroelectric Powerplant and Austin Dam.* Texas Water Development Board: 1968.

[16] Fig. 9 *The world's oil production (consumption). Fossil Fuels:* "*Building clinical pharmacology laboratory capacity in low- and middle-income countries:* Uganda". Afr J Lab Med. 2023

[17] White, Doug, *Building an Astrophysics/Astrochemistry Laboratory from Scratch,* The Physics Teacher, ER,2022.

[18] Fig. 10 *Brazos Wind Turbine Towers.* – Wind Farms USA 2005-2024.

[19] Ardani, Kristen, Eric O'Shaughnessy, Ran Fu, Chris McClurg, Joshua Huneycutt and Robert Margolis. *Installed Cost Benchmarks and Deployment Barriers for Residential Solar Photovoltaics with Energy Storage*: National Renewable Energy Laboratory. Golden, CO:2016.

[20] The Iron-Ridge® *BX System.* HEADQUARTERS Iron-Ridge, Inc. 28357Industrial,BoulevardHayward,CA,2023.

[21] US Energy *Most utility-scale fixed-tilt solar photovoltaic systems are tilted 20 degrees-30 degrees,* Online: US Energy Information Administration,Wash.DC2023.

[22] Fig.11 Grid-connected Microgrid System: MDPI,

[23] Fig. 12 Average Crude oil consumption; 2023 Geopolitical Outlook Global Specialty Insights Center Staff, Tianjin China, 2022.

[24] Jason Svarc - Founder, *Solar and energy storage specialist,* Clean Energy Reviews (CER) Quebec,2024.

[25] Daniel Hart, "*Power Electronics*", Published by McGraw-Hill, Avenue of the Americas, New York, NY 10020. Copyright © 2011

[26] Andrey Gorichenski, *Series, Parallel & Series-Parallel Connection of Solar Panels, Electrical Technology.*Florida, 2024.

[27] Fig. 13 Jude Obichere, *Time to Produce Energy Sources* Research Gate, January 2010.

[28] Fig. 14 Jude Obichere, *Time to Produce Energy Sources* Research Gate, January 2010.

[29] Fig. 15 *Solar Cells* Array; Getty Images: International-space-station, 2020.

[30] Fig. 16 *An diagram of apparatus by Becquerel* (1839); First photovoltaic Devices, Christiana Honsberg and Stuart Bowden(1839).

[31] H. Keshan, J. Thornburg and T. S. Ustun, *Comparison of lead-acid and lithium ion batteries for stationary storage in off-grid energy systems,*Kuala Lumpur, Malaysia, 2016.

[32] John and Willie Leone *Family Department of Energy and Mineral Engineering*, Pennsylvania The Pennsylvania State University © 2020.

[33] Fig. 17 *Structural Diagram of a Crystalline Silicon Solar Cell – Copper - cuprous oxide Pv cell.* 1930-32.

[34] Fig. 18 *Three Types of Solar Cell.*; The 3 Types of Solar Panels: Solar-Time, 2022.

[35] Dave Vernier Hydroelectric *Power Module*, Oregon USA.2021.

[36] *PSIM User manual* Copyright © 2001-2016 Powersim Inc. Version 10.0 Release January 2016.

[37] Dr. John Fuller proposed to the Department of Education Title III "*Solar Energy Experimentation Laboratory*", 2017.

[38] Fig. 19 *Solar Installations in the US. Chart*:, US records in 2023.
[39] Canary Media.com, *Chart-solar-installations-set-to-break-global-us-records*, US, 2023.

[40] Fig. 20 *Residential Solar Power Installation Cost.* Washington, D.C.2022.

[41] Fig. 21 *Cumulative US Community Solar Capacity Installations, 2022.*

[42] Fig. 22 *Future Overview Cumulative US Community Solar Installations. US, 2022.*

[43] Fig. 23 PVAMU *FY 2022 Energy Consumption*. PVAMU TAMU PO System Database, US, 2023.

[44] Fig. 24 PVAMU FY 2022 *Energy Consumption* PVAMU TAMU PO System Database.2023.

[45] Solar Energy Industries Association, Washington, D.C , SEIA, Research Data, 2022.

[46] Solar Energy Industries Association, Washington, D.C. SEIA, Research Data, 2022.

[47] Sol-Ark User manuals Copyright © 2023 Sol-Ark | Portable Solar LLC,2023.

[48] Solar/Wind Energy Training Systems 46120, Festo Didactic Inc. NJ 07724 USA,2019.

[49] Fig. 25 Ali Emadi *Irradiance PV IV Curve*, Mahankali, Muralidhar, *Handbook of Automotive Power Electronics and Motor Drives Institute of Technology,* Chicago, Illinois, USA.© 2005.

[50] Fig. 26 *Solar Cell Electric Circuit. Modeling and Performance Analysis of Simplified Two-Diode Model of Photovoltaic Cells* Department of Electrical and Electronics & Communication Engineering, DIT University, Dehradun, India, 2021.

[51] Fig. 27 *The Overload Request for Texas Outage. Review of* Extreme Cold Weather Event – ERCOT Presentation, US, 2021.

[52] Fig. 28 *Satellite Imagery of Texas The Overload Request for Texas Outage.* Extreme Cold Weather Event – ERCOT Presentation US. 2021.

[53] Fig. 29 *Roof Top Monofacial Solar Cells - Off Grid.* Rising The Energy Experts US, 2019.

[54] Fig. 30 *The Flow of the Renewable Energy PV System.* FESTO documents; Quebec, 2019.

[55] Fig. 31 *Power Curve and Irradiance Characteristics, PSIM,2022*.

[56] Fig. 31 *Power Curve and Irradiance Characteristics, PSIM,2022*.

[57] L. Pinter and C. Farkas, *"Impacts of electric vehicle chargers on the power grid,* Pisa, Italy, 2015. 10.1109/IYCE.2015.7180811

[58] Fig. 34 *Lead-Acid Battery Series Configurations*. Sol-Ark manual,2023.

[59] Fig. 35 Annette Evans,Tim J. Evans, *Lead Acid Battery breakdown*. Science Direct;2015.

[60] Ahmet Aktaş, Yağmur Kirçiçek, in Solar Hybrid Systems, *The Power Grid.*; Smart Energy Storage, 2021.

[61] Ali Najah Al-Shamani1,2, Mohd Yusof Hj Othman1, Sohif Mat1, M.H. Ruslan1, Azher M. Abed1,   K. Sopian1. Solar Energy Research Institute (SERI), *Design & Sizing of Stand-alone Solar Power Systems A house Iraq*, Musaib Technical College, Al-Furat Al-Awsat Technical University Babylon, Iraq, 2016.

[62] GovDelivery Communications Cloud on behalf of: *DOE Office of Clean Energy Demonstrations*, Washington DC, 2022.

[63] Fig. 36: Md. Aminul Islam, A. Merabet, +1 author H. Ibrahim *PV Cell breakdown*. , IEEE Electrical Power, 2013.

[64] Fig. 37: Carl R. Osterwald, *PV Panel testing example*. Standards, Calibration, and Testing of PV Modules and Solar Cells; National Renewable Energy Laboratory, 2020.

[65] Online Calculator NREL 2018.

[66] The National Academies Press. *America's Energy Future: Technology and Transformation*, Washington, DC: The National Academies Press 2009.

[67] Fig. 39 Robert W. Erickson, *Equivalent Circuit*. University of Colorado Boulder, 2016.

[68] Fig. 40 *Equivalent Circuit*. Robert W. Erickson, *Equivalent Circuit*. University of Colorado Boulder, 2016.

[69] Fig. 41. *V-I Power Curve Characteristics,* Alternative Energy.2020.

[70] Fig. 42 9 Bus System: Created in PowerWorld, 208.

[71] Md Razuan Hossain; M. Shamim Kaiser; Fahmid Iftekher Ali; Md Monjurul Alam Rizv N*etwork flow optimization by Genetic Algorithm and load flow analysis by Newton Raphson method in power system, 2015.*

[72] Fig. 43 9 Bus System: Created in PowerWorld,2022

[73] Fig. 44 9 Bus System: Created in PowerWorld,2022.

[74] Fig. 45 9 Bus System: Created in PowerWorld,2022.

[75] Fig. 46 a). Editorial Team Basic Dc to Dc *All About circuits June* 06, 2015.

[76] Editorial Team Basic Dc to Dc *All About circuits June* 06, 2015.

[77] Fig. 47 Robert W. Erickson, *The Output voltage of DC-DC converter.* University of Colorado Boulder, CO,2017.

[78] Fig. 48 Fig. 47 Robert W. Erickson, *The Output voltage of DC-DC converter.* University of Colorado Boulder, CO,2017.

[79] Fig. 49 *MPPT Application (Buck converter charge battery control output voltage), Electrical Engineering, 2016.*

[80] Fig. 50 *MPPT with Voltages and Current applications Clean Power,2019.*

[81] Fig. 51 *Buck converter during T_{on}* . Robert W. Erickson, *The Output voltage of DC-DC converter.* University of Colorado Boulder, CO,2017.

[82] Fig. 52 Solar Cell Datasheet: *Solar panels specs,*PSIM,2022.

[83] Fig. 53 *Solar Configurations*: Created by PSIM,2022.

[84] Fig. 54 *Solar Configurations* Schematic: Created by PSIM,2022.

[85] Fig. 55 *Solar Configurations:* I-V Power Curve Characteristics simulated by PSIM,2022.

[86] Fig. 56 *Solar Configurations: I-V Power Curve Characteristics* simulated by PSIM,2022.

[88] Fig. 57 Vikas Jaisinghani, *Maximum Power for MPPT*. 2015.

[89] Fig. 58 *Worst case conditions and IV Curves results*. Science Direct, 202.

[90] Fig. 59. Alternative Energy Tutorials Copyright © 2010 – 2024 All Rights Reserved. 2010-2024.

[91] Cara Marcy, *Most Utility-Scale, Fixed-Tilt Solar Photovoltaic Systems Are Tilted 20 Degrees To 30 Degrees*,TAMU,2017.

[92] Cara Marcy, Most Utility-Scale, Fixed-Tilt Solar Photovoltaic Systems Are Tilted 20 Degrees To 30 Degrees, TAMU,2017.

[93] Fig. 60 *Series configurations*. Cara Marcy, Most Utility-Scale, Fixed-Tilt Solar Photovoltaic Systems Are Tilted 20 Degrees To 30 Degrees,TAMU,2017.

[94] Fig. 62: Aya M. Elsherbiny *I-V Characteristic Curves, Smooth transition from grid to standalone solar diesel mode hybrid generation system with a* University, Egypt 1, 2016.

[95] Fig. 63 *Parallel and series combination (2S2P)*. Clean Power Cara Marcy, Most Utility-Scale, Fixed-Tilt Solar Photovoltaic Systems Are Tilted 20 Degrees To 30 Degrees, TAMU,2017.

[96] Fig. 64 *STORZ Batteries*: STORZ user guide manual,

[97] Discharging Lead vs Li-ion Battery @ 25°C. Impact of Temperature and Discharge, 2022.

[98] Rate on the Aging of a LiCoO2/LiNi0.8Co0.15Al0.05O2 Lithium-Ion Pouch Cell

[99] Fig. 65 *Lead Acids Batteries*: Local Model by Anthony Hill
Yao Wu2,3,1, Peter Keil2,1, Simon F. Schuster1 and Andreas Jossen1 Discharging Lead vs Li-ion Battery @ 25°C, 2017.

[100] Fig. 67 SOC rated at 80% Created in MATLAB

[101] Fig. 68 Lithium-ion vs Lead Acid: Generated by MATLAB

[102] Fig. 69 Storage comparison for Li-ion vs Lead Acid,

[103] Fig. 70 *Two / three batteries in series*. 2021

[104] Fig. 71 *Two / three batteries in parallel.* 2021

[105] Fig. 72 Sun orientation, Jason Svarc - Founder, "Solar and energy storage specialist", CEC accreditation license, 2019.

[106] Fig. 73 PSIM Professional 2022.2.0, PSIM

[107] Fig. 74 Simulating a Circuit. PSIM Online Manual

[108] PSIM Online Manual,2022.

[109] Fig. 75 PSIM Online Manual,2022.

[110] Fig. 76 PSIM Solar section,2022.

[111] PSIM Solar Online Manual,2022.

[112] Fig. 77 PSIM Solar schematic,2022.

[113] Fig. 78 *I-V Characteristics using PSIM,2022.*

[114] Fig. 79 *I-V Characteristics using PSIM Results,2022.*

[115] Fig. 80 *Solar Platform Modified output,2022.*

[116] Fig. 81 *Filtered output with an LC load*

[117] Fig. 82 *A Slice of the Solar Array Slice Schematic* created in PSIM software, 2022.

[118] Fig. 83 *A Slice of the Solar Array Slice Schematic* created in PSIM software, 2022.

[119] Fig. 84 Solar Array Results for string. Created in PSIM software

[120] Fig. 85 8 Solar Array Panels 3 Phase using PSIM Results

[121] Fig. 86 8-Solar Array Panels in series using PSIM Results

[122] Fig. 87 Solar Array Results for string 1 using PSIM Results

[123] M. R. Ruman, D. Paul, A. Barua, A. K. Sarker, A. Iqbal and S. Barua, *"Design and Implementation of SPWM Inverter,* Greater Noida, India, 2019.

[124] M. R. Ruman, D. Paul, A. Barua, A. K. Sarker, A. Iqbal and S. Barua, [125] *Design and Implementation of SPWM Inverter," 2019* Greater Noida, India, 2019.

[125] Fig. 88 Solar array filed test, modified sinewave. Model Platform created by Anthony Hill.2024.

[126] Fig. 89 Partial Shading: Pardhavi Kavya: Alternative Energy Tutorials Copyright © 2010 – 2024 All Rights Reserved.

[127] Fig. 90 Results at 200 W/m2 irradiance PSIM created by Anthony Hill,2024.

[128] Fig. 91 Simulations results s at 200 W/m2 irradiance. created by Anthony Hill,2024.

[129] Fig. 92 PV off-grid Model System. 300 Watt Model created by Anthony Hill,2024.

[130] Fig. 93 Solar model load results. 300 Watt Model created by Anthony Hill,2024.

[131] Fig. 94 Model modified sinewave and measurements. created by Anthony Hill,2024.

[132] Fig. 95 Photovoltaic Module Characteristic Curve Demonstration. by Anthony Hill,2024.

[133] Fig. 96 Solar model in the Field results. created by Anthony Hill,2024.

[134] Fig. 97 Solar Panels placements created by Anthony Hill,2024.

[135] Battery behavior during charging and discharging mode created by Anthony Hill,2024.

[136] Fig. 99 Battery behavior during charging and discharging Amp-Hours results

[137] Fig. 100 Discharging mode for Lead acid Batteries: MATLAB

[138] Fig. 101 12 volts battery charging: MATLAB

[139] Fig. 102 15 volts battery charging MATLAB

[140] Fig. 103 AC / DC Switches

[141] Fig. 104 Various type of Inverters

[142] Fig. 105 Wattage Consumptions

[143] Fig. 106 Oscilloscope and 60- and 100-watt loads.

[144] IronRidge, Inc. 28357 Industrial Boulevard Hayward, CA, 2024.

[145] IronRidge, Inc. 28357 Industrial Boulevard Hayward, CA,2024.

[146] Fig. 107 Ballasted mount. IronRidge, Inc. 28357 Industrial Boulevard Hayward, CA,2024.

[147] *Solar Mount process. Ballasted mount.* IronRidge, Inc. CA 2024.

[148] *US Scale for Fixed Title angles of 20° to 40° US Energy*, Washington, DC, 2024.

[149]*US Scale for Fixed Title angles of 20° to 40° US Energy* Information Administration 1000 Independence Ave., SW Washington, DC ,2021.

[150] *Fixed Titled Solar PV system. US Scale for Fixed Title angles of 20° to 40°* US Scale for Fixed Title angles of 20° to 40° US Energy Information Administration, SW Washington, DC ,2021.

[151] *Fixed Tilt Solar PV capacities US Scale for Fixed Title angles of 20° to 40° US Scale for Fixed Title angles of 20° to 40°* US Energy Information Administration, SW Washington, DC *,2021.*

[152] *Dual Axis Solar Tracking System.* US Scale for Fixed Title angles of 20° to 40° US Energy Information Administration Washington, DC ,2024.

[153] *Utility Scale for Fixed tilt Solar PV generating capacity, US Scale for Fixed Title angles of 20° to 40°* US Scale for Fixed Title angles of 20° to 40° US Energy Information Administration, *Washington, DC ,2024.*

[154] EPA Press Office *"EPA Proposed New Carbon Pollution Standards for Fossil Fuel-Fired Power Plants, EPA Washington DC,* 2020.

[155] EPA Press Office "EPA Proposed New Carbon Pollution Standards for Fossil Fuel-Fired Power Plants, EPA Washington DC, 2020.

[156] *An Overview of the proposed PV Site.*2023.

[157] *Renewable energy capacity 2022 by country*, Published by Lucía Fernández, 2023.

[158] Chris Mi San Diego State University USA, M. Abul Masrur *Hybrid Electric Vehicles,* University of Detroit Mercy USA, MA 2018 © 2018

[159] John Wiley &   Sons Ltd Samantha Houston, *Can the Electric Frid Handle EV charging? Transportation Tags: electric vehicle charging, EVs*, University of Detroit Mercy USA, MA 2018.

[160] Construction process of the off-grid PV system. G. M. Masters,

[161] *Renewable and Efficient Electric Power Systems*, 2nd ed. Hoboken, NJ, USA: Wiley, 2013.

[162] PV Facility system.

[163] Dr. John Fuller Solar Lab Proposal

[164] Fig. 118 PV Facility system.

[164] Dr. John Fuller "Solar Lab Proposal"

[165] Fig. 119 The Entry Gate

[166] Sol-Ark -2P. Sol-Ark Manual 2022.

[167] Sol-Ark -2P. Sol-Ark Manual 2023.

[168] Sol-Ark -2P. Sol-Ark Manual 2023.

[169] Fig. 121 E-Gauge Smart Meter. eGauge Website,2024.

[170] Fig. 122 Powerline Communication2024.

[171] Fig. 123 Sensor Hub, 2024.

[172] Fig. 124 Live Data Report. eGauge manual, 2024.

[173] Fig. 125 PV One Line Diagram. IES / Native /NASH,2024.

[174] Fig. 126 Preliminary Concept Online Drawing of PV Solar Platform IES-NASH,2022-23.

[175] J.F. Kurose, K.W. Ross, Pearson, 2020 *Computer Networking: a Top-Down Approach (8th ed.)*, 2010

[176] Fig. 127: Kurose, K.W. Ross, Pearson, 2020 *Computer Networking: a Top-Down Approach (8th ed.)* 2010.

[177] J.F. Kurose, K.W. Ross, Pearson, *2020 Computer Networking: a Top-Down Approach (8th ed.) 2010.*

[178] J.F. Kurose, K.W. Ross, Pearson, 2020 *Computer Networking: a Top-Down Approach (8th ed.)*2010.

[179] J.F. Kurose, K.W. Ross, Pearson, 2020 *Computer Networking: a Top-Down Approach (8th ed.)*2010.

[180] J.F. Kurose, K.W. Ross, Pearson, 2020 *Computer Networking: a Top-Down Approach (8th ed.*)2010.

[181] J.F. Kurose, K.W. Ross, Pearson, 2020 *Computer Networking: a Top-Down Approach (8th ed.)*,2010.

[182] In-Hand cellular modems manual, 2023.

[183] F. Kurose, K.W. Ross, Pearson, 2020 *Computer Networking: a Top-Down Approach (8th ed.),* 2020.

[184] Preliminary Concept Online Drawing of PV Solar Platform   IES-NASH,2022-23.PARU Solar Tracker.

[185] Preliminary Concept Online Drawing of PV Solar Platform   IES-NASH,2022-23. PARU Solar Tracker.

[186] IPCC, "Climate Change 2021: *The Physical Science Basis.* Contribution of Working Group I to the Sixth Assessment Report of the Intergovernmental Panel on Climate Change," Cambridge University Press, Cambridge UK, 2021.

[187] Preliminary Concept Online Drawing of PV Solar Platform   IES-NASH,2022-23. PARU Solar Tracker.

[188] Preliminary Concept Online Drawing of PV Solar Platform   IES-

NASH,2022-23. PARU Solar Tracker.

[189] PARU Solar Tracker November 2021.

[190] PARU Solar Tracker manual, 2023.

[191] United States Department of State and the United States Executive Office of the President, *The Long-Term Strategy of the United States*: Pathways to Net-Zero Greenhouse Gas Emissions, Washington DC. November 2021.

[192] In-Hand cellular modems manual, 2023.

APPENDICES

CURRICULUM VITAE

_____

ANTHONY HILL
adhill@pvamu.edu

Education.

Prairie View A&M University   Prairie View, TX

- B.A., Electrical Engineering. May 1991
- Master 's: Community Development May 2016
- M.S.: Electrical and Computing Engineering, May 2020
- Ph. D. in Electrical Engineering, August 2023

Work Experience.

- Company: Prairie View A&M University, College of Engineering
    Title: IT Professional I /Adjunct Professor, 2018-present
    Job: Manage Labs / Teach in the Electrical & Comp. Eng.

- Company: City of Hempstead
    Title: Dir. of Tech. & Utilities infrastructure 2015-2018
    Job: Manage Infrastructure & Supervise Utility usages

- Company: City of Hempstead
    Title: Director of Parks & Recreation-Tech. 2012-2015
    Job: Manage the Activities & Supervised Technology.

- Company: Hempstead I.S.D.
    Title: Director of Technology 1999 – 2012
    Job: Managed and implemented the Computer Network

Technical &

Work-related

- Certified Universal R3 Robotics, Security Awareness, Training in
    Fundamentals of Solar Photovoltaic Design and Installation,
    Training in Intel FPGA and Quartus Prime Software, e-Series Core
    Track Universal Robots, Teachers Certification Training in UR

Experiences &

Skills.

Publications

&Presentations.

[1]. The power flow analysis for electric power network: A tutorial article; **1st author:**

[2]. Performance analysis of reactive power control management for doubly fed induction generator wind turbines;

[3]. Alleviating power line congestion through the use of renewable generation.

All publications were published by World Journal of Advanced Engineering Technology and Sciences. (WJAETS)